Ma) to the Cenozoic age following subsequent to the Hercynian orogeny, particularly by the large-scale deformation caused by the Alpine orogeny starting in the Mesozoic, and also affected strongly by the geological restructuring resulted from the collision of the Eurasian and African plates in the Jurassic.

The effects of the orogeny that occurred mainly in the Mesozoic period are reflected in, among other things, the fact that the Shebenik-Pogradec ultrabasic massif was obduced over the external Albanides together with Mirdita zone in Jurassic period, that the lower Triassic to lower Jurassic of the Mirdita zone to the east of the Shebenik massif is marked by pronounced folding and faults in the NW-SE direction and that a tectonic melange consisting of schists, phyllitic sediments, serpentinite, limestones, etc., was developed between the Triassic and the ultrabasic massif zone.

It is considered that those rocks constituting the Mirdita zone and the ultrabasic rocks of the Shebenik-Pogradec massif were once flysch sediments and its oceanic crust of the Jurassic or earlier existed between the Eurasian plate and the African plate. The chemical composition of the Shebenik-Pogradec ultrabasic massif indicates that it is probable that at the stage of closing of the two plates an island arc environment accompanied by volcanic activity was produced.

In Cretaceous period, as a result of the widespread marine transgression sediments mainly consisting of limestone deposited regionally even in the Internal Albanides. After the Cretaceous sedimentation large scale marine regression caused by epeirogeny of the Cenozoic Alpine orogeny took place regionally to create an erosive and oxidizing environment which may resulted in nickeliferous laterite deposits widely over the ultrabasic rocks.

In the last part of the Cretaceous and into the Tertiary period the Internal Albanides, including the project area, underwent folding accompanied by upheaval, which resulted in formation of mountain ranges in the NNW-SSE direction, and that at the same time lowlands developed between the mountain ranges with accompaniment of faults. The Eocene, Oligocene and Neogene of the project area were probably deposited in such intermontane lowlands. Although a shallow-sea environment may remained in the Eocene, overall upheaval subsequently proceeded, resulting in inland lakes. During those period an erosive environment was dominant in the hinterland supplying such Tertiary systems but that it was not until the Neogene that the Shebenik-Pogradec ultrabasic massif experienced upheaval to such an extent that it became subject to a really intense erosive environment.

The geological structures formed from the end of the Cretaceous into the Tertiary are the gentle folds in the NNW-SSE direction, the faults in the same direction that occurred in the vicinity of the boundaries between mountain ranges and lowlands and the small faults perpendicular to those.

After the sedimentation that took place in the Neogene the water level in the inland lakes in the intermontane lowlands declined as a result of further erosion of the mountain ranges between Librazhd and Elbasan by what is presently the Shkumbin River and that gave the entire project area an erosive environment. There is still an inland lake environment on the NNW-SSE axis centering on Ohrit Lake on the east side of the area.

2-3-3 Chromite Deposits

As indicated in Table 2-2-11 (1)-(2), eleven chrome deposits in the Shebenik area have already been exploited, and there are another twenty-two for which the ore reserves have been calculated but which have not yet been exploited. Three of those eleven, as already mentioned, are still in operation: Katjel, Qershori Pojske and Pishkash-4. Besides those deposits, more than 300 chrome showings are known, as indicated in Table 2-2-11(2). The location of those chrome deposits and showings is shown in PL 2-2-1 and PL 2-2-3.

As shown in PL 2-2-1 and PL 2-2-3, chrome deposits and showings are distributed practically throughout the Shebenik-Pogradec ultrabasic massif, with the exception of the northwestern part of the Shebenik massif. In particular, many deposits and showings are distributed in the Pogradec massif, where harzburgite mainly occurs accompanied by dunite, and in the west half of the Shebenik massif south of the drainage basins of the Gobilla and Govates Rivers, tributaries of the Bushtrice River. Most of the deposits and showings involved in past exploration and development lie within those ranges.

Geologically, all such chrome deposits and showings belong to the Alpine podiform type hosted by harzburgite. They occur as chromitite accompanied by dunite envelope or schlieren rich in chrome spinel in dunite, the existence of dunite being a necessary condition for the existence of chromitite.

The dimensions of the ore bodies are as follows: width of several centimeters to 2 m, maximum strike length of 300 m, maximum dip length of 150 m. Most of the deposits that have been exploited have a width of about 1 m.

The ore has a variety of modes of occurrence, including massive, nodular, banded and disseminated, and there is considerable variety in that respect within the same ore body. Disseminated, banded and nodular chromitite is frequently accompanied by a texture of linear arrangement according to the chrome spinel, and nodular chromite is frequently accompanied by arrangement in the direction of the longitudinal axis of the nodule, which is oval. From experience it is known that such structures match the dip direction of the entire ore body, and that is an important factor in efficient exploration of chrome deposits.

The ore presently being mined in the area is that with a massive-nodular-disseminated and that has a grade of at least 25-30% Cr_2O_3. In the rich-ore part of the ore body that grade of ore occurs abundantly, but at the end of the ore body, closed by dunite, there is often a change to disseminated ore.

As for the scale of the ore bodies discovered so far, in the case of the Katjel deposit, the largest in the area, the strike length is 350 m, the dip length 300 m, and the average width 2 m. The deposit consists of a single homoclinally folded ore body with ore reserves of approximately 820,000 tons. In the case of the Qershori Pojske deposit, the next largest after Katjel, the strike length is 130 m, the dip length 100 m, and the average width 1.5 m. There is a single ore body with a monoclinal structure and ore reserves amounting to approximately 440,000 tons.

The ore body strike direction of both those deposits is N 30° W, which just about matches the structure of the harzburgite host. The entire ore body has a dip of approximately 20° in the south-southeast direction in the case of the Katjel deposit, accompanied by folding, and approximately 25-30° in the north-northeast direction in the case of the Qershori Pojske deposit.

Besides chrome deposits like those two with a structure that just about matches the structure of the harzburgite, there are other deposits and showings with structures that do not match that of the harzburgite, such as the Pishkash-4 deposit, which has a lenticular ore body that can be traced about 150 m in the dip direction and with a strike length of about 25 m in the N 10° W direction and an average width of 1.2 m, the Menik deposit, which has two intersecting ore bodies, one running NNE-SSW and the other WNW-ESE, and the No. 49 indication, with a cylindrical deposit inside pipe-shaped dunite with a diameter ranging from several meters to about 10 m.

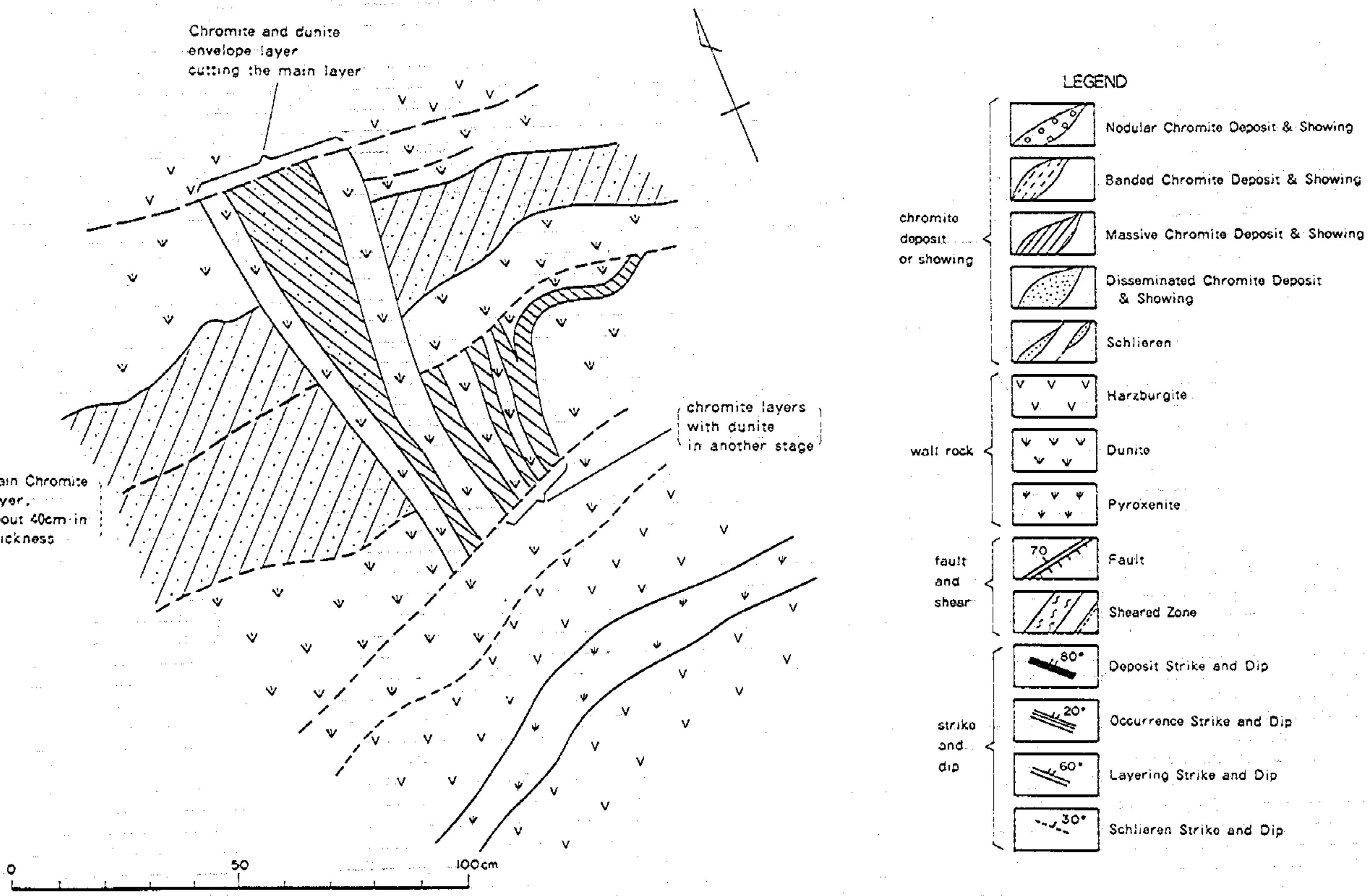

Fig. 2-3-2(1) Geological sketch of chromitite outcrops

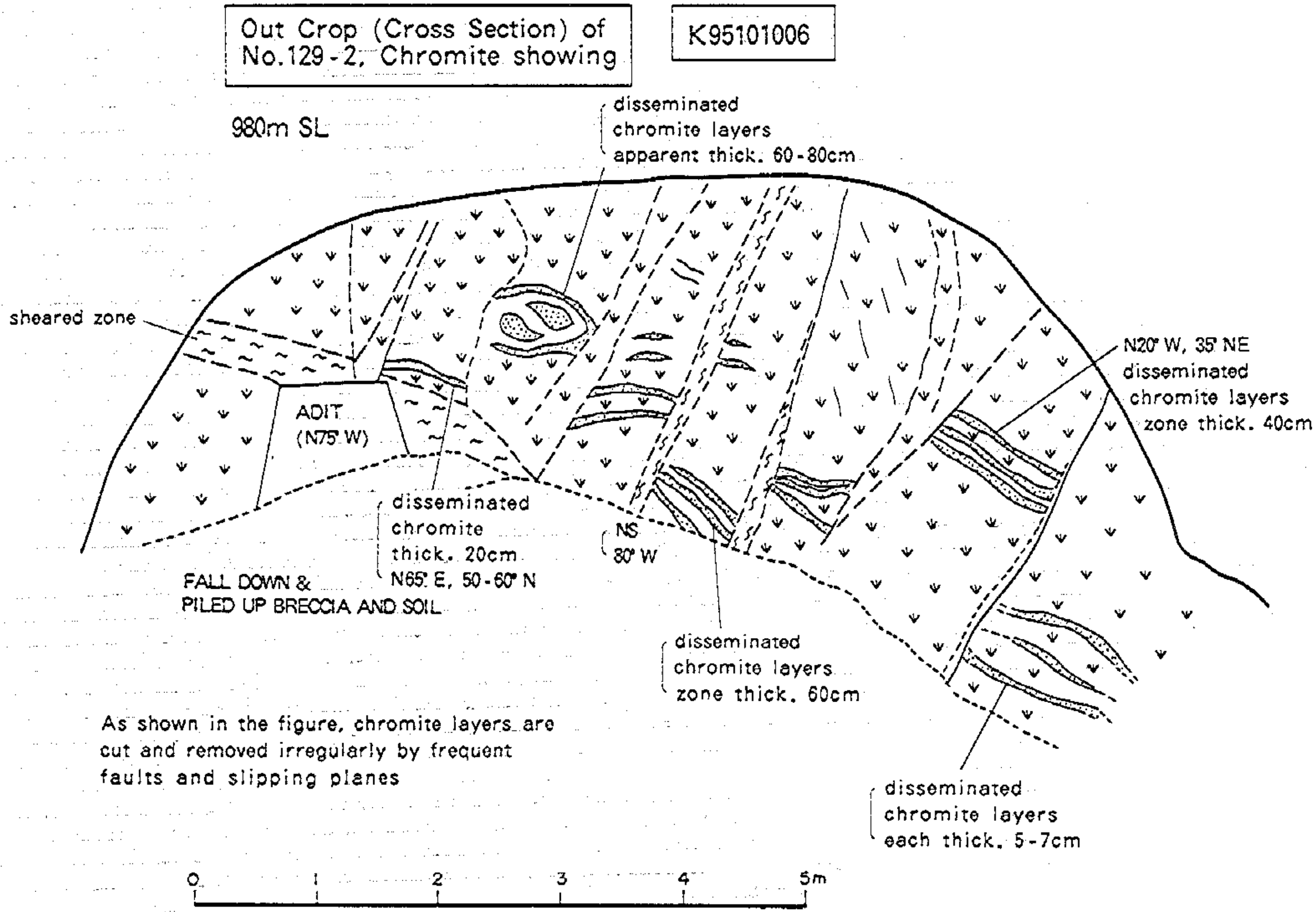

Fig. 2-3-2 (2) Geological sketch of chromitite outcrops

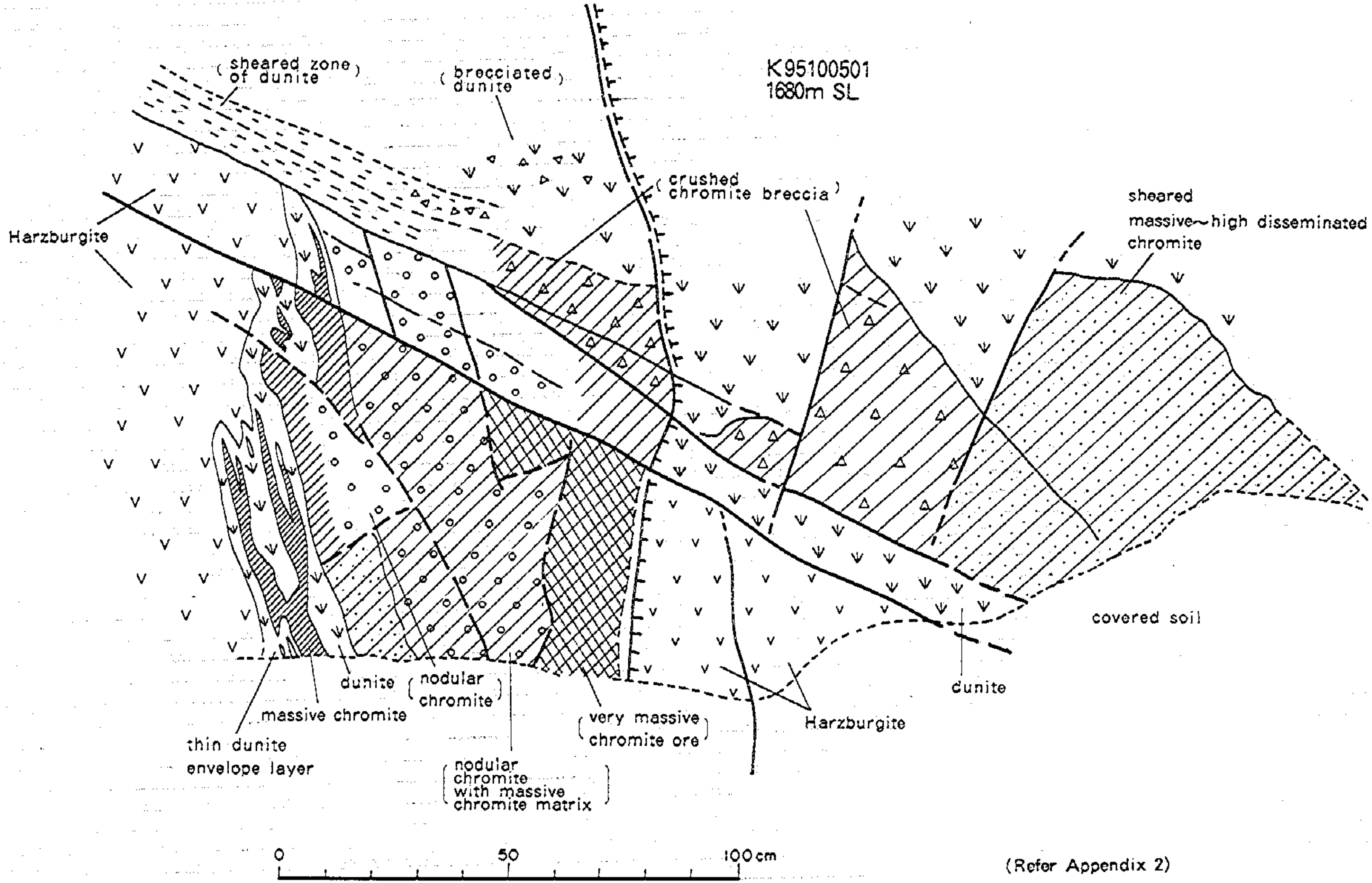

(Refer Appendix 2)

Fig. 2–3–2(3) Geological sketch of chromitite outcrops

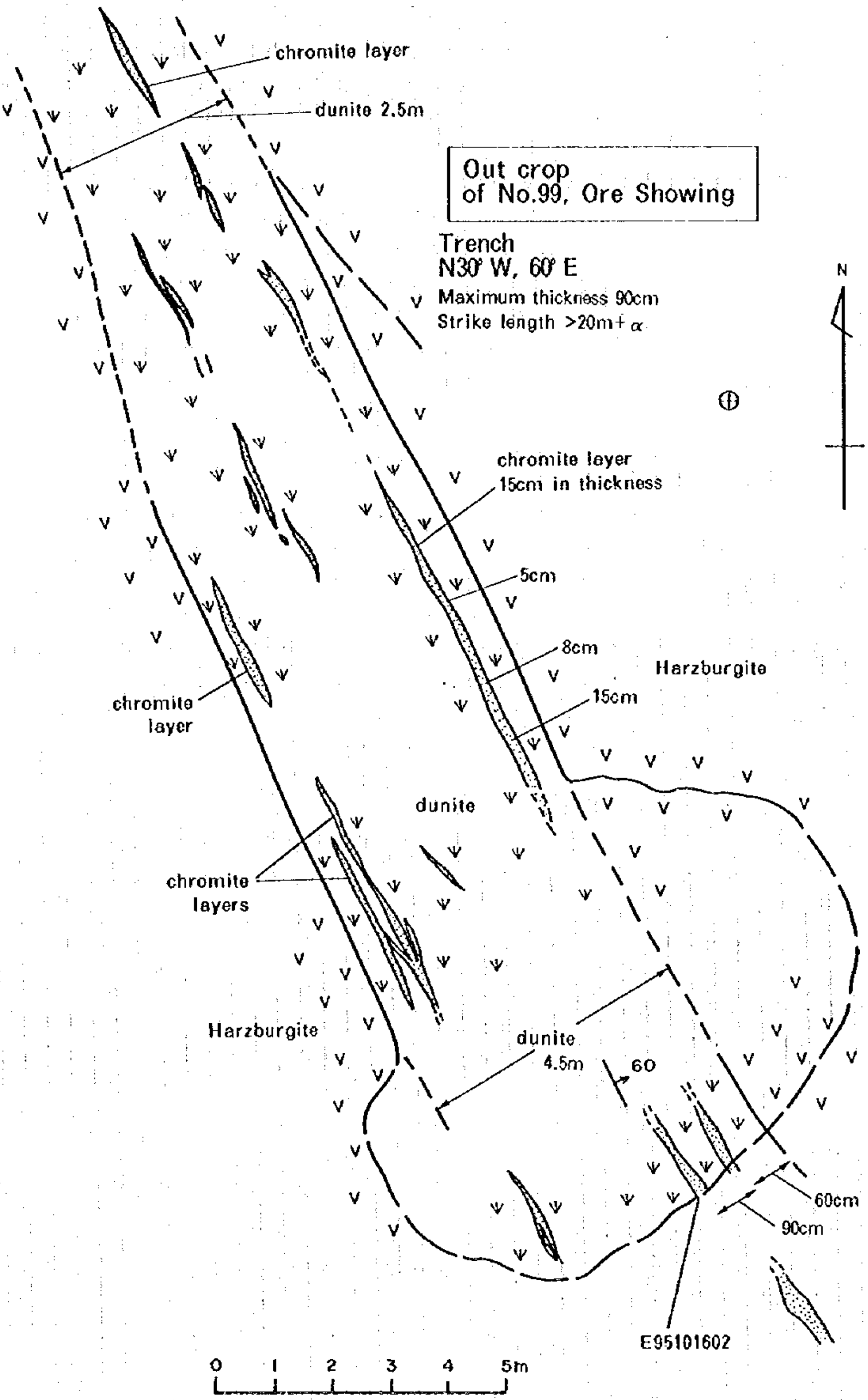

Fig. 2-3-2 (4) Geological sketch of chromitite outcrops

Such chromitite ore bodies in dunite are frequently displaced by faults with a dislocation of several meters to tens of meters and sometimes more than 100 m that develop 3-dimensionally at intervals of ten to tens of meters, and that makes exploration of chromite deposits in the area more difficult than it would otherwise be.

It might be added that in the case of many of the showings that have led to discovery of chrome deposits through drilling and gallery exploration, high-grade massive and nodular ore has been discovered in surface trenches and exploration galleries directly under them.

Fig.2-3-2(1) to Fig.2-3-2(4) and Apx.2 indicate sketches of typical mode of occurrence of chromitite in the area, including chromitites in multi-stages intersecting one another, chromitite dislocated by small faults, chromitite impregnated in marginal parts of dunite, small lenticular chromitites distributed intermittently in dunite etc.

2-3-4 Laboratory Tests

As a part of the geological survey, microscopic observation of rock thin sections and ore polished thin sections and chemical analyses of rock and ore samples as well as EPMA tests were carried out. PL.2-3-4 indicates localities of samples for laboratory tests.

(1) Microscopic Observation of Ore Polished Thin Sections and Rock Thin Sections

Table 2-3-1 gives the results of appraisal of rock thin sections for 50 samples, and Apx. 3 gives microphotographs of representative rock thin sections. The results of microscopic observation of ore polished thin sections are given in Table 2-3-2, and representative microphotographs thereof are given in Apx. 4.

Of a total of 50 samples for appraisal of rock thin section, 21 samples of harzburgite, 21 samples of dunite, 2 samples of pyroxenite, 2 samples of meta-amphibolite, 2 samples of hornblende gabbro, 1 sample of meta-basalt and 1 sample of sandstone taken from the Shebenik-Pogradec ultrabasic massif and its surroundings.

A total of 121 samples were used for microscopic observation of ore polished thin sections: 50 samples of chromitite taken from the Shebenik-Pogradec ultrabasic massif, 35 samples of the dunite that occurs as an envelope of the chromitite, 32 samples of the harzburgite distributed next to the dunite and 2 samples each of harzburgite, dunite and chromitite taken from two outcrops of the Bulqiza mine.

The following is a summary of the respective lithological characteristics of the samples of the above rock types.

-Harzburgite:

It consists mainly of olivine and contains small quantities of orthopyroxene, clinopyroxene (±) and chrome spinel. The olivine is mostly altered to serpentine-group minerals, and a mesh structure is often noted. Both the orthopyroxene and clinopyroxene, too, are often altered to serpentine-group minerals, sometimes having a bastite structure.

Except for the lherzolitic harzburgite distributed in the northwestern part of the Shebenik massif, only very small amounts of orthopyroxene exist in the harzburgite, which indicates that it is a harzburgite depleted in melt constituents.

Table 2-3-1 Results of microscopic observation on thin sections

No.	Sample number	Coordination X	Coordination Y	Rock	ol	opx	cpx	sp	opaq	serp	chl	carb	pl	others	Remarks
1	K95101307HZ	69060	38990	Serpentinized hurzburgite	△	△		+		◎	+			talc+	
2	K95101307DU	69060	38990	Serpentinized dunite	△			△		◎					
3	E95102202HZ	68770	38990	Serpentinized hurzburgite	+	+		+		◎	+				
4	E95102202DU	67770	38990	Serpentinized dunite	+			+		◎					
5	E95102201HZ	67080	38710	Serpentinized hurzburgite	△	△		+		◎					
6	E95102201DU	67080	38710	Serpentinized dunite	△			+	+	◎					
7	K95092505HZ	68310	42370	Serpentinized hurzburgite	○	○		+		◎	△	+			
8	K95092505DU	68310	42370	Serpentinized dunite	△			+		◎		+			
9	M95102203HZ	64730	42180	Serpentinized hurzburgite	○	○		+		○	+				
10	M95102203DU	64730	42180	Serpentinized dunite	△			+		◎		+			
11	K95102107HZ	64190	44280	Serpentinized hurzburgite	○	○		△		○					
12	K95102107DU	64190	44280	Serpentinized dunite	○			+	+	◎					
13	K95101801HZ	62700	52980	Serpentinized hurzburgite	○	○		+		○		+			
14	K95101801DU	62700	52980	Serpentinized dunite	○			○		◎					
15	M95101602HZ	61650	53550	Serpentinized hurzburgite	○	○		+		◎				epidote+	
16	M95101602DU	61650	53550	Serpentinized dunite	○			+		◎					
17	M95101703HZ	59920	52910	Serpentinized hurzburgite	○	○		+		◎					
18	M95101703DU	59920	52910	Serpentinized dunite	△			+		◎					
19	M95100810HZ	55470	53950	Serpentinized hurzburgite	△	△		+		◎	+				
20	M95100810DU	55470	53950	Serpentinized dunite	△			+		◎	+				
21	M95101605HZ	58830	55420	Serpentinized hurzburgite	○	○		+		○	+				
22	M95101605DU	58830	55420	Serpentinized dunite	○			△		◎					
23	M95101507HZ	61170	57530	Serpentinized hurzburgite	○	○		+		○					
24	M95101507DU	61170	57530	Serpentinized dunite	○			+		◎					
25	K95101702HZ	54830	59380	Serpentinized hurzburgite	○	○		+		○					
26	K95101702DU	54830	59380	Serpentinized dunite	△			+		◎	+				
27	E95101602HZ	58040	61670	Serpentinized hurzburgite	○	○		+		○	+				
28	E95101602DU	58040	61760	Serpentinized dunite	○			+		◎					

Table 2-3-1 Results of microscopic observation on thin sections

No.	Sample number	Coordination X	Coordination Y	Rock	Minerals ol	opx	cpx	sp	opaq	serp	chl	carb	pl	others	Remarks
29	K95100601HZ	54050	62390	Serpentinized hurzburgite	○	○		+		◎					
30	K95100501DU	54050	62390	Serpentinized dunite	○			+	+	◎					
31	E95100201HZ	54130	65350	Serpentinized hurzburgite	○	○		+		○	+				
32	E95100201DU	54130	65350	Serpentinized dunite	○			+		◎					
33	K95093005HZ	47550	63200	Serpentinized hurzburgite		Δ		+		◎					
34	E95100407DU	55500	68950	dunite	◎	Δ		+							
35	M95102102HZ	64560	45830	Serpentinized hurzburgite	○	○		+		◎					
36	M95102102DU	64560	45830	Serpentinized dunite	○			+		◎					
37	M95101807HZ	63250	51410	Serpentinized hurzburgite	○	Δ		+		◎		+			
38	M95101807DU	63250	51410	Serpentinized dunite	+			+		◎					
39	K95101603HZ	56150	57790	Serpentinized hurzburgite	○	○		+		○					
40	K95101603DU	56150	57790	Serpentinized dunite	○			+		◎					
41	E95100001SCH	53160	69130	hornblende gabbro					+				○	hornblende◎ quartz +	
42	M95100305PX	50250	67390	pyroxenite	Δ	○	○							hornblendeΔ	
43	E95100402HZ	56720	66290	Serpentinized hurzburgite	◎	○		+		Δ					
44	E95100404PX	57680	66310	altered pyroxenite		○	○		+		+		Δ	prehnite Δ epidote Δ	
45	E95100405AM	58000	66530	metagabbro			Δ							*	
46	E95100401DU	55000	65210	Serpentinized dunite	○			+		◎					
47	N95100503GB	50170	64650	metagabbro							○		○	**	
48	N95101703BT	62450	58230	greenstone (metabasalt)			○		+		Δ	○	○	epidote +	
49	K95102302BT	67000	46210	sandstone					+				+	***	
50	K95102307GB	68420	45290	hornblende gabbro								Δ	○	hornblende◎ epidote Δ prehnite Δ	

ol : olivine
opx : orthopyroxene
cpx : clinopyroxene
sp : chrome spinel
opaq : opaque minerals

serp : serpentine minerals
chl : chlorite
carb : carbonate minerals
pl : plagioclase

◎ : >40%
○ : 10~40%
Δ : 5~10%
+ : ≦5%

* : hornblende◎, titanite(sphene) +, prehnite +, epidote +, sericite +
** : hornblende◎, titanite(sphene) +, epidote +
*** : quartz○, muscovite +, K-feldspar +, lithic fragments +, cement minerals(matrix) ○

Table 2-3-2 Results of microscopic observation on polished-thin sections

No.	Sampe No.	Rock type	primary minerals						secondary minerals									Note
			ol	opx	cpx	sp	par	mi	ser	tc	chl	bru	mt	f.c.	tre	ca	di	
1	K95101307 HZ	Harzburgite	◎	○		△			◎	△	・		・		△			
2	K95101307 DU	Dunite	◎			△			◎				△					Antigorite (in vein)
3	K95101307 CR	Olivine chromitite	○			◎			○									Cracked, opaque
4	E95102202 HZ	Harzburgite	◎	○	△	△			◎									
5	E95102202 DU	Dunite	◎			△			◎									Relatively spinel rich.
6	E95102202 CR	Olivine chromitite	○			◎			△	△	△							
7	E95102201 HZ	Harzburgite	◎	○		△			◎									Relatively OPX poor.
8	E95102201 DU	Dunite	◎			△			◎			△						
9	E95102201 CR	Olivine chromitite	◎			○			◎				・					or spinel rich dunite.
10	K95101301 HZ	Harzburgite	◎	○		△			◎									
11	K95101302 DU	Dunite	◎	△		△		・	◎									Spinel has mineral inclusions.
12	K95101301 CR	Chromitite	△			◎				・	・							
13	E95102101 HZ	Harzburgite	◎	○	△	△			◎									Spinel has mineral inclusions.
14	E95102101 DU	Dunite	◎			△			◎									
15	E95102101 CR	Olivine chromitite	△			◎			△									
16	K95092505 HZ	Harzburgite	◎	○	△	△			◎									Relatively OPX poor.
17	K95092505 DU	Dunite	◎			△			◎									
18	K95092505 CR	Olivine chromitite	◎			◎			◎									ol:sp=1:1
19	K95102108 HZ	Harzburgite	◎	○		△			◎									Strongly foliated.
20	K95102108 DU	Dunite	◎	・		△			◎									
21	K95102108 CR	Olivine chromitite	○			◎			◎	・	・							
22	M95102203 HZ	Harzburgite	◎	○	・	△			◎	△					・			Protogranular~porphyroclastic.
23	M95102203 DU	Dunite	◎			・			◎									Relatively spinel poor.
24	M95102203 CR	Chromitite	△			◎			△	・	・		△			・		
25	K95102206 HZ	Harzburgite	◎	○	・	△			◎	・								
26	K95102206 DU	Dunite	◎			△			◎		・	・						Relatively spinel rich.
27	K95102206 CR	Chromitite	△			◎			△		・							olivine poor chromitite
28	E95110101 HZ	Harzburgite	◎	○	・	△			◎	・								
29	E95110101 DU	Dunite	◎			△			◎				・	・?				Spinel has inclusions.
30	E95110101 CR	Olivine chromitite	○			◎			○	・						・		Brecciated (sheared)
31	K95102107 HZ	Harzburgite	◎	○	・	・			◎									Porphyroclastic texture
32	K95102107 DU	Dunite	◎			△			◎							△		Olivine has relic fluid inclusions.
33	K95102107 CR	Olivine chromitite	○			◎			○	・								ol:sp=4:6
34	K95102104 HZ	Harzburgite	◎	○	・	△			◎									Porphyroclastic texture
35	K95102104 DU	Dunite	◎			△			◎									
36	K95102104 CR	Sp-rich dunite	◎			○			◎									Four spinel rich seam.
37	K95102102 HZ	Harzburgite	◎	○	△	△			○									Porphyroclastic texture
38	K95102102 DU	Dunite	◎	・		△			○						△			Porphyroclastic texture
39	K95102102 CR	Olivine chromitite	○			◎			○									ol:sp=3:7
40	K95101801 HZ	Harzburgite	◎	○	・	△			◎	・								Porphyroclastic texture
41	K95101801 DU	Dunite	◎			△			◎						・			
42	K95101801 CR	Olivine chromitite	◎			○			◎									ol:sp=4:1
43	M95101802 HZ	Harzburgite	◎	○	・	△			◎									OPX-aggregation
44	M95101802 DU	Dunite	◎			△			◎									
45	M95101802 CR	Olivine chromitite	○			◎			○									ol:sp=2:8
46	M95101703 HZ	Harzburgite	◎	○	・	△			◎	・					・			
47	M95101703 DU	Dunite	◎			△			◎			・	・					
48	M95101703 CR	Olivine chromitite	○			◎			○		・							ol:sp=2:8
49	M95101704 HZ	Harzburgite	◎	○	・	△			◎							・		Protogranular texture
50	M95101704 DU	Dunite	◎			△			◎		・		・			・		
51	M95101704 CR	Olivine chromitite	◎			○			◎									ol:sp=7:3, Fine grained spinel.
52	K95092904 HZ	Harzburgite	◎	○		△			◎	・								Strongly serpentinized.
53	K95092904 DU	Dunite	◎			△			◎							△		Relatively spinel rich.
54	K95092904 CR	Olivine chromitite	◎			○			◎									ol:sp=6:4, Fine grained spinel.
55	K95092911 HZ	Harzburgite	◎	○	△	△			◎						・			
56	K95092911 DU	Dunite (+harz.)	◎	○		△			◎									
57	K95092911 CR	Olivine chromitite	○			◎			○									ol:sp=3:7
58	M95100810 HZ	Harzburgite	◎	○	△	△			◎							△		OPX is aggregated and kinked.
59	M95100810 DU	Dunite	◎			△			◎							△		
60	M95100810 CR	Olivine chromitite	◎			◎			◎									ol:sp=5:5
61	M95101605 HZ	Harzburgite	◎	○	・	△			◎	・								Porphyroclastic texture.
62	M95101605 DU	Dunite	◎		・	△			◎									
63	M95101605 CR	Olivine chromitite	○			◎			○									ol:sp=4:6
64	M95101509 HZ	Harzburgite	◎	○		△			◎						△			Spinel has inclusions.
65	M95101509 DU	Dunite	◎		・	△			◎		・	・						
66	M95101509 CR	Olivine chromitite	△			◎	△		・	・								Fresh, ol:sp=2:8,

Table 2-3-2 Results of microscopic observation on polished-thin sections

No.	Sampe No.	Rock type	primary minerals: ol	opx	cpx	sp	par	mi	secondary minerals: ser	tc	chl	bru	mt	f.c.	tre	ca	di	Note
67	M95101507 HZ	Harzburgite	◎	○	·	△			◎	△								
68	M95101507 DU	Dunite	◎			△			◎									Relatively spinel rich.
69	M95101507 CR	Olivine chromitite	○		·	◎			△		·				△			ol:sp=3:7
70	K95101705 HZ	Harzburgite	◎	○	△	△			◎						△			
71	K95101705 DU	Dunite	◎			○			◎									Spinel rich layer.
72	K95101705 CR	Olivine chromitite	○			◎			○									ol:sp=4:6
73	K95101702 HZ	Harzburgite	◎	○	△	△			◎	·								
74	K95101702 DU	Dunite	◎			·			◎									
75	K95101702 CR	Olivine chromitite	○			◎			△		△		·					ol:sp=3:7
76	E95101601 HZ	Harzburgite	◎	○	△	△			◎									Relatively OPX poor.
77	E95101601 DU	Dunite	◎		·	△			◎	·	·							
78	E95101601 CR	Olivine chromitite	△		·	◎	·		△		·							ol:sp=2:8~1:9, Spinel has inclusions.
79	E95101602 HZ	Harzburgite	◎	○	·	△			◎	·								
80	E95101602 DU	Dunite	◎			·			◎									
81	E95101602 CR	Olivine chromitite	◎			◎			◎									ol:sp=1:1
82	K95100501 HZ	Harzburgite	◎	○	△	△			◎									Coarse grain spinel has incusions.
83	K95100501 DU	Dunite	◎		·	·			◎									Relatively CPX rich.
84	K95100501 CR	Chromitite	△			◎			△									Olivine poor chromitite
85	E95100501 HZ	Harzburgite	◎	○	·	·			◎	·								Relatively pyroxene poor.
86	E95100501 DU	Dunite	◎			·			◎			△						Relatively spinel poor.
87	E95100501 CR	Olivine chromitite	◎			○			◎	△	△							
88	M95100306 HZ	Harzburgite	◎	○	△	△			◎	△					·			Relatively CPX rich. Porphyroclastic.
89	M95100306 DU	Ol chr + Dunite	◎			◎			◎									
90	M95100306 CR	Olivine chromitite	○			◎			○									ol:sp=2:8
91	E95100201 HZ	Harzburgite	◎	○	○	△			○									Porphyroclastic texture.
92	E95100201 DU	Dunite	◎			△			◎									
93	E95100201 CR	Olivine chromitite	◎			◎			◎	△								ol:sp=5:5~6:4
94	K95093005 HZ	Harzburgite	◎	○		△			◎	·			·					
95	K95093005 CR	Olivine chromitite	◎						◎	△	△							ol:sp=6:4, Orbicular texture.
96	N95100602 HZ	Harzburgite	◎	○	·	△			◎	△			·		·			
97	N95100602 CR	Olivine chromitite	△			◎			△	△								ol:sp=2:8, grading.
98	E95100407 DU	Harzburgite	◎	○	·	△			△									Porphyroclastic texture.
99	K95101305 CR	Chromitite	△			◎			△		·		△			○		Crushed and veined.
100	K95102207 CR	Olivine chromitite	◎			◎			◎				△					ol:sp=4:6, Crushed.
101	K95102203 CR	Olivine chromitite	◎			○			◎									ol:sp=8:2
102	K95102106 CR	Olivine chromitite	○			◎			○	△								
103	M95102102 CR	Sp-rich dunite	◎			△			◎									Layered structure, ol:sp=90:10~95:5
104	M95101807 HZ	Harzburgite	◎	○	·	△			◎	·								Relatively OPX-poor.
105	M95101807 DU	Dunite	◎	·		△			◎									
106	M95101807 CR	Olivine chromitite	◎			◎			◎	·								ol:sp=5:5~4:6
107	E95101803 CR	Olivine chromitite	◎			◎			◎	△								ol:sp=6:4
108	K95101802 CR	Ol poor Chromitite	△			◎			△									Crushed
109	K95092912 CR	Spinel rich dunite	◎			○			◎									Spinel rich layer
110	K95101005 CR	Olivine chromitite	○			◎			○		△							ol:sp=3:7~2:8
111	K95101603 CR	Olivine chromitite	○			◎			○	△	△							Orbicular texture, ol:sp=3:7~2:8
112	E95101502 CR	Olivine chromitite	○			◎			○	△	△							ol:sp=3:7
113	K95101701 CR	Olivine chromitite	○			◎			○	·	△							ol:sp=3:7
114	K95100904 CR	Olivine chromitite	△			◎			△									ol:sp=1:9
115	K95100305 CR	Olivine chromitite	△			◎			△	·						△		ol:sp=1:9
116	K95100504 HR	Dunite (?)	◎			△			◎				△			○		Chalcopyrite, pentlandite, pyrrhotite and antigorite
117	N95102701 HZ	Harzburgite	◎	○	△	△			○						·			Protogranular texture
118	N95102701 DU	Dunite	◎			△			○									Antigorite
119	N95102701 CRM	Olivine chromitite	△			◎			△		△		·					ol:sp=1:9~5:95
120	N95102702 HZ	Harzburgite	◎	○	△	△			○	·								OPX is relatively poor.
121	N95102702 DU	Dunite	◎		·	△			○									
122	N95102702 CR	Olivine chromitite	◎			◎			△									ol:sp=6:4

Legend; ◎, abundant; ○, common; △, minor; · rare

ol: olivine, opx: ortho pyroxene, cpx: clino pyroxene, sp: chromian spinel, par: pargasite, mi: mica,
ser: serpentine (chrysotile/lizardite), tc: talc, chl: chlorite, bru: brucite, mt: magnetite,
f.t.: ferrit chromite, tre: tremolite, di: diopside, ca: carbonate,

The chrome spinel is mostly accompanied by orthopyroxene and can be considered to be a subsolidus crystalline facies of orthopyroxene. Most of the crystals are euhedral to a comparatively high degree. The color under the microscope is dark reddish brown to opaque, which indicates that there is a fairly high degree of depletion of harzburgite containing chrome spinel.

It is a noteworthy fact that harzburgite containing mica, hornblende and other hydrous minerals are noted in the chrome spinel crystals, although only very rarely. Chrome spinel containing hydrous minerals is normally noted in chromitite, and it is necessary to give further study to the connection between hydrous minerals and chromitite as regards genesis.

Most of the harzburgite has a porphyroblastic structure, but some of the samples have a structure that is close to protogranular. In the samples with porphyroblastic structure there are comparatively fine-grained olivine, etc. produced by recrystallization around the somewhat deformed coarse-grained olivine and orthopyroxene. The samples with porphyroblastic structure have undergone hardly any deformation and are practically equigranular. The grain boundaries of the crystals are curved, and in particular the chrome spinel has a comparatively complicated holly-leaf like morphology.

In the way of secondary minerals, almost all of the samples contain large quantities of chrysotile, lizardite and other serpentine-group minerals, and some of them contain talc, chlorite, brucite, magnetite, tremolite, calcite, etc.

It might be added that besides the above minerals, occurrence of chalcopyrite, pentlandite, pyrrhotite and other sulfide minerals in small quantities was confirmed under a reflecting microscope in a sample of harzburgite taken from the northwestern part of the Shebenik massif (sample N95100504Hz).

-Dunite:

It consists mostly of olivine, with accompaniment of a small amount of chrome spinel. Sometimes it also includes extremely small quantities of clinopyroxene and orthopyroxene.

Just as in the harzburgite samples, in almost all of the samples the olivine is altered to chrysotile, lizardite and other serpentine-group minerals, and sometime it is accompanied by extremely small quantities of talc, chlorite, brucite, magnetite, tremolite, calcite, etc. But there are also frequently samples containing olivine that has not undergone alteration.

Again as in the case of the harzburgite samples, the chrome spinel looks dark reddish brown to opaque under the microscope. That indicates that its composition is high in Cr# and low in Al. The chrome spinel in the dunite is characterized by considerable variation in form (especially grain size) and mode.

-Chromitite:

It consists of olivine and chrome spinel. The relative quantities of olivine and chrome spinel are extremely variable, and many of the samples are comparatively rich in olivine and can therefore be called olivine chromitite.

As in the case of both the harzburgite and dunite samples, in many of the chromitite samples the olivine is altered to chrysotile, lizardite and other serpentine-group minerals. But in some of the samples the olivine retains a fresh matrix with accompaniment of mainly pyroxene and hornblende, and in others it coexists with chrome spinel. There is therefore the possibility that primary information on the period in which the chrome spinel was produced can be extracted from such samples.

The chrome spinel has many crystals that are euhedral to a high degree, and the grain size is quite variable, with large and small grains mixed together and frequent fragmentation. But it is noteworthy that much of the chrome spinel has not undergone alternation to ferrite-chromite, etc. and that uvarovite and other minerals that would indicate that has undergone alteration do not occur in it.

-Pyroxenite:

These samples consist mainly of clinopyroxene and orthopyroxene and have a coarse granular structure. The clinopyroxene and orthopyroxene make up about 80% of the rock. One of the samples has accompaniment of small quantities of olivine and hornblende, and the other of plagioclase and opaque mineral.

The sample with accompaniment of olivine and hornblende is comparatively fresh. But in the sample with accompaniment of plagioclase and opaque mineral, the plagioclase has undergone substantial saussuritization and changed to albite with accompaniment of small quantities of epidote and chlorite, with prehnite and plagioclase occurring as minute veins.

-Hornblende gabbro:

This rock consists mainly of green hornblende and anorthitic plagioclase. Besides occurrence of carbonate mineral as secondary mineral, prehnite and epidote occur as minute veins.

-Meta-amphibolite:

A sample consisting of hornblende, clinopyroxene, plagioclase and titanaugite and a sample consisting of hornblende and plagioclase were examined under the microscope. The first sample was taken from the Mirdita zone, and the second from the Shebenik massif.

Both have a holocrystalline equigranular structure, and the hornblende is green. The plagioclase has undergone substantial saussuritization and changed to albite with accompaniment of epidote and chlorite, with sericite produced as a secondary mineral. That indicates that there is not much difference in altered mineral composition of analogous rocks between the Mirdita zone and the Shebenik massif.

-Meta-basalt:

This sample consists of clinopyroxene, carbonate minerals, plagioclase, chlorite, epidote and opaque mineral. It is basalt that has a porphyritic structure and that has undergone considerable alteration, carbonate minerals making up about 30%. The plagioclase is rich in albite component. The clinopyroxene partly remains as relic, and secondarily produced diopside is to be noted.

It is considered to be a rock facies indicating the upper part of the ophiolite member.

-Sandstone:

The sample consists of crystal and lithic fragments and inter-crystalline material. The crystal fragments are of quartz (about 40%), plagioclase (about 5%), potassium feldspar (about 5%), muscovite (about 5%), opaque mineral and (about 10%). Lithic fragments are about 5%. Inter-crystalline material (about 30%) binds them. Both the lithic fragments and fragmental crystals are relatively well rounded.

Table 2-3-3 Results of chemical analysis on rocks

Hurzburgite

SAMPLE DESCRIPTION	Al2O3 %	CaO %	Cr2O3 %	Fe2O3 %	K2O %	MgO %	MnO %	Na2O %	P2O5 %	SiO2 %	TiO2 %	LOI %	TOTAL %	Bi ppm
K95101307-HZ	0.7	0.6	0.38	7.23	0.01	36.2	0.1	0.14	<0.01	38.8	<0.01	13.8	97.93	<0.1
E95100201-HZ	0.36	0.4	0.49	7.85	0.02	40.1	0.11	0.06	<0.01	42.1	<0.01	6.42	97.91	<0.1
K95093005-HZ	1.05	0.0	0.43	7.62	0.02	35.1	0.1	0.07	0.01	39.0	<0.01	14.6	98.00	<0.1
M95101703-HZ	0.35	0.2	0.34	7.47	0.02	37.0	0.1	0.06	<0.01	38.5	<0.01	13.8	97.79	<0.1
M95100810-HZ	0.35	0.2	0.28	7.62	0.02	36.2	0.09	0.06	<0.01	37.2	<0.01	15.6	97.61	<0.1
M95101605-HZ	0.33	0.3	0.37	7.64	0.02	39.2	0.1	0.06	<0.01	38.7	<0.01	11.3	97.93	0.1
E95101602-HZ	0.47	0.4	0.4	7.41	0.02	38.0	0.1	0.05	<0.01	39.5	<0.01	11.8	98.08	<0.1
M95101507-HZ	0.92	0.6	0.4	7.56	0.02	36.4	0.1	0.06	<0.01	39.0	0.01	12.9	97.90	0.1
K95100501-HZ	0.57	0.5	0.49	7.53	0.02	38.7	0.1	0.09	<0.01	40.0	<0.01	10.3	98.24	<0.1
K95101702-HZ	0.35	0.4	0.42	7.43	0.02	38.0	0.1	0.06	0.01	38.7	<0.01	12.7	98.13	<0.1
M95101802-HZ	0.44	0.3	0.49	7.14	0.02	36.7	0.1	0.06	<0.01	38.6	<0.01	13.9	97.72	0.1
K95101801-HZ	0.6	0.1	0.43	7.03	0.03	37.0	0.1	0.11	<0.01	39.2	<0.01	12.8	97.66	<0.1
M95102102-HZ	0.44	0.4	0.33	7.40	0.02	39.0	0.1	0.06	<0.01	38.9	<0.01	11	97.60	<0.1
K95092505-HZ	0.47	0.5	0.43	7.19	0.01	37.7	0.1	0.07	<0.01	37.9	<0.01	14.1	98.46	<0.1
E95102202-HZ	0.54	0.2	0.42	7.58	0.02	34.9	0.1	0.06	<0.01	38.2	<0.01	15.7	97.76	<0.1
M95101603-HZ	0.5	0.5	0.4	7.45	0.02	37.7	0.11	0.09	<0.01	38.8	<0.01	12.3	97.88	<0.1
E95102201-HZ	0.41	0.1	0.4	7.11	0.03	36.6	0.09	0.08	<0.01	38.2	<0.01	15.5	98.43	<0.1
M95101807-HZ	0.34	0.1	0.35	7.43	0.02	35.7	0.1	0.08	<0.01	38.5	<0.01	15.2	97.83	<0.1
M95102203-HZ	0.38	0.4	0.43	7.52	0.01	37.4	0.11	0.06	<0.01	40.4	<0.01	11.2	97.57	<0.1
K95102107-HZ	0.49	0.3	0.41	7.61	0.03	39.0	0.11	0.11	<0.01	39.2	<0.01	10.4	97.69	<0.1
Maximum	1.05	0.6	0.49	7.85	0.01	40.1	0.11	0.14	0.01	42.1	0.01	15.7	98.46	0.1
Average	0.50	0.33	0.40	7.44	0.02	37.3	0.10	0.07	0.00	38.97	0.00	12.75	97.91	0.02
Minimum	0.33	0.0	0.28	7.03	0.02	34.9	0.09	0.05	<0.01	37.2	<0.01	6.42	97.57	0
Standard dev.	0.14	0.1	0.04	0.16	0.01	1.2	0.00	0.02	0.00	0.66	0.00	1.75	0.1942	0.03

Dunite

SAMPLE DESCRIPTION	Al2O3 %	CaO %	Cr2O3 %	Fe2O3 %	K2O %	MgO %	MnO %	Na2O %	P2O5 %	SiO2 %	TiO2 %	LOI %	TOTAL %	Bi ppm
E95100107-DU	0.68	0.1	0.47	8.71	0.02	42.7	0.11	0.06	<0.01	43.2	<0.01	1.65	98.02	0.1
E95100201-DU	0.19	0.1	0.32	6.78	0.02	37.9	0.09	0.08	<0.01	36.7	<0.01	16.3	98.46	<0.1
M95101807-DU	0.17	0.0	0.2	7.54	0.02	35.6	0.09	0.08	<0.01	38.0	<0.01	16.2	97.93	<0.1
K95100501-DU	0.23	0.2	0.45	6.92	0.02	40.0	0.09	0.07	<0.01	34.9	<0.01	15	97.88	<0.1
M95102102-DU	0.21	0.1	0.58	6.16	0.02	35.3	0.08	0.06	0.01	40.0	<0.01	15.4	97.55	<0.1
E95101602-DU	0.25	0.1	0.5	7.40	0.02	40.0	0.09	0.06	<0.01	35.6	<0.01	14.4	98.47	<0.1
M95100810-DU	0.2	0.6	0.16	6.67	0.02	36.6	0.05	0.06	<0.01	37.5	<0.01	15.6	97.76	<0.1
K95101702-DU	0.17	0.1	0.36	6.18	0.02	39.5	0.08	0.06	<0.01	35.3	<0.01	16.3	98.01	<0.1
K95102107-DU	0.19	0.2	0.41	7.06	0.02	41.1	0.09	0.06	<0.01	31.6	<0.01	14.3	98.09	<0.1
E95102202-DU	0.23	0.1	0.51	6.44	0.03	35.6	0.08	0.08	<0.01	38.6	<0.01	16.1	97.74	<0.1
E95102201-DU	0.25	0.1	0.57	5.85	0.03	39.7	0.07	0.06	<0.01	34.4	<0.01	17.3	98.30	<0.1
K95092505-DU	0.34	0.2	0.43	6.36	0.03	37.3	0.09	0.07	<0.01	34.2	<0.01	18.7	97.66	<0.1
M95102203-DU	0.22	0.1	0.71	6.05	0.02	38.0	0.08	0.06	<0.01	35.6	<0.01	17.6	98.48	<0.1
K95101801-DU	1.07	0.1	5.57	6.88	0.02	39.4	0.07	0.07	0.01	33.2	0.01	14	100.35	0.1
M95101507-DU	0.24	0.1	0.42	7.44	0.02	40.7	0.09	0.06	<0.01	36.1	<0.01	12.7	97.93	<0.1
M95101802-DU	0.21	0.1	0.44	6.64	0.02	39.6	0.09	0.07	<0.01	34.6	<0.01	16.2	98.00	<0.1
M95101703-DU	0.21	0.1	0.42	7.01	0.01	38.8	0.09	0.06	<0.01	34.3	<0.01	17	97.97	<0.1
K95101307-DU	0.46	0.1	1.03	8.15	0.06	35.0	0.11	0.11	<0.01	38.3	0.01	15.1	98.11	<0.1
M95101605-DU	0.21	0.1	0.45	7.67	0.02	40.8	0.1	0.06	<0.01	36.5	<0.01	12.3	98.20	<0.1
M95101603-DU	0.23	0.1	0.41	7.33	0.02	39.4	0.09	0.07	<0.01	35.1	<0.01	11.8	97.62	<0.1
Maximum	1.07	0.6	5.57	8.71	0.06	42.7	0.11	0.11	0.01	43.2	0.01	18.7	100.35	0.1
Average	0.30	0.15	0.74	6.97	0.02	38.6	0.09	0.07	0.00	36.3	0.00	14.83	98.14	0.01
Minimum	0.17	0.0	0.2	5.85	0.01	35.0	0.05	0.06	<0.01	33.2	<0.01	1.65	97.55	0
Standard dev.	0.13	0.1	0.51	0.57	0.01	1.8	0.01	0.01	0.00	1.81	0.00	1.97	0.3689	0.02

Table 2-3-4 Results of chemical analysis on chromitites

Chromitite

SAMPLE DESCRIPTION	Ag ppm	Ba ppm	Be ppm	Bi ppm	Cd ppm	Co ppm	Cu ppm	Mn ppm	Mo ppm	Ni ppm	Sr ppm	V ppm	Zn ppm	Al %	Ca %	Fe %	K %	Mg %	Na %	Ti %	Pb %	Cr2O3 %
K95101307-CR	<1.0	<100	<10	<20	<10	10	10	160	<10	1550	<10	10	20	0.2	0.05	1.3	<.1	8.2	<.05	<.05	<.001	38.60
E95102202-CR	<1.0	<100	<10	<20	<10	10	<10	230	<10	460	<10	20	20	0.5	0.05	1.45	<.1	4.4	<.05	<.05	<.001	52.00
E95102701-CR	<1.0	<100	<10	<20	<10	80	<10	500	<10	2430	<10	30	20	0.15	0.05	3.4	<.1	14.9	<.05	<.05	<.001	17.80
K95101301-CR	<1.0	<100	<10	<20	<10	10	<10	160	<10	360	<10	60	20	0.6	0.05	1.3	<.1	2.45	<.05	<.05	<.001	41.90
E95102201-CR	<1.0	<100	<10	<20	<10	10	<10	230	<10	370	<10	20	<20	0.1	0.05	1.15	<.1	3.4	<.05	<.05	<.001	55.00
K95092505-CR	<1.0	<100	<10	<20	<10	10	<10	180	<10	1040	<10	20	<20	0.1	<.05	1.5	<.1	6.85	<.05	<.05	<.001	43.30
K95102108-CR	<1.0	<100	<10	<20	<10	10	<10	180	<10	1050	<10	10	<20	0.05	<.05	1.4	<.1	7.7	<.05	<.05	<.001	41.50
M95102203-CR	1	<100	<10	<20	<10	<10	10	220	<10	190	20	10	20	0.2	1.1	1.8	<.1	3.3	<.05	<.05	<.001	53.50
K95102206-CR	<1.0	<100	<10	<20	<10	<10	<10	140	<10	360	<10	10	<20	0.1	<.05	0.8	<.1	2.25	<.05	<.05	<.001	53.20
E95110101-CR	<1.0	<100	<10	<20	<10	20	10	240	<10	1900	10	20	<20	0.05	1.75	1.55	<.1	11.1	<.05	<.05	<.001	14.80
K95102107-CR	1	<100	<10	<20	<10	30	<10	290	<10	1570	<10	20	20	0.15	0.05	1.3	<.1	10.3	<.05	<.05	<.001	35.90
K95102104-CR	<1.0	<100	<10	<20	<10	80	<10	560	<10	2640	<10	30	20	0.1	0.05	3.65	<.1	16.2	<.05	<.05	<.001	14.80
K95102102-CR	<1.0	<100	<10	<20	<10	40	<10	370	<10	1820	<10	30	20	0.15	0.05	2.25	<.1	11.6	<.05	<.05	<.001	32.70
K95101801-CR	1	<100	<10	<20	<10	40	<10	340	<10	1840	<10	20	40	0.05	<.05	2.45	<.1	13.4	<.05	<.05	<.001	26.90
M95101802-CR	<1.0	<100	<10	<20	<10	30	<10	300	<10	1140	<10	30	<20	0.15	0.05	1.85	<.1	7.8	<.05	<.05	<.001	41.50
M95101703-CR	<1.0	<100	<10	<20	<10	10	<10	230	<10	900	<10	20	<20	0.35	0.15	1.5	<.1	7.3	<.05	<.05	<.001	43.30
M95101701-CR	<1.0	<100	<10	<20	<10	10	<10	180	<10	1160	<10	20	<20	0.1	<.05	1.25	<.1	7.85	<.05	<.05	<.001	41.50
K95092904-CR	<1.0	<100	<10	<20	<10	20	<10	300	<10	1430	10	20	<20	0.1	1.1	2.45	<.1	8.9	<.05	<.05	<.001	37.40
K95092914-CR	<1.0	<100	<10	<20	<10	20	<10	200	<10	1260	<10	20	<20	0.2	0.5	1.15	<.1	7.3	<.05	<.05	<.001	42.70
M95100810-CR	<1.0	<100	<10	<20	<10	20	<10	200	<10	1750	<10	30	<20	0.15	0.6	2.05	<.1	8.75	<.05	<.05	<.001	39.60
M95101605-CR	1	<100	<10	<20	<10	10	<10	200	<10	1120	<10	10	<20	0.1	<.05	1.45	<.1	6.65	<.05	<.05	<.001	41.40
M95101509-CR	<1.0	<100	<10	<20	<10	20	<10	240	<10	750	<10	10	<20	0.05	0.15	1.3	<.1	4.9	<.05	<.05	<.001	53.20
M95101507-CR	<1.0	<100	<10	<20	<10	20	<10	230	<10	800	<10	30	<20	0.45	0.1	1.3	<.1	5	<.05	<.05	<.001	45.60
K95101705-CR	<1.0	<100	<10	<20	<10	20	<10	310	<10	1210	<10	20	20	0.15	<.05	1.65	<.1	7.4	<.05	<.05	<.001	40.20
K95101702-CR	<1.0	<100	<10	<20	<10	10	<10	160	<10	700	<10	20	<20	0.2	<.05	1.05	<.1	4.95	<.05	<.05	<.001	50.30
E95101601-CR	<1.0	<100	<10	<20	<10	20	80	300	<10	490	<10	110	20	0.65	0.05	1.6	<.1	3.3	<.05	<.05	<.001	46.70
E95101602-CR	1	<100	<10	<20	<10	20	<10	180	<10	850	<10	20	<20	0.2	<.05	1.1	<.1	5.3	<.05	<.05	<.001	45.00
K95100501-CR	<1.0	<100	<10	<20	<10	10	<10	130	<10	410	<10	20	<20	0.1	<.05	1.05	<.1	7.75	<.05	<.05	<.001	10.60
E95100501-CR	<1.0	<100	<10	<20	<10	170	<10	910	<10	1660	<10	60	40	0.1	0.05	5.9	<.1	17.6	<.05	<.05	<.001	9.94
M95100306-CR	<1.0	<100	<10	<20	<10	10	<10	210	<10	980	<10	10	<20	0.2	0.05	1.3	<.1	4.8	<.05	<.05	<.001	46.80
E95100201-CR	<1.0	<100	<10	<20	<10	40	<10	300	<10	1380	<10	20	<20	0.05	<.05	1.9	<.1	12	<.05	<.05	<.001	32.70
K95093005-CR	<1.0	<100	<10	<20	<10	40	20	310	<10	1230	<10	70	20	2.1	0.4	2.05	<.1	8.75	<.05	<.05	<.001	24.00
N95100602-CR	<1.0	<100	<10	<20	<10	40	<10	310	<10	1140	<10	70	20	1	0.15	1.65	<.1	8.35	<.05	<.05	<.001	26.90
E95100107-DU	<1.0	<100	<10	<20	<10	130	<10	950	<10	2520	<10	50	20	0.3	0.45	5.9	<.1	25.2	0.1	<.05	<.001	0.58
K95101305-CR	<1.0	<100	<10	<20	<10	10	<10	230	<10	300	<10	10	<20	0.1	4.2	0.95	<.1	1.65	<.05	<.05	<.001	46.10
K95102707-CR	<1.0	<100	<10	<20	<10	20	<10	200	<10	660	<10	20	<20	0.1	0.05	1.9	<.1	3.75	<.05	<.05	<.001	51.90
K95102203-CR	<1.0	<100	<10	20	<10	20	<10	200	<10	1710	<10	20	<20	0.15	0.05	1.8	<.1	11.2	0.05	<.05	<.001	31.80
K95102106-CR	1	<100	<10	<20	<10	10	<10	160	<10	980	<10	10	<20	0.05	<.05	1.15	<.1	5.6	<.05	<.05	<.001	46.80
M95102102-CR	1	<100	<10	<20	<10	80	<10	440	<10	3710	<10	20	<20	0.05	<.05	3.1	<.1	15.2	<.05	<.05	<.001	12.40
M95101807-CR	1	<100	<10	<20	<10	40	<10	300	<10	1490	<10	20	<20	0.05	<.05	2.2	<.1	10.6	<.05	<.05	<.001	32.20
E95101803-CR	<1.0	<100	<10	20	<10	20	<10	200	<10	1430	<10	10	<20	0.05	0.3	1.25	<.1	10.1	<.05	<.05	<.001	33.20
K95101802-CR	<1.0	<100	<10	<20	<10	10	<10	200	<10	410	<10	10	<20	0.3	0.05	2.25	<.1	2.7	<.05	<.05	<.001	59.10
K95092917-CR	<1.0	<100	<10	20	<10	30	<10	330	<10	1250	<10	20	<20	0.1	0.05	1.8	<.1	9.65	<.05	<.05	<.001	38.00
K95101005-CR	<1.0	<100	<10	<20	<10	10	<10	160	<10	730	<10	<10	<20	0.05	<.05	1	<.1	4.6	<.05	<.05	0.00	52.50
K95101003-CR	<1.0	<100	<10	<20	<10	<10	<10	110	<10	600	<10	<10	<20	0.1	<.05	0.65	<.1	2.65	<.05	<.05	<.001	55.90
E95101502-CR	<1.0	<100	<10	20	<10	30	<10	310	<10	2880	<10	20	<20	0.15	<.05	1.65	<.1	8	<.05	<.05	<.001	40.90
K95101701-CR	<1.0	<100	<10	40	<10	60	<10	430	<10	2350	<10	30	20	0.3	0.05	2.3	<.1	12	<.05	<.05	<.001	29.20
K95100904-CR	<1.0	<100	<10	20	<10	20	<10	210	<10	500	<10	30	20	0.3	0.05	1.4	<.1	3.95	<.05	<.05	<.001	50.10
K95100305-CR	<1.0	<100	<10	40	<10	30	20	350	<10	750	<10	20	20	0.45	0.05	1.9	<.1	6.45	<.05	<.05	<.001	35.80
Maximum	1	<100	<10	40	<10	130	80	950	<10	3710	20	110	40	2.1	4.2	5.9	<.1	25.2	0.1	<.05	0.00	59.10
Average	-	-	-	-	-	28	-	284	-	1235	-	26	-	0.23	-	1.84	-	7.93	-	-	-	38.07
Minimum	<1.0	<100	<10	<20	<10	<10	<10	110	<10	300	<10	<10	<20	0.05	<.05	0.65	<.1	1.65	<.05	<.05	<.001	0.58
Standard dev.						19		104		569	-	14	-	0.18		0.66	-	3.47	-		-	10.79

Other Rocks

SAMPLE DESCRIPTION	Ag ppm	Ba ppm	Be ppm	Bi ppm	Cd ppm	Co ppm	Cu ppm	Mn ppm	Mo ppm	Ni ppm	Sr ppm	V ppm	Zn ppm	Al %	Ca %	Fe %	K %	Mg %	Na %	Ti %	Pb %	Cr2O3 %
N95100504-HZ	<1.0	<100	<10	<20	<10	110	100	650	<10	2050	40	40	20	0.2	5.5	5.4	<.1	16.8	<.05	<.05	<.001	0.96
E95100601-SCH	<1.0	<100	<10	<20	<10	50	60	1660	<10	90	70	380	80	6.75	6.15	8.45	0.2	1.75	2.85	0.9	<.001	0.07
M95100205-PX	<1.0	<100	<10	<20	<10	70	<10	1320	<10	380	<10	130	20	0.65	7.1	4.7	<.1	14.5	0.65	<.05	<.001	0.41
E95100402-HZ	<1.0	<100	<10	20	<10	120	<10	880	<10	2350	<10	50	20	0.25	0.45	5.45	<.1	23.3	<.05	<.05	<.001	0.38
E95100401-PX	<1.0	<100	<10	<20	<10	60	100	1020	<10	350	110	190	40	6.65	9.8	5.4	<.1	8.35	0.75	0.25	<.001	0.16
E95100405-AM	<1.0	<100	<10	<20	<10	60	60	1170	<10	220	120	250	40	7.8	8	6.65	0.4	6	1.9	0.55	<.001	0.09
E95100401-DU	<1.0	<100	<10	20	<10	120	<10	710	<10	2540	<10	30	20	0.05	0.15	4.65	<.1	23.3	<.05	<.05	<.001	1.08
N95100503-GB	<1.0	<100	<10	<20	<10	50	<10	1050	<10	230	90	240	40	5.15	10.3	5.35	0.1	6.75	0.9	<.05	<.001	0.13
N95101703-BT	<1.0	<100	<10	<20	<10	60	80	890	<10	340	190	180	40	6.85	11.1	5.55	0.1	2.65	3.1	0.45	<.001	0.09
K95102302-BT	<1.0	100	<10	<20	<10	20	10	310	20	80	40	50	40	4.8	0.35	2.85	1.2	1.15	1.4	0.2	0.00	0.01
K95102202-GB	<1.0	200	<10	<20	<10	30	10	900	<10	70	340	140	40	9.6	7.55	4.8	1	2.3	2.75	0.55	<.001	0.03

Table 2-3-5(1) Mole fraction of Cr, Al and Fe in harzburgites and dunites

Harzburgite

Sample Number	Fe %	Cr %	Al %	Mg %	Cr/Fe wt ratio	Cr/Mg wt ratio	Cr/Al wt ratio	Cr/Fe mol ratio	Cr/Mg mol ratio	Cr/Al mol ratio	mol % Cr	mol % Al	mol % Fe
K95101307-Hz	5.06	0.26	0.37	21.83	0.05	0.01	0.70	0.055	0.006	0.364	4.58	12.56	82.86
E95102202-Hz	5.30	0.29	0.29	21.05	0.05	0.01	1.01	0.058	0.006	0.522	4.98	9.54	85.49
E95102201-Hz	4.97	0.27	0.22	22.07	0.06	0.01	1.26	0.059	0.006	0.654	5.14	7.86	87.00
K95092505-Hz	5.03	0.29	0.25	22.70	0.06	0.01	1.18	0.063	0.006	0.614	5.39	8.79	85.82
K95102203-Hz	5.26	0.29	0.20	22.37	0.06	0.01	1.46	0.060	0.006	0.759	5.27	6.95	87.78
K95102107-Hz	5.34	0.28	0.26	23.52	0.05	0.01	1.08	0.056	0.006	0.561	4.87	8.68	86.44
K95101801-Hz	4.92	0.29	0.32	22.31	0.06	0.01	0.93	0.064	0.006	0.481	5.36	11.16	83.48
M95101802-Hz	4.99	0.34	0.23	22.13	0.07	0.02	1.44	0.072	0.007	0.747	6.17	8.26	85.57
M95101703-Hz	5.22	0.23	0.19	22.31	0.04	0.01	1.26	0.048	0.005	0.652	4.27	6.55	89.19
M95100810-Hz	5.33	0.19	0.19	21.83	0.04	0.01	1.03	0.039	0.004	0.537	3.48	6.48	90.05
M95101605-Hz	5.34	0.25	0.17	23.64	0.05	0.01	1.45	0.051	0.005	0.752	4.55	6.05	89.40
M95101507-Hz	5.29	0.27	0.49	21.95	0.05	0.01	0.56	0.056	0.006	0.292	4.46	15.29	80.24
K95101702-Hz	5.20	0.29	0.19	23.40	0.06	0.01	1.55	0.059	0.006	0.805	5.24	6.51	88.25
E95101602-Hz	5.18	0.27	0.25	22.92	0.05	0.01	1.10	0.057	0.006	0.571	4.91	8.59	86.50
K95100501-Hz	5.27	0.34	0.30	23.34	0.06	0.01	1.11	0.068	0.007	0.577	5.76	9.99	84.25
E95100201-Hz	5.49	0.34	0.19	24.18	0.06	0.01	1.76	0.066	0.006	0.913	5.77	6.31	87.92
K95100407-Hz	5.33	0.29	0.56	21.17	0.06	0.01	0.53	0.059	0.006	0.275	4.65	16.93	78.42
M95102102-Hz	5.18	0.23	0.23	23.52	0.04	0.01	0.97	0.047	0.004	0.503	4.11	8.17	87.72
MP5101807-Hz	5.20	0.24	0.18	21.53	0.05	0.01	1.33	0.049	0.005	0.691	4.41	6.39	89.19
M95101603-Hz	5.21	0.27	0.26	22.73	0.05	0.01	1.03	0.056	0.006	0.537	4.86	9.05	86.09
Maximun	5.49	0.34	0.56	24.18	0.10	0.01	0.02	0.072	0.007	0.913	6.17	16.93	90.05
Average	5.21	0.28	0.27	22.52	0.09	0.01	0.01	0.057	0.006	0.590	4.91	9.01	86.08
Minimum	4.92	0.19	0.17	21.05	0.09	0.00	0.01	0.039	0.004	0.275	3.48	6.05	78.42
Standard Dev.	0.15	0.04	0.10	0.87	0.00	0.00	0.00	0.008	0.001	0.165	0.63	2.99	3.03

Dunite

Sample Number	Fe %	Cr %	Al %	Mg %	Cr/Fe wt ratio	Cr/Mg wt ratio	Cr/Al wt ratio	Cr/Fe mol ratio	Cr/Mg mol ratio	Cr/Al mol ratio	mol % Cr	mol % Al	mol % Fe
K95101307-Du	5.70	0.70	0.24	21.11	0.10	0.01	0.01	0.133	0.016	1.502	10.87	7.24	81.89
E95102202-Du	4.50	0.35	0.12	21.47	0.08	0.01	0.00	0.083	0.008	1.488	7.30	4.91	87.79
E95102201-Du	4.09	0.39	0.13	23.91	0.07	0.01	0.00	0.102	0.008	1.530	8.76	5.72	85.52
K95092505-Du	4.45	0.29	0.16	22.49	0.08	0.01	0.01	0.071	0.006	0.931	6.19	6.65	87.16
K95102203-Du	4.23	0.49	0.12	22.92	0.08	0.01	0.00	0.123	0.010	2.165	10.45	4.83	84.73
K95102107-Du	4.94	0.28	0.10	24.78	0.09	0.01	0.00	0.061	0.005	1.448	5.53	3.82	90.65
K95101801-Du	4.81	3.81	0.57	23.76	0.09	0.07	0.02	0.851	0.075	3.492	40.62	11.63	47.75
M95101802-Du	4.64	0.30	0.11	23.88	0.08	0.01	0.00	0.070	0.006	1.406	6.22	4.43	89.35
M95101703-Du	4.92	0.29	0.11	23.40	0.09	0.01	0.00	0.063	0.006	1.342	5.65	4.21	90.14
M95100810-Du	4.67	0.31	0.11	22.07	0.08	0.01	0.00	0.072	0.007	1.543	6.47	4.20	89.33
M95101605-Du	5.36	0.31	0.11	24.60	0.10	0.01	0.00	0.062	0.006	1.438	5.58	3.88	90.54
M95101507-Du	5.20	0.29	0.13	24.54	0.09	0.01	0.00	0.059	0.005	1.174	5.34	4.55	90.10
K95101702-Du	4.32	0.25	0.09	23.82	0.08	0.00	0.00	0.061	0.005	1.421	5.54	3.90	90.56
E95101602-Du	5.18	0.34	0.13	24.12	0.09	0.01	0.00	0.071	0.007	1.342	6.32	4.71	88.98
K95100501-Du	4.84	0.31	0.12	24.12	0.09	0.01	0.00	0.068	0.006	1.313	6.10	4.65	89.26
E95100201-Du	4.74	0.22	0.10	22.86	0.08	0.00	0.00	0.050	0.004	1.130	4.53	4.01	91.45
K95100407-Du	6.11	0.32	0.36	25.72	0.11	0.01	0.01	0.057	0.006	0.464	4.79	10.34	84.86
M95102102-Du	4.31	0.40	0.11	21.29	0.08	0.01	0.00	0.099	0.009	1.853	8.59	4.63	86.78
MP5101807-Du	5.27	0.14	0.09	21.47	0.09	0.00	0.00	0.028	0.003	0.789	2.62	3.32	94.06
M95101603-Du	5.13	0.30	0.12	23.76	0.09	0.01	0.00	0.063	0.006	1.283	5.67	4.42	89.91
Maximun	6.11	3.81	0.57	25.72	0.11	0.07	0.02	0.851	0.075	3.492	40.62	11.63	94.06
Average	4.87	0.50	0.16	23.30	0.09	0.01	0.01	0.112	0.010	1.452	8.16	5.30	86.54
Minimum	4.09	0.14	0.09	21.11	0.07	0.00	0.00	0.028	0.003	0.464	2.62	3.32	47.75
Standard Dev.	0.51	0.79	0.11	1.30	0.01	0.02	0.00	0.175	0.015	0.598	7.89	2.17	9.54

Table 2-3-5(2) Mole fraction of Cr, Al and Fe in chromitites

Sample Number	Al wt%	Fe* wt%	Cr wt%	Mg wt%	Cr/Fe wt ratio	Cr/Mg wt ratio	Cr/Al wt ratio	Al mol%	Fe* mol%	Cr mol%	Mg mol%	Mol Ratio Al	Mol Ratio Fe*	Mol Ratio Cr
K95101307-CR	0.20	1.30	26.41	8.20	20.32	3.22	3.22	0.007	0.023	0.508	0.053	1.376	4.322	94.302
K65102202-CR	0.50	1.45	35.58	4.40	24.54	8.09	8.09	0.019	0.026	0.684	0.060	2.543	3.563	93.894
K65102201-CR	0.15	3.40	12.18	14.90	3.58	0.82	0.82	0.006	0.061	0.234	0.140	1.849	20.249	77.902
K95101301-CR	0.60	1.30	30.72	2.45	23.63	12.54	12.54	0.022	0.023	0.591	0.053	3.495	3.658	92.847
E95102201-CR	0.10	1.15	37.63	3.40	32.72	11.07	11.07	0.004	0.021	0.724	0.047	0.495	2.753	96.752
K95092505-CR	0.10	1.50	29.63	6.85	19.75	4.32	4.32	0.004	0.027	0.570	0.062	0.617	4.474	94.909
K95102108-CR	0.05	1.40	28.39	7.70	20.28	3.69	3.69	0.002	0.025	0.546	0.058	0.323	4.375	95.302
M95102203-CR	0.20	1.80	36.81	3.30	20.45	11.15	11.15	0.007	0.032	0.708	0.074	0.992	4.311	94.697
K95102206-CR	0.10	0.80	36.40	2.25	45.50	16.18	16.18	0.004	0.014	0.700	0.033	0.516	1.995	97.489
E95110101-CR	0.05	1.55	18.41	11.05	11.87	1.67	1.67	0.002	0.028	0.354	0.064	0.483	7.236	92.281
K95102107-CR	0.15	1.30	24.56	10.25	18.89	2.40	2.40	0.006	0.023	0.472	0.053	1.109	4.644	94.247
K95102104-CR	0.10	3.65	10.13	16.20	2.77	0.63	0.63	0.004	0.065	0.195	0.150	1.405	24.774	73.821
K95102102-CR	0.15	2.25	22.37	11.55	9.94	1.94	1.94	0.006	0.040	0.430	0.093	1.168	8.462	90.371
K95101801-CR	0.05	2.45	18.41	13.35	7.51	1.38	1.38	0.002	0.044	0.354	0.101	0.464	10.976	88.560
M95101802-CR	0.15	1.85	28.39	7.80	15.35	3.64	3.64	0.006	0.033	0.546	0.076	0.951	5.665	93.385
M95101703-CR	0.35	1.50	29.63	7.30	19.75	4.06	4.06	0.013	0.027	0.570	0.062	2.128	4.406	93.466
M95101704-CR	0.10	1.25	28.39	7.85	22.72	3.62	3.62	0.004	0.022	0.546	0.051	0.648	3.912	95.440
K95092904-CR	0.10	2.45	25.59	8.90	10.44	2.88	2.88	0.004	0.044	0.492	0.101	0.687	8.128	91.185
K95092911-CR	0.20	1.15	29.22	7.30	25.40	4.00	4.00	0.007	0.021	0.562	0.047	1.257	3.491	95.253
M95100810-CR	0.15	2.05	26.41	8.75	12.88	3.02	3.02	0.006	0.037	0.508	0.084	1.010	6.672	92.318
M95101605-CR	0.10	1.45	30.38	6.65	20.95	4.57	4.57	0.004	0.026	0.584	0.060	0.604	4.229	95.167
M95101509-CR	0.05	1.30	36.40	4.90	28.00	7.43	7.43	0.002	0.023	0.700	0.053	0.256	3.210	96.534
M95101507-CR	0.45	1.30	31.20	5.00	24.00	6.24	6.24	0.017	0.023	0.600	0.053	2.606	3.637	93.757
K95101705-CR	0.15	1.65	27.50	7.40	16.67	3.72	3.72	0.006	0.030	0.529	0.068	0.986	5.238	93.777
K95101702-CR	0.20	1.05	34.42	4.95	32.78	6.95	6.95	0.007	0.019	0.662	0.043	1.077	2.732	96.190
E95101601-CR	0.65	1.60	31.61	3.30	19.76	9.58	9.58	0.024	0.029	0.608	0.066	3.646	4.336	92.017
E95101602-CR	0.20	1.10	30.79	5.30	27.99	5.81	5.81	0.007	0.020	0.592	0.045	1.197	3.181	95.622
K95100501-CR	0.10	1.05	7.25	2.75	6.91	2.64	2.64	0.004	0.019	0.139	0.043	2.288	11.606	86.106
E95100501-CR	0.10	5.90	6.80	17.55	1.15	0.39	0.39	0.004	0.106	0.131	0.243	1.543	43.992	54.465
M95100306-CR	0.20	1.30	32.02	4.80	24.63	6.67	6.67	0.007	0.023	0.616	0.053	1.147	3.600	95.253
E95100201-CR	0.05	1.90	22.03	11.95	11.60	1.84	1.84	0.002	0.034	0.424	0.078	0.403	7.403	92.194
K95093005-CR	2.10	2.05	16.42	8.75	8.01	1.88	1.88	0.078	0.037	0.316	0.084	18.086	8.530	73.385
N95100602-CR	1.00	1.85	18.41	8.35	9.95	2.20	2.20	0.037	0.033	0.354	0.076	8.738	7.810	83.452
E95100407-CR	0.30	5.90	0.40	25.20	0.07	0.02	0.02	0.011	0.106	0.008	0.243	8.938	84.927	6.135
K95101305-CR	0.10	0.95	31.54	1.65	33.20	19.12	19.12	0.004	0.017	0.607	0.039	0.591	2.712	96.698
K95102207-CR	0.10	1.90	37.56	3.75	19.77	10.02	10.02	0.004	0.034	0.722	0.078	0.488	4.476	95.037
K95102203-CR	0.15	1.80	21.76	11.2	12.09	1.95	1.95	0.006	0.032	0.418	0.074	1.219	7.065	91.717
K95102106-CR	0.05	1.15	32.02	5.60	27.84	5.72	5.72	0.002	0.021	0.616	0.047	0.290	3.226	96.483
M95102102-CR	0.05	3.10	8.42	15.20	2.71	0.55	0.55	0.002	0.056	0.162	0.128	0.845	25.322	73.833
M95101807-CR	0.05	2.20	22.03	10.60	10.01	2.08	2.08	0.002	0.039	0.424	0.091	0.399	8.472	91.129
E95101803-CR	0.05	1.25	22.72	10.05	18.17	2.26	2.26	0.002	0.022	0.437	0.051	0.402	4.854	94.744
K95101802-CR	0.30	2.25	40.64	2.70	18.06	15.05	15.05	0.011	0.040	0.782	0.093	1.335	4.836	93.829
K95929012-CR	0.10	1.80	26.00	9.65	14.44	2.69	2.69	0.004	0.032	0.500	0.074	0.692	6.014	93.295
K95101005-CR	0.05	1.00	35.92	4.60	35.92	7.81	7.81	0.002	0.018	0.691	0.041	0.261	2.520	97.219
K95101603-CR	0.10	0.65	38.25	2.65	58.84	14.43	14.43	0.004	0.012	0.736	0.027	0.494	1.550	97.956
E95101502-CR	0.15	1.65	27.98	8.00	16.96	3.50	3.50	0.006	0.030	0.538	0.068	0.970	5.154	93.877
K95101701-CR	0.30	2.30	19.98	12.00	8.69	1.66	1.66	0.011	0.041	0.384	0.095	2.547	9.434	88.019
K95100904-CR	0.30	1.40	34.28	3.95	24.48	8.68	8.68	0.011	0.025	0.659	0.058	1.599	3.605	94.796
K95100305-CR	0.45	1.90	24.49	6.45	12.89	3.80	3.80	0.017	0.034	0.471	0.078	3.196	6.520	90.283
Maximum	2.10	5.90	40.64	25.20	58.84	19.12	19.12	0.078	0.106	0.782	0.243	18.086	84.927	97.956
Average	0.23	1.84	26.21	7.93	18.67	5.30	5.30	0.009	0.033	0.504	0.076	1.844	8.740	89.416
Minimum	0.05	0.65	0.40	1.65	0.07	0.02	0.02	0.002	0.012	0.008	0.027	0.256	1.550	6.135
tandard Deviatio	0.33	1.05	9.23	4.65	11.31	4.51	4.51	0.012	0.019	0.177	0.043	2.943	13.310	14.534

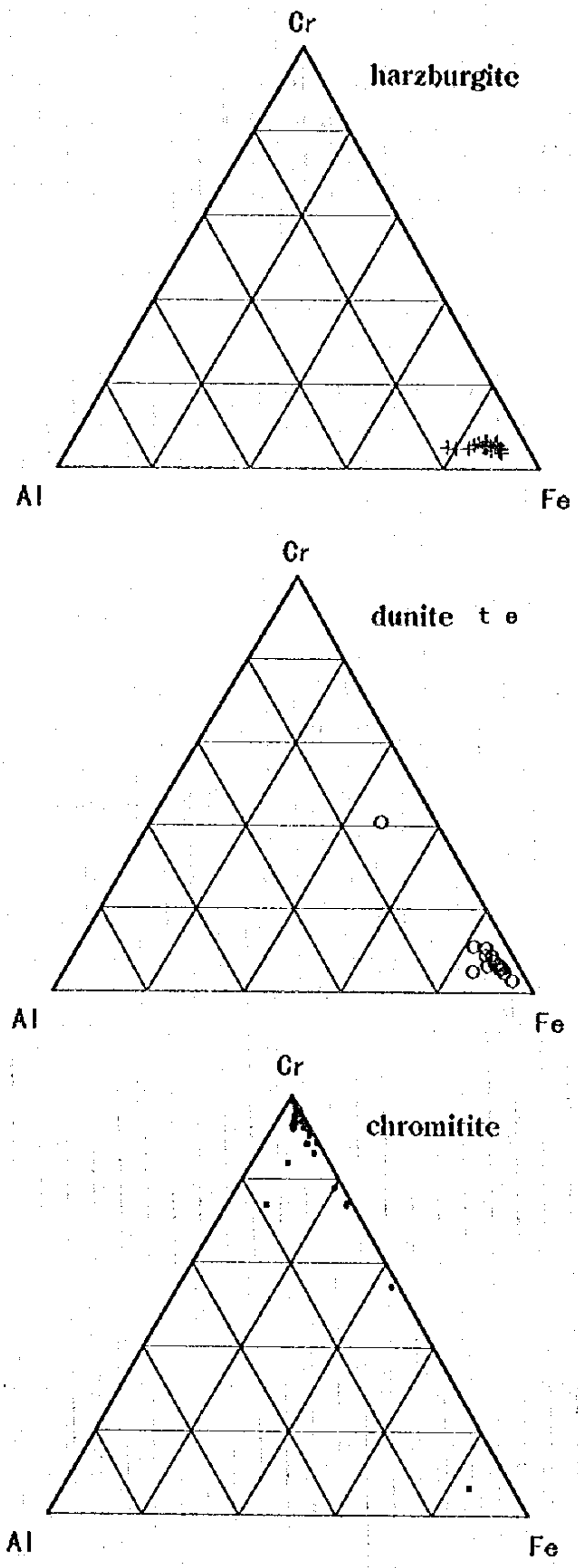

Fig. 2-3-3 Cr-Al-Fe proportion of harzburgite, dunite and chromitite

(2) Chemical Analysis of Rock and Ore Samples

A total 100 samples were used for chemical analysis: 20 samples of harzburgite, 20 samples of dunite, 49 samples of chromitite and 11 samples of other rocks. Table 2-3-3 gives the results of the rock samples, and Table 2-3-4 the results of the chromitite samples. Fig. 2-3-1 is a Cr-Al-Fe diagram compiled on the basis of those results.

As can be seen from those tables and that figure, although the chemical compositions of harzburgite and dunite are somewhat similar, harzburgite, dunite and chromitite all have different characteristics as regards chemical composition.

Regarding composition with respect to main components, both harzburgite and dunite have high ignition loss values of 10-18%, which corroborates the fact that they are samples that underwent serpentinization as a whole. However, there were also some fresh samples with low values of 1.6-6.42%. As a trend the harzburgite has somewhat higher Al_2O_3, Fe_2O_3, SiO_2 and CaO contents and somewhat lower Cr_2O_3 and MgO contents than the dunite. The average Cr_2O_3 contents of the harzburgite and the dunite are 0.4% and 0.78%, respectively, and both have low K_2O, Na_2O, MnO, P_2O_5 and TiO_2 contents.

On the other hand, the chromitite samples have a high average Cr_2O_3 content of 40%, and their Al and Fe contents are far lower than those of the harzburgite and the dunite.

The rather similar compositions of the harzburgite and the dunite and the fact that the chromitite is very rich in Cr can be clearly seen from the Cr-Al-Fe diagram of Fig. 2-3-3. It might be noted that of the chromitite samples, the two with a high percentage of Al were taken in the northwestern part of the Shebenik massif and that those with a high percentage of Fe were taken at Cervenake, Kotodesh and elsewhere upstream of the Gobilla Marsh.

The base metal contents of the rocks constituting the Shebenik-Pogradec ultrabasic massif are, for harzburgite and dunite, 0.2-0.25% Ni, 0.01-0.02% Co, both comparatively high, and 0.06-0.10% Mn, which is not so high, and, for the chromitite, 0.05-0.37% Ni, comparatively high, and low values in the order of 0.0n% for Mn. In all of the rocks the values of the Ag, Ba, Be, Bi, Cd, Co, Cu, Pb, Zn, Mo, Sr, V, K and Na contents were generally extremely low, near the limit of detection.

Table 2-3-5(1)-(2) gives the Cr/Fe, Cr/Mg and Cr/Al weight and mole ratios, of the chromitite, dunite and harzburgite. Those values are high for the chromitite, but they are nearly as low as for the dunite in the disseminated chromitite that could very well be called olivine chromitite.

Table 2−3−6 Statistics of Platinum Group Elements in the West and East Zones

	Pt	Pd	Os	Ir	Ru	Rh	Au	Re
Shebenik-Pogradec Massif (6 Samples)								
Maximum (ppb)	<5	<2	54	57	93	13	11	<5
Average (ppb)	<5	<2	29	35	75	11	5	<5
Minimum (ppb)	<5	<2	17	25	57	8	2	<5
Standard Deviation (ppb)	-	-	11	8	12	2	3	-
Bulqiza Massif (2 Samples)								
Maximum (ppb)	23	20	110	91	130	10	12	<5
Average (ppb)	-	-	62	54	91	9	7	<5
Minimum (ppb)	<5	<2	14	17	58	8	2	<5
Standard Deviation (ppb)	-	-	48	37	36	1	5	-
West of Korce (11 Samples)								
Maximum (ppb)	3080	4340	170	300	350	240	160	<5
Average (ppb)	555	733	60	70	120	48	70	<5
Minimum (ppb)	10	12	2	2	7	2	4	<5
Standard Deviation (ppb)	500	764	45	45	92	42	37	-

Besides above 19 chromitite samples from different locations were attempted to analyze for platinum group elements. The samples are of six samples from the Shebenik-Pogradec ultrabasic massif, two samples from Bulqiza mine and eleven samples from western zone near Korce. Table 2-3-6 indicates their statistics values such as maximum, average, minimum and standard deviation. The chromitite samples from the western zone are highly concentrated in the platinum group elements compared with those of the eastern zone and show about 100 times in Pt and Pd, 1-1.5 times in Os, 1.5-2 time in Ir, 5 times in Rh and 10 times in Au, but Re is very low in both zones.

(3) EPMA Tests

(3)-1 Purpose of the EPMA Tests

It is expected that data that is determined concerning the chemical composition of the chrome spinel of the dunite, harzburgite and chromitite will serve as useful information in exploration of large-scale chromitite deposits. Regarding the so-called podiform type of chromitite, which occurs in the orogenic zone, there is a most recent model according to which the chromitite is produced by mixture of the secondary melt that resulted from interaction between magma and wall rock with the primitive melt (e.g. Arai, 1992; Arai and Yurimoto, 1994; 1995; Matsumoto et al., 1995; Matsumoto, 1996). That model is, basically, a model that shows that Irvine's model (1975), which proved that the origin of stratiform type chromitite can be ascribed to melt mixing, can also be applied to deposits of the podiform type. That can also be seen from the Chugoku region and Hokkaido examples in Japan (MITI, 1993, 1994, 1995), and Zhou (1994), too, has presented the same idea.

Looking at podiform type chromitite throughout the world, one sees a tendency for the Cr# (Cr/(Cr + Al)) of the chrome spinel in the harzburgite to have a relatively low value (about 0.4-0.6) and that the podiform type chromitite for which that value is higher is of high grade, but the ore body tends not to be very large (e.g. Arai, 1994). In other words, attention is focused on podiform chromitite for which the Cr# of the chrome spinel in the harzburgite is relatively low (about 0.4-0.6).

Next, regarding harzburgite and dunite, it is necessary to be able to determine from the chemical composition of the chrome spinel the phenomena that are thought to have produced many secondary melts by interaction. In other words, attention is being focused on chrome spinel in harzburgite with a high TiO_2 content and high Fe# ($Fe^{+3}/(Cr+Al+Fe^{+3})$), chrome spinel in dunite with a low TiO_2 content and spinel in dunite and harzburgite with high Cr# and low V_2O_3 as regards the relationship between Cr# and V_2O_3 (MITI, 1994, 1995; Matsumoto et al, 1995; Matsumoto, 1996).

The purpose of the EPMA tests is to extract zones with high probability of endowment with chromitite by focusing attention on the above-mentioned relationships concerning the chrome spinel contained in the harzburgite, dunite an chromitite as a basis for formulation of survey policy for the remaining years of the project.

(3)-2 Test Conditions

The test conditions are as follows:

- Test apparatus : model JAX-733 (wavelength dispersion) of Nihondenshi Co., Ltd.
- Acc. Voltage : 15 kV
- X-ray angle : 40°

·Probe current	: 12 nA (12 x 10-9 A)
·Probe diameter	: 1 micron
·Elements tested	: Cr, Al, Fe, Mg, Ti, Mn, V
·Standard sample	: Chromite (Acoje Mine), $MnSiO_4$ (Mn-Olivine), V_2O_3, Al_2O_3, Fe_2O_3, MgO, TiO_2

(3)-3 Samples for the Tests

The tests were carried out with respect to the chrome spinel contained in each of 96 samples from 32 points, with harzburgite, dunite and chromitite as a set, taken from chrome deposits and showings practically throughout the area except for the northwestern part of the Shebenik-Pogradec ultrabasic massif, 4 samples from 2 points, with harzburgite and chromitite as a set, 1 sample of dunite from 1 point and 14 samples of chromitite from 14 points. Furthermore, for the purpose of comparison with the results of testing of those 6 samples with harzburgite, dunite and chromitite as a set were taken from two outcrops at the Bulqiza mine, Albania's largest chrome mine, and the same tests were carried out on them. The total number of samples tested was 121, the breakdown being 36 harzburgite samples, 35 dunite samples and 50 chromitite samples.

(3)-4 Results of the Tests

The results of EPMA test are given in Table 2-3-7, a Cr-Al-Fe^{+3} diagram in Fig. 2-3-4, and the tendency of the different components with respect to Cr# in Fig. 2-3-5 to Fig.2-3-8. In order to show the overall trend in the Shebenik-Pogradec ultrabasic massif, which stretches approximately 55 km from north to south, six zones of that massif are shown in Fig. 2-3-14, and Fig. 2-3-9 shows the Cr-Al-Fe^{+3} diagram and Fig.2-3-10 to Fig.2-3-13 show Cr# versus other indices in prepared for each of them.

The characteristics of each of the elements that can be seen from the test results are as follows. It should be noted that the expressions of the values that have been used are those generally used for analysis of spinel assay results.

a) Cr#; Cr/(Cr+Al) Atomic Ratio

For the samples taken all together the Cr# ranges from 0.5 to 0.9, which indicates considerable variation in the Cr/Al ratio, but for a large number of the samples it is concentrated in the range 0.65-0.85. (see Fig. 2-3-4).

Among the different rock facies, Cr# is low for harzburgite, high for chromitite and the values for dunite is between the two. It is particularly noteworthy that for dunite and chromitite the values lie in the comparative narrow range of 0.7-0.8. On the other hand, although the range of variation is wider in the case of harzburgite, 0.6-0.8, in the set samples in all cases the Cr# was lower for harzburgite than for dunite and chromitite.

Fig. 2-3-9 shows how the Cr# of harzburgite differs from zone to zone. One sees a trend of slight decline in the value proceeding from north to south. As will be discussed later, the Cr# of the chrome spinel in the harzburgite is considered to be an important factor in formation of chromitite on a large scale. From that viewpoint zones III, V and VI are the most promising, followed by zone IV.

The Cr# values of the samples from the Bulqiza mine belong to an even lower group than those from the Shebenik-Pogradec ultrabasic massif.

Table 2-3-7 Results of EPMA analysis

No.	Sampe No.	TiO2	Al2O3	Cr2O3	V2O3	FeO*	MnO	MgO	Total	Ti	Al	Cr	V	Fe*	Mn	Mg	Total	FE2+	FE3+	Cr#	Mg#	Fe3+#
1	K95101307 HZ	0.03	18.31	50.72	0.33	20.19	0.34	9.67	99.59	0.001	0.692	1.286	0.009	0.542	0.009	0.462	3.000	0.531	0.009	0.650	0.465	0.004
2	K95101307 DU	0.06	8.53	61.58	0.21	18.31	0.35	10.46	99.49	0.001	0.335	1.620	0.006	0.510	0.010	0.519	3.000	0.475	0.033	0.829	0.522	0.016
3	K95101307 CR	0.13	9.83	61.99	0.08	12.78	0.22	15.07	100.10	0.003	0.369	1.563	0.002	0.341	0.006	0.716	3.000	0.278	0.056	0.809	0.720	0.028
4	E95102202 HZ	0.04	18.01	52.03	0.31	17.78	0.30	11.16	99.62	0.001	0.674	1.307	0.008	0.473	0.008	0.529	3.000	0.465	0.006	0.660	0.532	0.003
5	E95102202 DU	0.09	8.50	61.84	0.13	17.52	0.34	10.96	99.37	0.002	0.333	1.624	0.003	0.487	0.009	0.542	3.000	0.451	0.031	0.830	0.546	0.016
6	E95102202 CR	0.07	9.46	62.31	0.12	13.15	0.27	13.77	99.14	0.002	0.362	1.601	0.003	0.358	0.007	0.667	3.000	0.328	0.026	0.816	0.670	0.013
7	E95102201 HZ	0.13	17.83	52.92	0.23	16.02	0.29	12.40	99.83	0.003	0.662	1.318	0.006	0.422	0.008	0.582	3.000	0.410	0.005	0.666	0.587	0.003
8	E95102201 DU	0.12	10.43	59.51	0.13	16.72	0.30	11.86	99.08	0.003	0.403	1.543	0.003	0.459	0.008	0.580	3.000	0.413	0.040	0.793	0.584	0.020
9	E95102201 CR	0.12	10.63	61.12	0.09	13.95	0.25	13.78	99.94	0.003	0.402	1.552	0.002	0.375	0.007	0.659	3.000	0.335	0.034	0.794	0.663	0.017
10	K95101301 HZ	0.03	24.81	44.83	0.18	16.38	0.26	13.35	99.84	0.001	0.889	1.078	0.005	0.417	0.007	0.605	3.000	0.391	0.025	0.548	0.608	0.012
11	K95101302 DU	0.03	11.77	56.37	0.29	19.38	0.31	10.28	98.42	0.001	0.460	1.478	0.008	0.537	0.009	0.508	3.000	0.486	0.050	0.763	0.511	0.025
12	K95101301 CR	0.06	22.39	48.45	0.20	12.59	0.18	15.73	99.59	0.001	0.799	1.161	0.005	0.319	0.005	0.710	3.000	0.285	0.031	0.592	0.713	0.016
13	E95102101 HZ	0.02	15.69	54.15	0.38	18.51	0.28	10.54	99.56	0.001	0.596	1.381	0.010	0.499	0.008	0.506	3.000	0.487	0.011	0.698	0.510	0.005
14	E95102101 DU	0.19	20.06	45.79	0.46	20.25	0.27	11.72	98.74	0.005	0.747	1.144	0.012	0.535	0.007	0.552	3.000	0.438	0.088	0.605	0.558	0.045
15	E95102101 CR	0.09	8.54	62.95	0.12	13.02	0.22	14.34	99.27	0.002	0.327	1.615	0.003	0.353	0.006	0.694	3.000	0.301	0.048	0.832	0.697	0.024
16	K95092505 HZ	0.04	15.78	53.70	0.27	18.20	0.31	10.75	99.05	0.001	0.601	1.373	0.007	0.492	0.009	0.518	3.000	0.476	0.014	0.695	0.521	0.007
17	K95092505 DU	0.09	9.39	58.46	0.16	20.50	0.37	9.73	98.70	0.002	0.371	1.550	0.004	0.575	0.011	0.487	3.000	0.506	0.064	0.807	0.490	0.032
18	K95092505 CR	0.14	9.78	60.90	0.08	14.35	0.24	13.93	99.44	0.004	0.373	1.556	0.002	0.388	0.007	0.671	3.000	0.323	0.058	0.807	0.675	0.029
19	K95102108 HZ	0.04	14.21	54.78	0.32	18.91	0.34	10.59	99.19	0.001	0.545	1.409	0.008	0.514	0.009	0.514	3.000	0.480	0.033	0.721	0.517	0.017
20	K95102108 DU	0.04	10.46	58.73	0.20	18.53	0.34	10.76	99.06	0.001	0.407	1.535	0.005	0.512	0.010	0.530	3.000	0.464	0.046	0.790	0.533	0.023
21	K95102108 CR	0.09	12.34	58.43	0.12	13.83	0.23	14.24	99.27	0.002	0.465	1.476	0.003	0.370	0.006	0.678	3.000	0.316	0.049	0.761	0.682	0.025
22	M95102203 HZ	0.05	10.52	58.11	0.28	20.41	0.38	8.84	98.58	0.001	0.417	1.546	0.008	0.574	0.011	0.443	3.000	0.550	0.022	0.788	0.446	0.011
23	M95102203 DU	0.12	9.80	60.02	0.10	17.69	0.34	11.05	99.12	0.003	0.382	1.569	0.003	0.489	0.010	0.545	3.000	0.448	0.035	0.804	0.548	0.018
24	M95102203 CR	0.08	9.90	62.75	0.09	12.53	0.21	14.25	99.81	0.002	0.375	1.595	0.002	0.337	0.006	0.683	3.000	0.312	0.020	0.810	0.686	0.010
25	K95102206 HZ	0.03	13.39	55.65	0.39	18.53	0.33	10.52	98.83	0.001	0.517	1.442	0.010	0.508	0.009	0.514	3.000	0.479	0.027	0.736	0.517	0.014
26	K95102206 DU	0.10	9.48	60.66	0.15	17.76	0.31	11.33	99.79	0.003	0.367	1.575	0.004	0.488	0.009	0.555	3.000	0.439	0.044	0.811	0.559	0.022
27	K95102206 CR	0.10	12.23	58.84	0.14	13.30	0.21	14.90	99.71	0.002	0.457	1.475	0.004	0.353	0.006	0.704	3.000	0.291	0.057	0.764	0.708	0.029
28	E95110101 HZ	0.01	13.11	56.19	0.39	19.29	0.36	9.84	99.19	0.000	0.508	1.460	0.010	0.530	0.010	0.482	3.000	0.511	0.019	0.742	0.485	0.010
29	E95110101 DU	0.10	10.43	59.56	0.12	17.15	0.34	11.29	98.99	0.002	0.405	1.552	0.003	0.473	0.010	0.555	3.000	0.439	0.029	0.793	0.558	0.015
30	E95110101 CR	0.14	9.58	60.56	0.09	14.25	0.23	14.35	99.20	0.003	0.365	1.547	0.002	0.385	0.006	0.691	3.000	0.302	0.076	0.809	0.696	0.038
31	K95102107 HZ	0.02	15.31	54.68	0.35	18.09	0.33	10.87	99.64	0.001	0.581	1.392	0.009	0.487	0.009	0.521	3.000	0.472	0.014	0.705	0.525	0.007
32	K95102107 DU	0.06	9.43	59.03	0.24	19.75	0.38	9.77	98.66	0.002	0.373	1.566	0.007	0.554	0.011	0.489	3.000	0.504	0.047	0.808	0.492	0.024
33	K95102107 CR	0.17	10.25	60.75	0.08	12.50	0.21	15.32	99.28	0.004	0.386	1.537	0.002	0.334	0.006	0.730	3.000	0.263	0.063	0.799	0.735	0.032
34	K95102104 HZ	0.03	17.47	53.35	0.26	16.69	0.28	11.83	99.91	0.001	0.651	1.335	0.007	0.441	0.007	0.558	3.000	0.437	0.003	0.672	0.561	0.002
35	K95102104 DU	0.06	9.94	60.41	0.17	17.64	0.34	11.06	99.62	0.002	0.386	1.572	0.005	0.485	0.009	0.542	3.000	0.451	0.031	0.803	0.546	0.015
36	K95102104 CR	0.12	10.46	60.15	0.09	15.64	0.28	12.92	99.67	0.003	0.399	1.540	0.002	0.424	0.008	0.624	3.000	0.370	0.048	0.794	0.628	0.024
37	K95102102 HZ	0.02	23.76	46.71	0.25	15.86	0.24	13.14	99.98	0.001	0.855	1.128	0.006	0.405	0.006	0.598	3.000	0.397	0.007	0.569	0.601	0.004
38	K95102102 DU	0.05	18.01	51.83	0.23	17.83	0.31	11.44	99.69	0.001	0.673	1.299	0.006	0.473	0.008	0.540	3.000	0.454	0.017	0.659	0.544	0.008
39	K95102102 CR	0.15	9.83	62.15	0.07	13.58	0.25	14.04	100.06	0.004	0.372	1.579	0.002	0.365	0.007	0.672	3.000	0.321	0.036	0.809	0.677	0.018
40	K95101801 HZ	0.02	16.40	54.22	0.27	17.05	0.30	11.53	99.78	0.001	0.616	1.367	0.007	0.455	0.008	0.548	3.000	0.447	0.007	0.689	0.551	0.003
41	K95101801 DU	0.07	13.29	56.24	0.16	17.60	0.29	11.92	99.56	0.002	0.505	1.434	0.004	0.475	0.008	0.573	3.000	0.421	0.050	0.740	0.576	0.025
42	K95101801 CR	0.10	10.37	60.28	0.11	15.13	0.26	13.40	99.64	0.003	0.395	1.539	0.003	0.409	0.007	0.645	3.000	0.349	0.055	0.796	0.649	0.027
43	M95101802 HZ	0.04	16.61	53.63	0.25	17.09	0.31	11.54	99.47	0.001	0.625	1.354	0.006	0.457	0.008	0.549	3.000	0.445	0.010	0.684	0.552	0.005
44	M95101802 DU	0.07	12.35	58.45	0.21	17.00	0.30	11.62	100.00	0.002	0.471	1.494	0.006	0.460	0.008	0.560	3.000	0.434	0.023	0.760	0.564	0.011

Table 2-3-7 Results of EPMA analysis

No.	Sampe No.	TiO2	Al2O3	Cr2O3	V2O3	FeO*	MnO	MgO	Total	Ti	Al	Cr	V	Fe*	Mn	Mg	Total	FE2+	FE3+	Cr#	Mg#	Fe3+#
45	M95101802 CR	0.08	9.83	62.45	0.13	13.41	0.23	13.87	100.00	0.002	0.373	1.589	0.003	0.361	0.006	0.665	3.000	0.330	0.028	0.810	0.669	0.014
46	M95101703 HZ	0.04	14.05	55.46	0.32	19.59	0.34	9.77	99.59	0.001	0.540	1.431	0.008	0.535	0.010	0.475	3.000	0.518	0.015	0.726	0.479	0.008
47	M95101703 DU	0.08	12.21	58.12	0.19	18.49	0.34	10.31	99.75	0.002	0.471	1.504	0.005	0.506	0.010	0.503	3.000	0.490	0.012	0.761	0.506	0.006
48	M95101703 CR	0.16	11.00	60.52	0.08	13.00	0.24	14.71	99.70	0.004	0.414	1.527	0.002	0.347	0.006	0.700	3.000	0.294	0.046	0.787	0.704	0.023
49	M95101704 HZ	0.04	21.50	48.73	0.23	17.01	0.28	12.32	100.11	0.001	0.785	1.193	0.006	0.440	0.007	0.568	3.000	0.426	0.012	0.603	0.571	0.006
50	M95101704 DU	0.11	13.69	57.14	0.20	16.83	0.33	11.66	99.95	0.003	0.519	1.453	0.005	0.453	0.009	0.559	3.000	0.434	0.014	0.737	0.563	0.007
51	M95101704 CR	0.10	9.63	60.85	0.09	14.06	0.24	13.82	98.80	0.002	0.370	1.566	0.002	0.383	0.007	0.670	3.000	0.324	0.054	0.809	0.674	0.027
52	K95092904 HZ	0.04	17.15	51.27	0.26	19.50	0.30	10.87	99.38	0.001	0.647	1.297	0.007	0.522	0.008	0.519	3.000	0.476	0.044	0.667	0.522	0.022
53	K95092904 DU	0.07	9.39	59.79	0.13	19.08	0.37	10.18	99.01	0.002	0.369	1.577	0.004	0.532	0.011	0.506	3.000	0.487	0.041	0.810	0.509	0.021
54	K95092904 CR	0.13	9.26	61.57	0.10	14.18	0.25	13.61	99.09	0.003	0.355	1.585	0.003	0.386	0.007	0.661	3.000	0.333	0.047	0.817	0.665	0.024
55	K95092911 HZ	0.01	15.49	53.54	0.26	19.09	0.33	10.67	99.39	0.000	0.589	1.366	0.007	0.515	0.009	0.513	3.000	0.481	0.034	0.699	0.516	0.017
56	K95092911 DU	0.06	10.63	59.04	0.13	18.73	0.34	10.77	99.70	0.001	0.411	1.533	0.003	0.515	0.010	0.527	3.000	0.467	0.045	0.788	0.530	0.022
57	K95092911 CR	0.10	9.85	60.53	0.08	13.05	0.26	14.48	98.35	0.003	0.377	1.555	0.002	0.355	0.007	0.702	3.000	0.293	0.057	0.805	0.705	0.028
58	M95100810 HZ	0.02	17.06	52.43	0.27	18.61	0.32	10.90	99.59	0.000	0.643	1.325	0.007	0.498	0.009	0.519	3.000	0.475	0.021	0.673	0.522	0.011
59	M95100810 DU	0.11	10.75	58.10	0.14	19.25	0.35	10.61	99.30	0.003	0.418	1.514	0.004	0.531	0.010	0.521	3.000	0.472	0.053	0.784	0.525	0.027
60	M95100810 CR	0.14	9.72	59.51	0.11	13.89	0.23	14.70	98.30	0.003	0.372	1.527	0.003	0.377	0.006	0.711	3.000	0.282	0.088	0.804	0.716	0.044
61	M95101605 HZ	0.02	13.19	56.48	0.27	18.93	0.34	10.23	99.47	0.001	0.508	1.459	0.007	0.518	0.009	0.498	3.000	0.496	0.020	0.742	0.501	0.010
62	M95101605 DU	0.05	11.92	57.68	0.22	18.05	0.34	10.73	98.98	0.001	0.462	1.500	0.006	0.496	0.009	0.526	3.000	0.468	0.026	0.764	0.529	0.013
63	M95101605 CR	0.12	10.21	61.28	0.07	13.42	0.27	13.66	99.01	0.003	0.390	1.573	0.002	0.364	0.007	0.661	3.000	0.333	0.025	0.801	0.665	0.013
64	M95101509 HZ	0.02	15.40	54.80	0.28	18.38	0.33	10.42	99.63	0.001	0.586	1.399	0.007	0.496	0.009	0.502	3.000	0.492	0.003	0.705	0.505	0.001
65	M95101509 DU	0.05	11.55	58.43	0.25	18.22	0.31	10.65	99.45	0.001	0.447	1.516	0.007	0.500	0.009	0.521	3.000	0.473	0.025	0.772	0.524	0.012
66	M95101509 CR	0.06	7.82	62.44	0.14	15.41	0.25	12.41	98.53	0.002	0.306	1.640	0.004	0.428	0.007	0.614	3.000	0.381	0.044	0.843	0.617	0.022
67	M95101507 HZ	0.04	26.50	43.40	0.23	15.29	0.24	13.60	99.29	0.001	0.946	1.040	0.006	0.387	0.006	0.614	3.000	0.381	0.004	0.524	0.617	0.002
68	M95101507 DU	0.06	14.69	54.49	0.24	18.72	0.31	10.64	99.14	0.001	0.562	1.399	0.006	0.508	0.009	0.515	3.000	0.479	0.027	0.713	0.518	0.013
69	M95101507 CR	0.06	12.91	57.42	0.20	14.18	0.22	13.39	98.37	0.001	0.492	1.467	0.005	0.383	0.006	0.645	3.000	0.350	0.031	0.749	0.648	0.015
70	K95101705 HZ	0.04	17.86	51.76	0.30	17.84	0.28	11.53	99.60	0.001	0.668	1.298	0.008	0.473	0.008	0.545	3.000	0.449	0.022	0.660	0.548	0.011
71	K95101705 DU	0.18	12.08	58.44	0.11	15.13	0.27	13.15	99.36	0.005	0.459	1.488	0.003	0.407	0.007	0.631	3.000	0.361	0.037	0.764	0.636	0.019
72	K95101705 CR	0.14	11.32	59.12	0.07	13.87	0.22	14.01	98.74	0.003	0.431	1.509	0.002	0.375	0.006	0.674	3.000	0.320	0.048	0.778	0.678	0.024
73	K95101702 HZ	0.02	12.76	56.57	0.33	18.35	0.34	10.57	98.95	0.001	0.493	1.468	0.009	0.504	0.010	0.517	3.000	0.476	0.026	0.748	0.520	0.013
74	K95101702 DU	0.10	11.97	58.49	0.22	17.23	0.33	11.30	99.64	0.003	0.460	1.506	0.006	0.469	0.009	0.549	3.000	0.444	0.020	0.766	0.553	0.010
75	K95101702 CR	0.14	10.96	60.23	0.07	13.02	0.26	14.49	99.17	0.003	0.415	1.530	0.002	0.350	0.007	0.694	3.000	0.300	0.043	0.787	0.698	0.022
76	E95101601 HZ	0.03	16.77	51.79	0.32	18.80	0.31	11.03	99.04	0.001	0.635	1.315	0.008	0.505	0.008	0.528	3.000	0.466	0.038	0.674	0.531	0.019
77	E95101601 DU	0.08	10.61	58.38	0.24	20.17	0.35	9.50	99.32	0.002	0.416	1.535	0.007	0.561	0.010	0.471	3.000	0.522	0.035	0.787	0.474	0.018
78	E95101601 CR	0.07	17.61	52.03	0.25	15.43	0.24	13.64	99.27	0.002	0.651	1.291	0.006	0.405	0.006	0.638	3.000	0.356	0.046	0.665	0.642	0.023
79	E95101602 HZ	0.03	18.13	52.17	0.30	17.12	0.29	11.69	99.73	0.001	0.676	1.304	0.008	0.453	0.008	0.551	3.000	0.443	0.008	0.659	0.554	0.004
80	E95101602 DU	0.07	14.27	54.66	0.23	17.69	0.32	11.43	98.66	0.002	0.546	1.404	0.006	0.480	0.009	0.553	3.000	0.440	0.037	0.720	0.557	0.019
81	E95101602 CR	0.13	11.78	59.28	0.14	13.26	0.23	14.68	99.50	0.003	0.442	1.494	0.004	0.353	0.006	0.698	3.000	0.296	0.051	0.772	0.702	0.026
82	K95100501 HZ	0.01	17.28	52.76	0.28	17.16	0.27	11.70	99.46	0.000	0.648	1.327	0.007	0.456	0.007	0.555	3.000	0.440	0.015	0.672	0.558	0.008
83	K95100501 DU	0.07	11.81	55.76	0.20	19.45	0.32	10.74	98.34	0.002	0.460	1.457	0.005	0.538	0.009	0.529	3.000	0.465	0.070	0.760	0.533	0.035
84	K95100501 CR	0.08	10.49	60.88	0.13	12.31	0.21	15.22	99.31	0.002	0.395	1.539	0.003	0.329	0.006	0.725	3.000	0.270	0.056	0.796	0.729	0.028
85	E95100501 HZ	0.04	12.57	57.15	0.35	18.22	0.35	10.11	98.80	0.001	0.489	1.491	0.009	0.503	0.010	0.497	3.000	0.495	0.005	0.753	0.501	0.003
86	E95100501 DU	0.12	8.16	58.83	0.43	23.20	0.41	7.51	98.64	0.003	0.330	1.595	0.012	0.665	0.012	0.384	3.000	0.606	0.054	0.829	0.388	0.027
87	E95100501 CR	0.10	7.09	61.42	0.26	21.04	0.37	8.49	98.77	0.003	0.286	1.660	0.007	0.602	0.011	0.432	3.000	0.559	0.037	0.853	0.436	0.019
88	M95100306 HZ	0.04	11.68	56.54	0.32	19.54	0.34	9.54	98.01	0.001	0.461	1.497	0.009	0.547	0.010	0.476	3.000	0.517	0.028	0.765	0.480	0.014

Table 2-3-7 Results of EPMA analysis

No.	Sampe No.	TiO2	Al2O3	Cr2O3	V2O3	FeO*	MnO	MgO	Total	Ti	Al	Cr	V	Fe*	Mn	Mg	Total	FE2+	FE3+	Cr#	Mg#	Fe3+#
89	M95100306 DU	0.12	13.11	57.68	0.10	14.59	0.24	13.61	99.44	0.003	0.494	1.457	0.003	0.390	0.006	0.648	3.000	0.346	0.038	0.747	0.652	0.019
90	M95100306 CR	0.15	12.74	57.78	0.08	13.94	0.22	14.12	99.03	0.004	0.480	1.462	0.002	0.373	0.006	0.673	3.000	0.320	0.045	0.753	0.678	0.023
91	E95100201 HZ	0.02	12.05	58.25	0.32	18.61	0.33	9.94	99.51	0.001	0.467	1.515	0.008	0.512	0.009	0.488	3.000	0.506	0.005	0.764	0.491	0.002
92	E95100201 DU	0.07	6.49	62.59	0.19	20.95	0.37	8.59	99.25	0.002	0.261	1.687	0.005	0.597	0.011	0.437	3.000	0.556	0.038	0.866	0.440	0.019
93	E95100201 CR	0.07	6.21	64.50	0.18	15.42	0.28	11.99	98.64	0.002	0.245	1.709	0.005	0.432	0.008	0.599	3.000	0.395	0.033	0.875	0.603	0.017
94	K95093005 HZ	0.04	31.30	36.54	0.21	16.37	0.21	14.49	99.17	0.001	1.091	0.854	0.005	0.405	0.005	0.639	3.000	0.357	0.046	0.439	0.642	0.023
95	K95093005 CR	0.24	28.40	38.83	0.17	15.96	0.23	15.41	99.23	0.005	0.994	0.912	0.004	0.397	0.006	0.682	3.000	0.309	0.077	0.478	0.688	0.039
96	N95100602 HZ	0.02	25.91	41.57	0.25	18.61	0.22	12.96	99.54	0.000	0.928	0.999	0.006	0.473	0.006	0.587	3.000	0.408	0.064	0.518	0.590	0.032
97	N95100602 CR	0.08	26.37	42.80	0.14	13.36	0.17	16.14	99.05	0.002	0.928	1.011	0.003	0.334	0.004	0.718	3.000	0.277	0.053	0.521	0.721	0.026
98	E95100407 DU	0.04	23.93	45.96	0.25	16.13	0.26	13.15	99.73	0.001	0.863	1.111	0.006	0.413	0.007	0.600	3.000	0.395	0.015	0.563	0.603	0.008
99	K95101305 CR	0.15	13.20	56.53	0.15	13.50	0.22	14.67	98.41	0.004	0.497	1.429	0.004	0.361	0.006	0.699	3.000	0.294	0.060	0.742	0.704	0.030
100	K95102207 CR	0.05	8.67	61.11	0.13	15.75	0.26	12.41	98.38	0.001	0.339	1.601	0.004	0.436	0.007	0.613	3.000	0.382	0.051	0.825	0.616	0.026
101	K95102203 CR	0.12	9.76	61.20	0.11	13.97	0.23	13.75	99.13	0.003	0.373	1.571	0.003	0.379	0.006	0.665	3.000	0.329	0.044	0.808	0.669	0.022
102	K95102106 CR	0.10	9.90	61.49	0.11	12.88	0.18	14.67	99.32	0.002	0.375	1.564	0.003	0.347	0.005	0.704	3.000	0.291	0.050	0.806	0.707	0.025
103	M95102102 CR	0.09	8.11	62.84	0.10	15.31	0.28	12.68	99.41	0.002	0.314	1.632	0.003	0.421	0.008	0.621	3.000	0.374	0.043	0.839	0.624	0.021
104	M95101807 HZ	0.04	14.49	56.48	0.28	17.09	0.32	11.25	99.95	0.001	0.549	1.436	0.007	0.459	0.009	0.539	3.000	0.455	0.003	0.723	0.542	0.001
105	M95101807 DU	0.11	13.37	56.24	0.23	18.04	0.31	11.33	99.62	0.003	0.510	1.439	0.006	0.488	0.009	0.547	3.000	0.446	0.037	0.738	0.551	0.019
106	M95101807 CR	0.04	9.46	61.69	0.18	13.96	0.21	13.39	98.93	0.001	0.364	1.592	0.005	0.381	0.006	0.652	3.000	0.344	0.035	0.814	0.655	0.018
107	E95101803 CR	0.09	8.43	63.15	0.07	12.87	0.20	14.76	99.58	0.002	0.321	1.612	0.002	0.348	0.006	0.710	3.000	0.285	0.058	0.834	0.714	0.029
108	K95101802 CR	0.09	8.23	63.23	0.09	15.23	0.27	12.47	99.60	0.002	0.318	1.641	0.002	0.418	0.007	0.610	3.000	0.384	0.029	0.838	0.613	0.015
109	K95092912 CR	0.08	7.02	64.67	0.11	14.49	0.26	13.18	99.79	0.002	0.271	1.676	0.003	0.397	0.007	0.644	3.000	0.351	0.042	0.861	0.647	0.021
110	K95101005 CR	0.07	6.92	64.71	0.10	14.32	0.26	12.99	99.37	0.002	0.269	1.687	0.003	0.395	0.007	0.638	3.000	0.357	0.035	0.862	0.642	0.017
111	K95101603 CR	0.08	9.05	61.84	0.09	13.50	0.22	14.29	99.07	0.002	0.346	1.586	0.002	0.366	0.006	0.691	3.000	0.304	0.058	0.821	0.694	0.029
112	E95101502 CR	0.06	11.28	59.62	0.17	14.60	0.28	13.38	99.38	0.001	0.429	1.521	0.004	0.394	0.008	0.644	3.000	0.351	0.040	0.780	0.647	0.020
113	K95101701 CR	0.09	10.14	62.45	0.12	12.97	0.24	13.81	99.82	0.002	0.385	1.591	0.003	0.350	0.007	0.663	3.000	0.332	0.013	0.805	0.667	0.007
114	K95100904 CR	0.05	11.01	59.84	0.19	14.51	0.26	13.50	99.37	0.001	0.419	1.527	0.005	0.392	0.007	0.650	3.000	0.345	0.044	0.785	0.653	0.022
115	K95100305 CR	0.05	20.74	48.57	0.23	15.03	0.20	14.44	99.24	0.001	0.753	1.184	0.006	0.387	0.005	0.663	3.000	0.332	0.053	0.611	0.667	0.027
116	N95102701 HZ	0.05	18.32	51.51	0.21	17.21	0.30	11.74	99.34	0.001	0.684	1.290	0.005	0.456	0.008	0.555	3.000	0.440	0.014	0.653	0.558	0.007
117	N95102701 DU	0.16	12.84	54.74	0.10	20.25	0.32	10.43	98.84	0.004	0.497	1.421	0.003	0.556	0.009	0.510	3.000	0.482	0.066	0.741	0.514	0.033
118	N95102701 CRM	0.07	13.42	58.03	0.14	13.28	0.25	14.24	99.42	0.002	0.503	1.458	0.003	0.353	0.007	0.675	3.000	0.320	0.029	0.744	0.678	0.015
119	N95102702 HZ	0.03	13.25	56.70	0.26	18.07	0.33	10.91	99.56	0.001	0.508	1.457	0.007	0.491	0.009	0.528	3.000	0.466	0.024	0.742	0.531	0.012
120	N95102702 DU	0.12	12.07	56.79	0.17	18.95	0.34	10.88	99.31	0.003	0.465	1.469	0.005	0.519	0.009	0.531	3.000	0.462	0.051	0.759	0.535	0.026
121	N95102702 CR	0.17	11.59	57.79	0.09	14.38	0.23	14.63	98.87	0.004	0.438	1.465	0.002	0.386	0.006	0.699	3.000	0.294	0.083	0.770	0.704	0.042

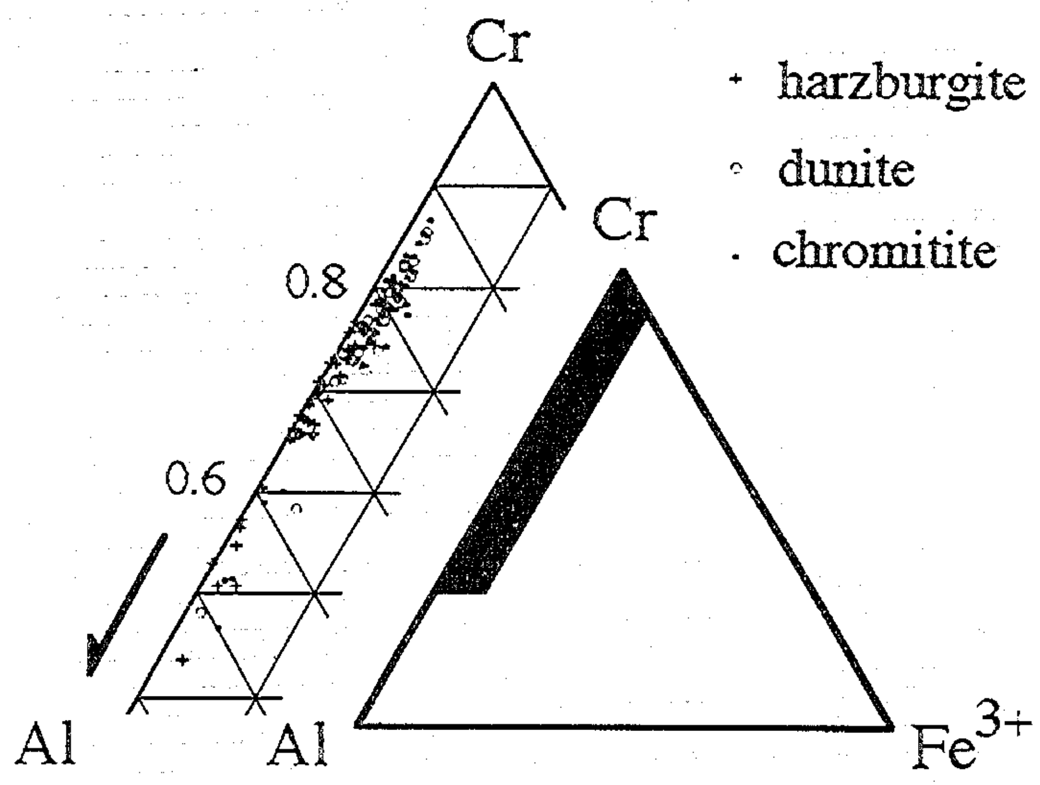

Fig. 2-3-4 Cr-Al-Fe^{+3} proportion of chrome spinels

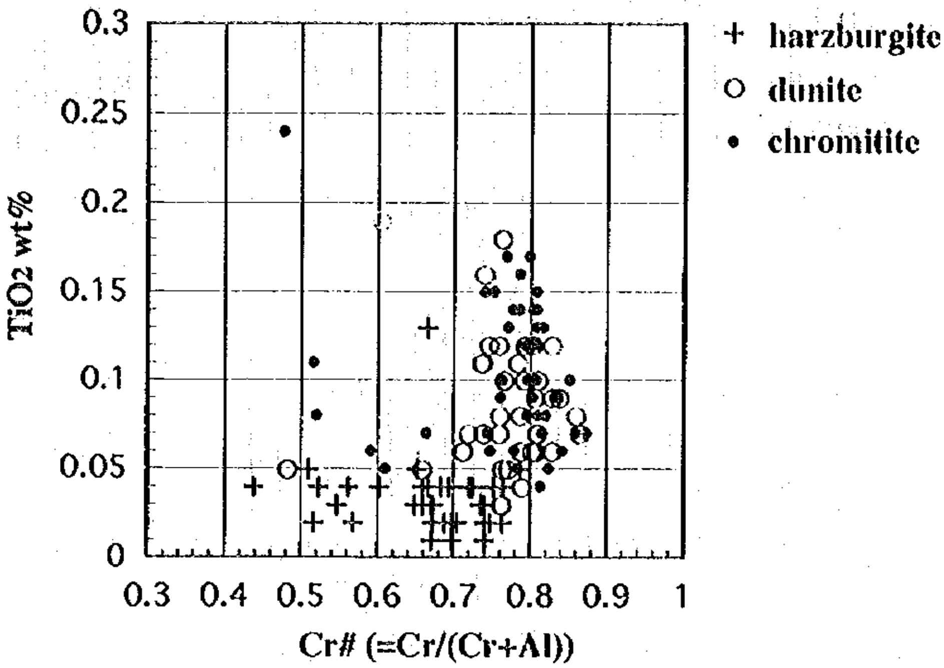

Fig. 2-3-5 Relationship between Cr# and TiO_2 wt% in chrome spinels

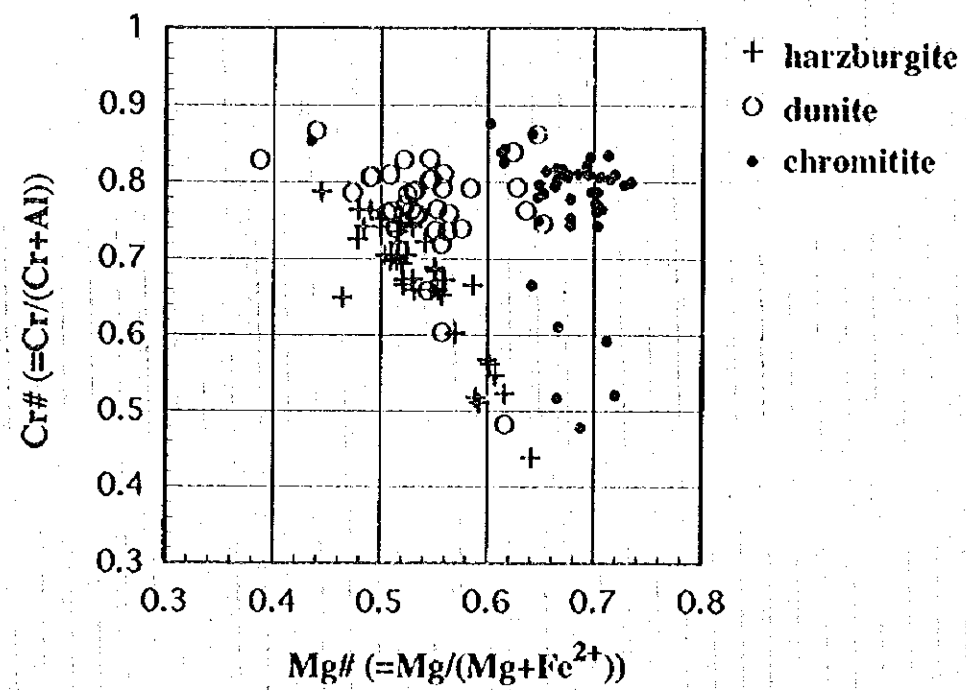

Fig. 2-3-6 Relationship between Cr# and Mg# in chrome spinels

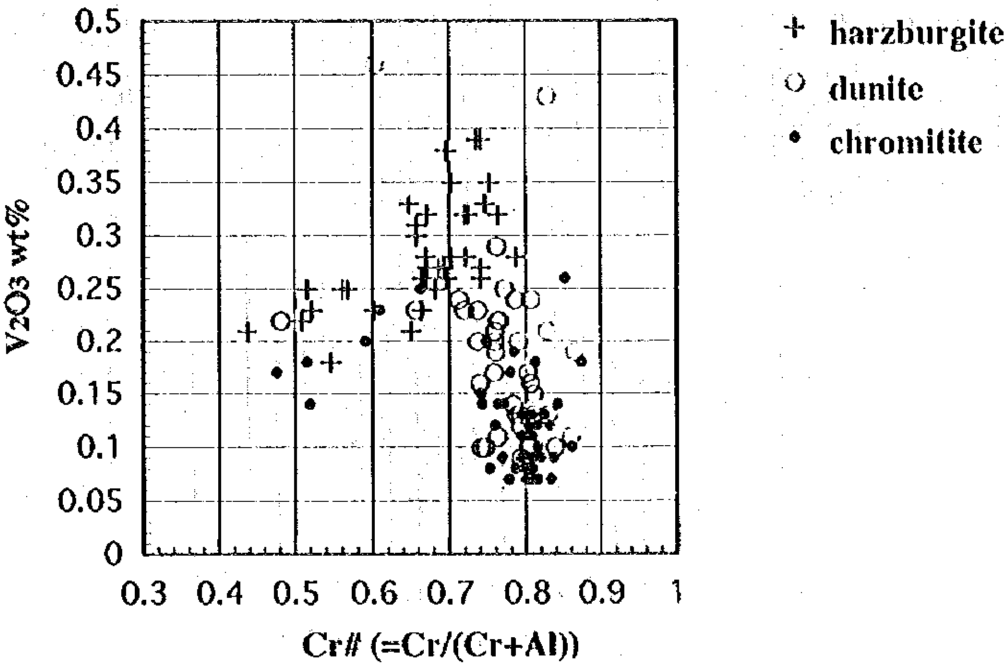

Fig. 2-3-7 Relationship between Cr# and V_2O_3 wt% in chrome spinels

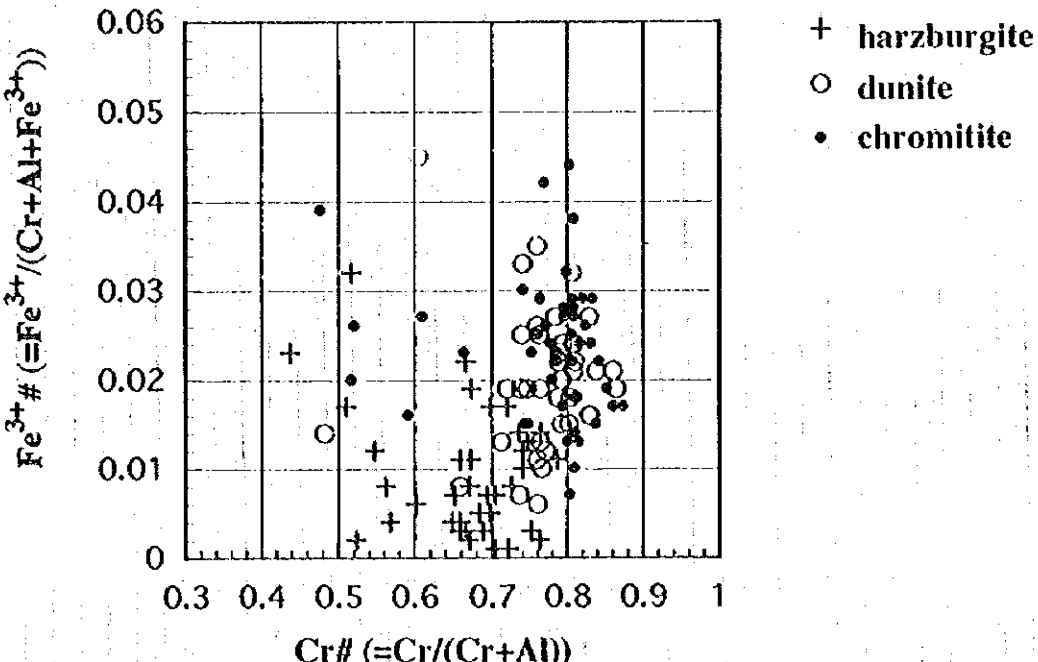

Fig. 2-3-8 Relationship between Cr# and Fe^{+3} # in chrome spinels

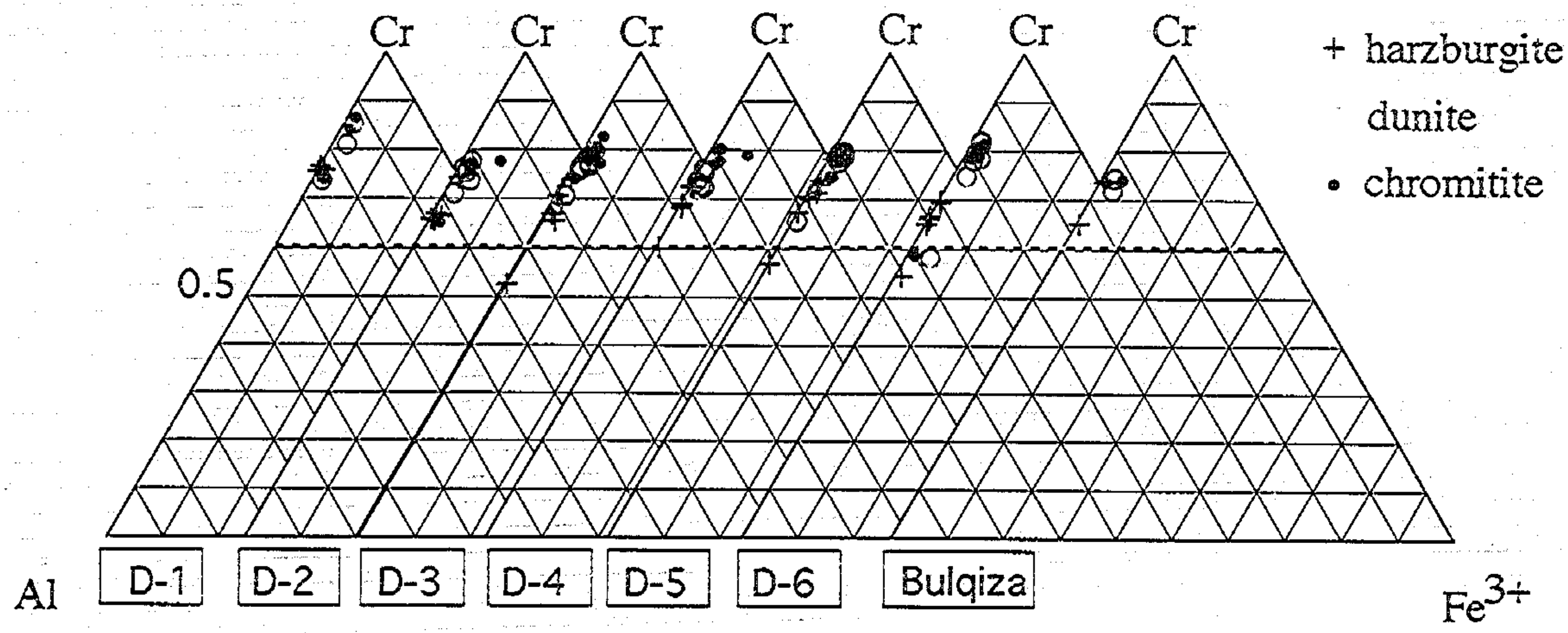

Fig. 2–3–9 Cr–Al–Fe^{+3} proportion of chrome spinels in each zone

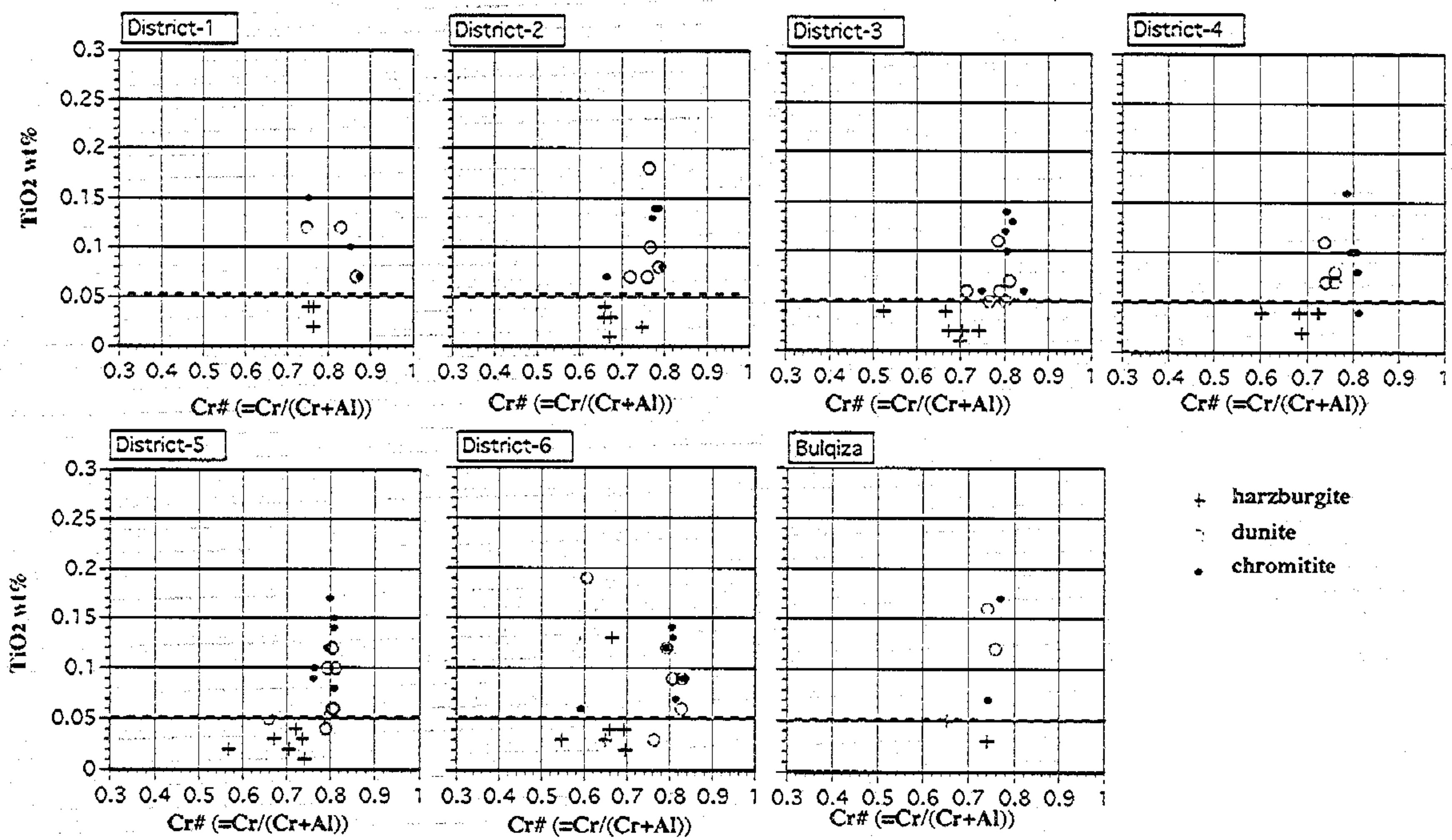

Fig. 2–3–10 Relationships between Cr# and TiO_2 wt% in chrome spinels in each zone

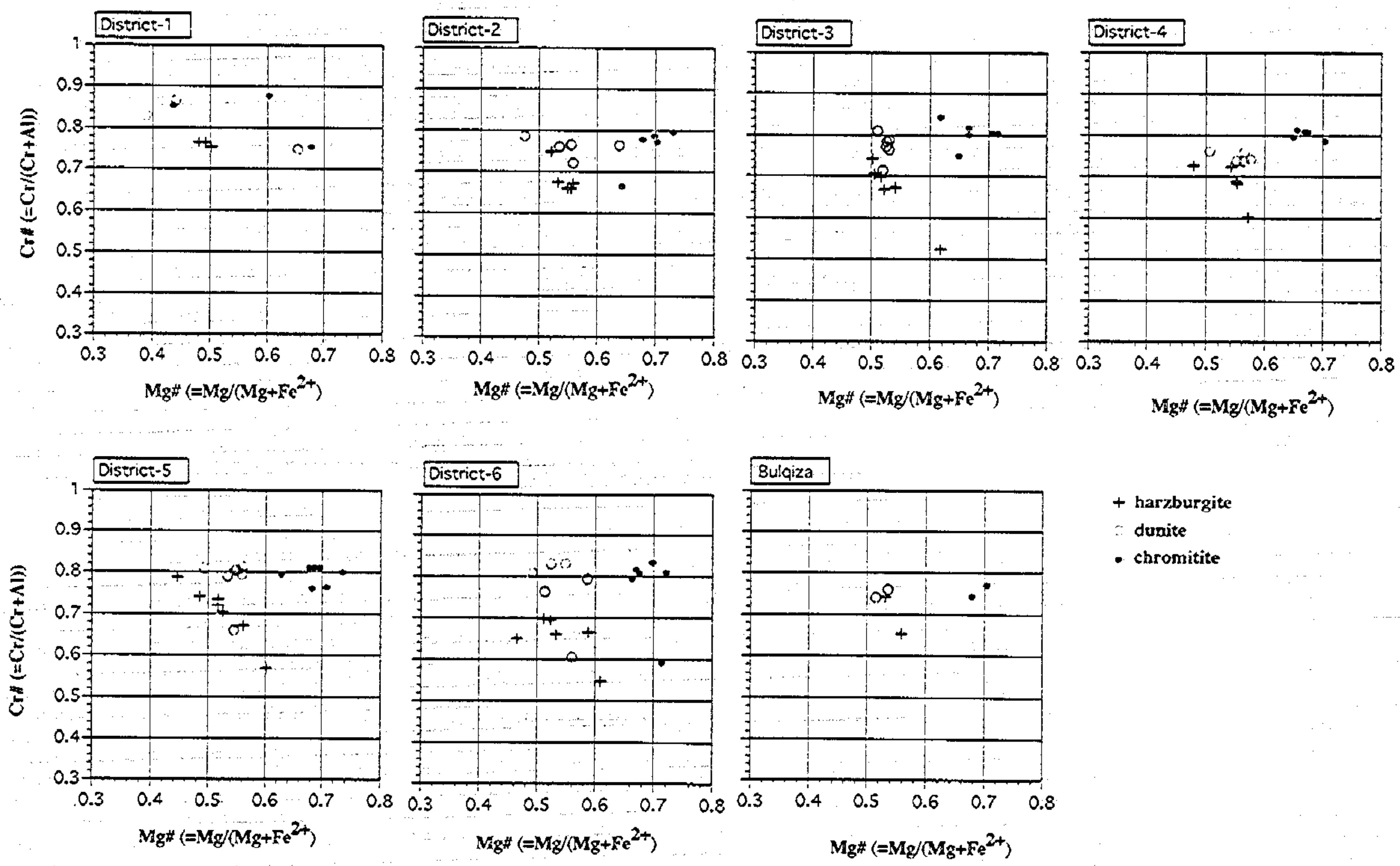

Fig. 2-3-11 Relationships between Cr# and Mg# in chrome spinels in each zone

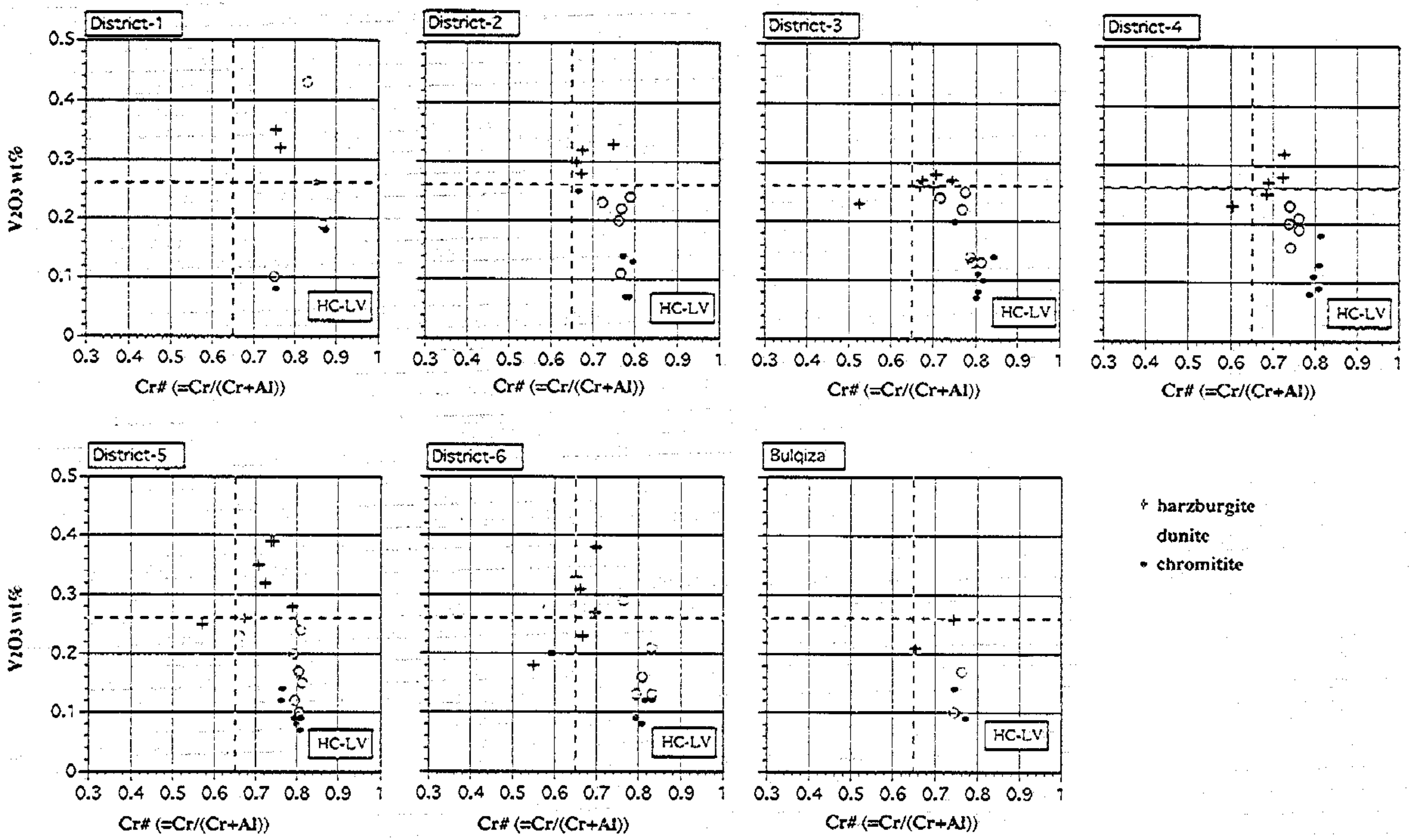

Fig. 2–3–12 Relationships between Cr# and V_2O_3 wt% in chrome spinels in each zone

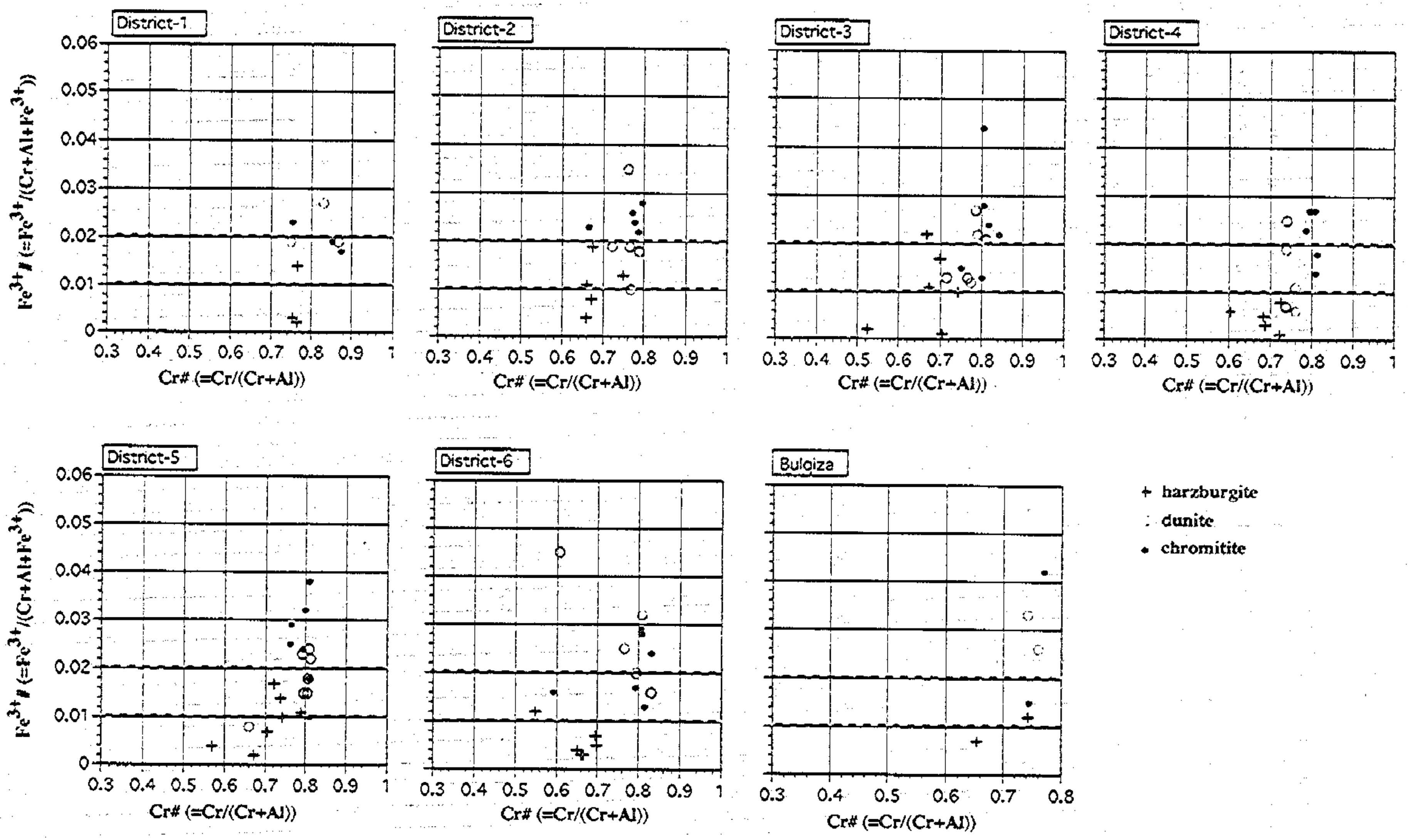

Fig. 2–3–13 Relationships between Cr# and Fe^{+3} # in chrome spinels in each zone

b) TiO_2 wt%

The TiO_2 content is lower than 0.2 wt% for all of the samples. Considered separately for the different rock facies, it is lowest in the harzburgite (0.05 wt% or lower), and the values in the dunite and the chromitite are higher (see Fig. 2-3-5). That is in harmony with the tendency that is generally seen in the peridotite.

However, there are some samples contrary to the general trend, i.e. in them the TiO_2 content of the chrome spinel in the dunite is low whereas that of the chrome spinel in harzburgite is high. That fact indicates the existence of spinel with an intermediate composition between that of dunite and that of harzburgite. The samples indicating that tendency are 2 dunite samples from zone III, 2 dunite samples and 1 harzburgite sample from zone IV, 1 dunite sample and 1 harzburgite sample from zone VI and 1 harzburgite sample from the Bulqiza mine.

c) Fe^{+3}#; $Fe^{+3}/(Cr+Al+Fe^{+3})$ Atomic Ratio

In all of the samples Fe^{+3}# is 0.05 or lower. For the different rock species it is lowest for the harzburgite less than 0.01 and for the dunite and the chromitite the values are comparatively high, above 0.01.

However, in some harzburgite samples the value is comparatively high, above 0.01, and it is even higher, above 0.02 for dunite. Looking at the zone distribution of such samples, one sees that 2 of the 7 samples from zone I (1 dunite sample and 1 harzburgite sample), 4 of the 10 samples from zone II (1 dunite sample and 3 harzburgite samples), 7 of the 12 samples from zone III (3 dunite samples and 4 harzburgite samples), 1 of the 10 samples from zone IV (dunite), 7 of the 14 samples from zone V (3 dunite samples and 4 harzburgite samples) and 5 of the 16 samples from zone VI (3 dunite samples and 2 harzburgite samples) are such samples.

Among sample from the Bulqiza mine 3 of the 4 samples from(2 dunite samples and 1 harzburgite sample) also have comparatively high Fe^{+3}# values.

d) V_2O_3 wt%

For all of the samples taken together the V_2O_3 content is less than 0.5 wt%. For the different rock facies the values tend to be comparatively high for harzburgite and lower for dunite and chromitite.

Looking at both the V_2O_3 content and the Cr# of the dunite and the harzburgite, ones sees that all four of the samples from the Bulqiza mine have a comparatively low V_2O_3 content (0.26% or lower) and a comparatively high Cr# (0.5 or higher). That same trend is to be seen particularly in the case of harzburgite in 2 of 6 samples from zone III, 1 of 5 samples from zone IV and 1 of 6 samples from zone VI.

e) Mg#; $Mg/(Fe^{+2} + Mg)$ Atomic Ratio

For all of the samples Mg# tends to be high in the chromitite and low in the dunite and harzburgite.

It has been confirmed that at subsolidus a Mg exchange reaction occurs between the chrome spinel and the olivine surrounding it (Arai, 1980). It was therefore expected that Mg# varies according to the quantity of chrome spinel, and the above-mentioned tendency of Mg# for the chromitite, dunite and harzburgite are in line with that interpretation.

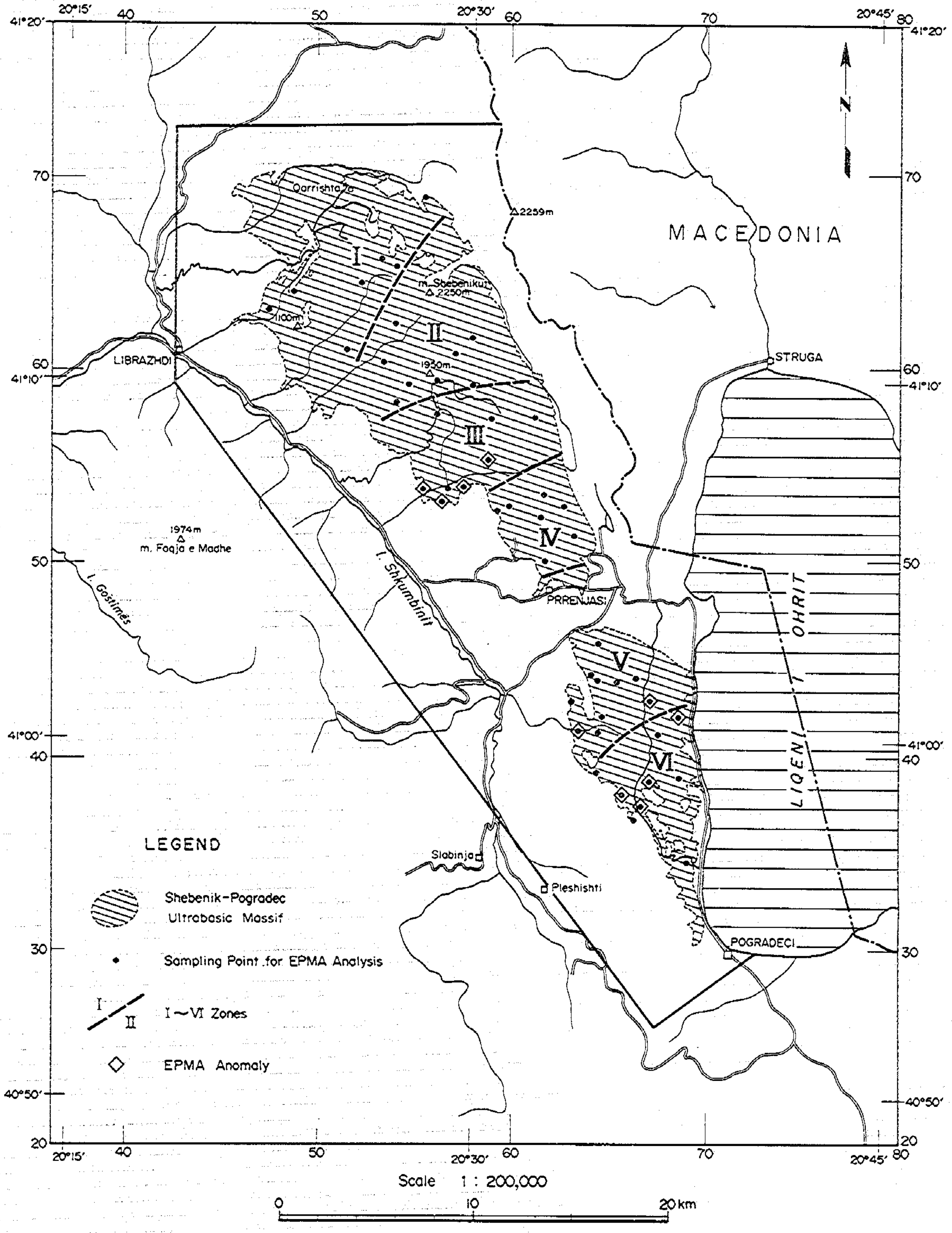

Fig. 2-3-14 Location of promising showings selected by EPMA analysis

f) MnO wt%

The MnO content was 0.4 wt% or lower in all of the samples. The trend is for comparatively lower values in the chromitite than in the harzburgite and dunite.

(3)-5 Analysis of the Test Results

From the results of study of chrome deposits so far the following four geochemical parameters are considered to be important for indication of large deposits of chromitite:

1) Cr# of the chrome spinel in the harzburgite
2) Ti content of the chrome spinel in the harzburgite and dunite
3) Fe^{+3}# of the chrome spinel in the harzburgite and dunite
4) The relationship between V_2O_3 content and the Cr# of the chrome spinel in the harzburgite and dunite

It is an observed fact that, as already mentioned, the value of the Cr# of the chrome spinel in the harzburgite is 0.4-0.5 (never higher than about 0.65) in the vicinity of large chrome deposits throughout the world, and at the same time it has been shown that the Cr content of the orthopyroxene is higher in the harzburgite with higher degree of depletion, and that there is a negative correlation between the Cr content of the orthopyroxene and Cr# of chrome spinel in the harzburgite (Arai, 1995; 1996). Such results back up the chromitite formation hypothesis (Arai, 1995) according to which the Cr in the melt was enriched by interaction between the wall rock mantle and the melt passing within it (mantle-melt interaction), and chromitite became densely concentrated by the process expounded by Irvine (1975). It is hoped, therefore, that the possibility that zones in which the Cr# of the chrome spinel of the harzburgite host is relatively low are zones with dense concentration of large quantities of Cr resulting from decomposition of orthopyroxene in view of the fact that the scale of the chromitite that is formed varies approximately according to the Cr content of the orthopyroxene selectively decomposed from the wall rock is correct.

Samples with intermediate values for the Ti content and Fe^{+3}# of the chrome spinel in the harzburgite and dunite are considered to be of significance as intermediate rock facies resulting from mantle-melt interaction (Matsumoto et al., 1995; 1996). They are important indicators in the sense that it is hoped that zones with comparatively prevalent distribution of intermediate values of Ti content and Fe^{+3}# are zones with larger quantities of dense concentration of Cr resulting from decomposition of orthopyroxene since such intermediate values are an indication of occurrence of mantle-melt interaction, which results in such decomposition of orthopyroxene.

Furthermore, it is expected that, as regards the V_2O_3 content and the Cr# of the chrome spinel in the harzburgite and dunite, a lower V_2O_3 content and a higher Cr# are brought about by selective fusion of the orthopyroxene in the harzburgite (MITI, 1994; 1995; Matsumoto et al., 1995; 1996), and in that sense that is also considered to the an important indicator.

The frequency with which those important indicators have values that are favorable to dense concentration of Cr is obtained as the zone index by the following formula:

Zone index = favorable indicator frequency/(4 indicators x number of samples) x 100.

The values of the zone index for the different zones are as follows:

Zone I : 8.3% (favorable in 2 instances/4 indicators x 6 samples)
Zone II : 10.3% (favorable in 4 instances/4 indicators x 10 samples)
Zone III : 25.5% (favorable in 12 instances/4 indicators x 8 samples)

Zone IV : 5.0% (favorable in 2 instances/4 indicators x 10 samples)

Zone V : 21.4% (favorable in 12 instances/4 indicators x 14 samples)

Zone VI : 18.8% (favorable in 9 instances/4 indicators x 12 samples)

Bulqiza : 37.5%(favorable in 6 instances/4 indicators x 4 samples))

Of which Bulqiza, Zone III, Zone V and Zone VI shows higher in the zone index as in the declining order and Zone II, Zone I, Zone IV are low in the values.

Of the points at which samples were taken with harzburgite, dunite and chromitite as a set, those for which the indicator values were favorable in three instances and those for which they were favorable in two instances are as follows:

- 3 instances of favorable indicators at 1 point:

  Zone III: K95092904 (Bushtrice showing), K9502911 (Menik deposit)

  Zone V : K95102108 (Bregu i Pishes showing)

  Zone VI: E95102201 (Shulleri i Kopri showing)

- 2 instances of favorable indicators at 1 point:

  Zone III: M95100810 (Qarri i Zi deposit), M95101605 (Mbi Shtepite e Celes showing)

  Zone V : K95102206 (Guri i Pellumbit showing)

  Zone VI: K95101301(Kroi i Farkuar showing), K95092505 (Qershori Pojske deposit), K95101302 (Cervenake).

As for the samples from the Bulqiza mine the indicator values were favorable in three instances for the samples taken from both outcrops.

The conclusions regarding the results of the EPMA tests concerning the Shebenik-Pogradec ultrabasic massif are as follows:

(1) Considering the Cr# of the chrome spinel in the harzburgite of the project area, the probability of there being any chromitite concentrations of the same scale or greater than the Bulqiza mine is low.

(2) However, if in the neighborhood of the above mentioned deposits and showings with favorable indicators for concentration of chromitite or in the neighborhood of points with a value of the Cr# in the harzburgite of no more than 0.6 there are areas in which the same kind of harzburgite is widely distributed and in which dunite occurs in large quantities, it is possible that there is endowment with chromitite ore bodies of the same scale as the Bulqiza mine.

2-4 Magnetic Survey

2-4-1 Survey Areas

Ground magnetic survey was carried out in the two areas indicated in Fig. 2-4-1 (Pishkash area and Kotodesh area). One lies north, and one south, of the Prenjas flatlands separating the Shebenik massif and the Pogradec massif.

2-4-2 Method of Measurement

(1) Setting of Measuring Lines

Since most of the dunite and chromitite distributed in the two areas has a directionality of N 30° W, for the sake of making it easier to catch magnetic anomalies the measuring line direction was set at N 60° E in both areas, and the measuring line interval and measuring point interval at 100 m and

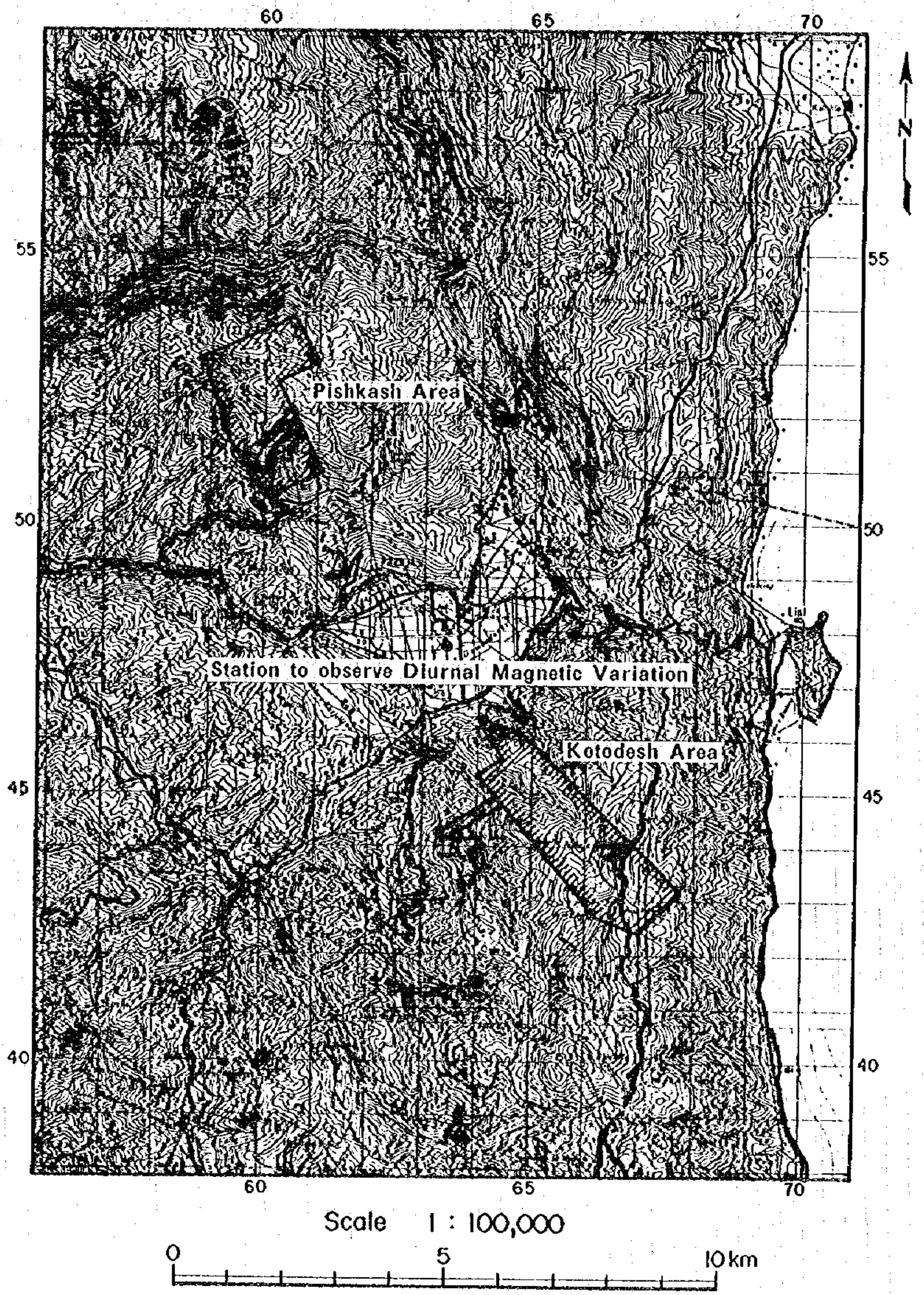

Fig. 2-4-1 Location of geophysical prospecting

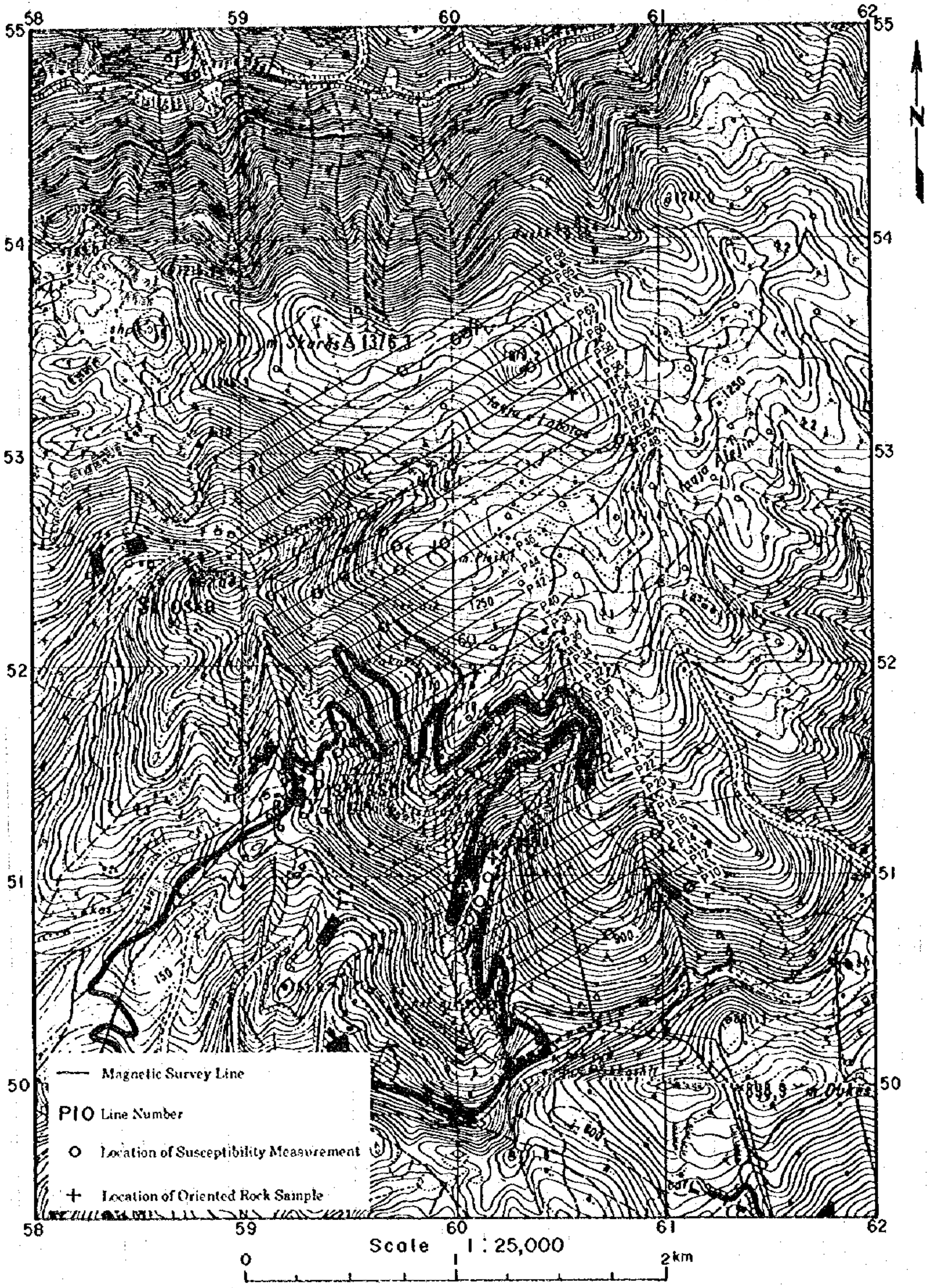

Fig. 2-4-2 Location of geophysical lines, oriented rock samples and magnetic susceptibility measurement in Pishkash area

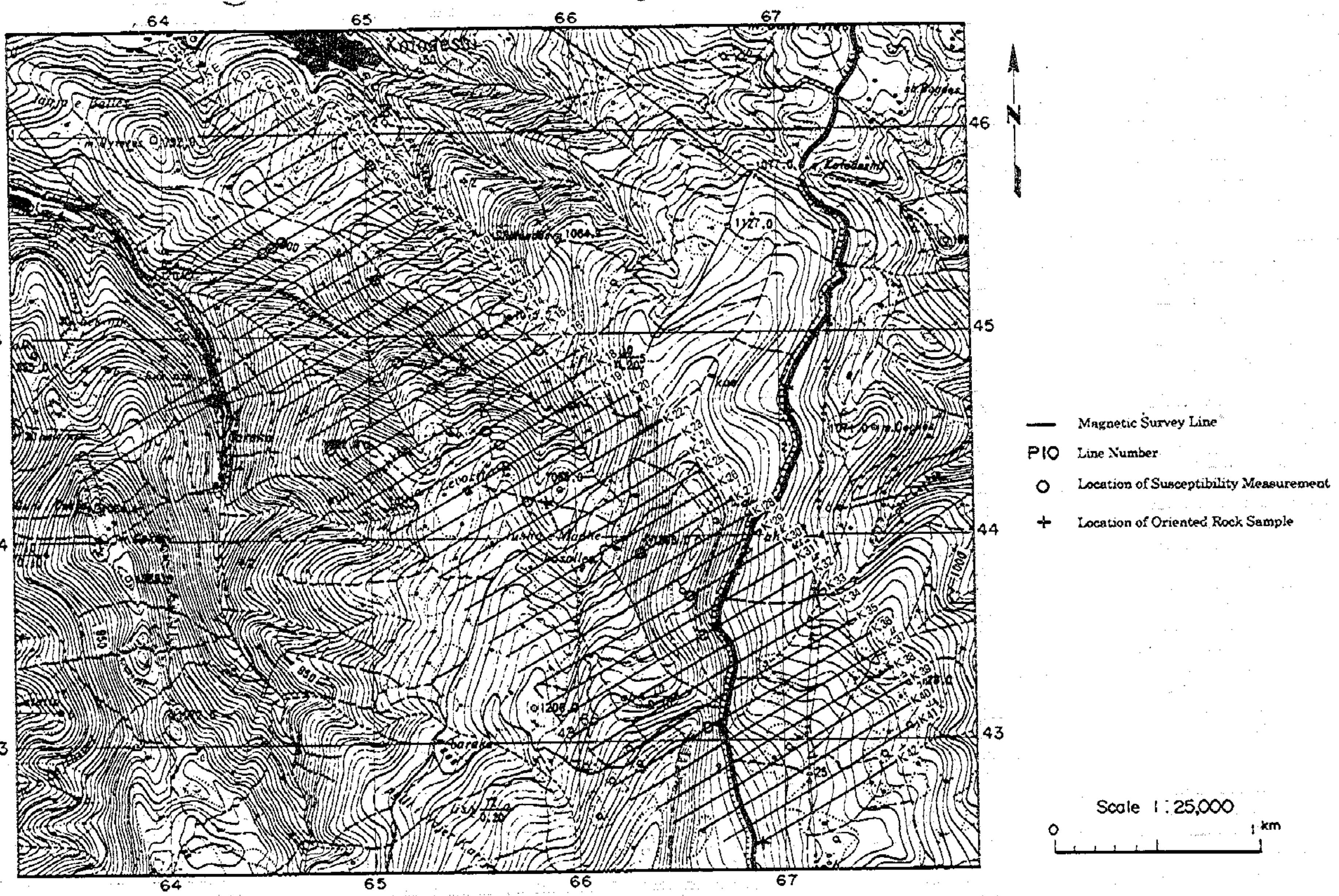

Fig. 2-4-3 Location of geophysical lines, oriented rock samples and magnetic susceptibility measurement in Kotodesh Area

20 m, respectively. All of the measuring lines were set by transit surveying with triangulation points in the vicinity of both areas as the datum points (see Fig.2-4-2 and Fig.2-4-3).

For the purpose of determining how magnetic survey reflects a known deposit, two measuring lines (1 km each) were set across the Katjel deposit as extensions outside the scope of the survey.

(2) Survey Method

Besides measuring total magnetic intensity at the measuring points on the different measuring lines set in the Pishkash and Kotodesh areas, supplementary measuring points were set at intervals of 10 m at places where anomalies in total magnetic intensity were noted for measurement at them as well. At the same time as such measurement local magnetic susceptibility was measured, and oriented rock samples were collected.

Table 2-4-1 below gives the surface areas of the two areas, the total measuring line length, the number of measuring points, the number of magnetic susceptibility measuring points and the number of oriented rock samples collected.

Table 2–4–1 Works of Magnetic Survey

Target Area	Area(km^2)	No. of Line	Line-km	Point	Susceptibility	No. of Oriented Sample
Pishkash	4.2	30	43.17	2187	66	10
Kotodesh	5.6	49	55.74	2835	26	10
Total	9.8	79	98.91	5022	92	20

The equipment used in the magnetic survey and measurement were as follows:

- Total magnetic intensity: Proton Magnetometer, model MP-2, Scintrex, Canada
- Magnetic susceptibility: Magnetic susceptibility meter,
  Kappameter, model KT-5, Czechoslovakia (local measurement)
  Barington, model SM2, U.K. (oriented rock samples)
- Natural remnant magnetization: Spinner Magnetometer, model SMM-85, Natsuhara Giken, Japan
  AC Demagnetizer, model DEM-8601, Natsuhara Giken, Japan

At each measuring point the value of the total magnetic intensity was taken as the average of two measurements. However, in cases in which the difference between the two measured values was greater than 5 nT, more measurements were made, and when stable values were obtained, the value of the total magnetic intensity was taken as the average of those stable values.

At the same time as measurement of total magnetic intensity at the different measuring points total magnetic intensity was observed at intervals of 5 minutes at a fixed observation point set in a field south of Prenjas approximately at the midpoint between the two areas in order to monitor magnetic storms influence on the measured values. However, no magnetic storms that would affect the measured values were observed during the period of the survey.

(3) Analysis Methods

Since no magnetic storms were observed during the period of the survey, the average of the fixed-point measured values obtained on December 8 was taken as the standard for obtaining the diurnal variation during the period of the survey, and that value was used to correct the values measured on the different days for diurnal variation.

The measured values corrected for diurnal variation were used for reduction to the pole and upward continuation, profile curve matching analysis was carried out with respect to the magnetic anomalies obtained in those ways.

Since reduction to the pole is vertical primary differentiation of pseudo gravity to make the magnetic field correspond to the gravity field and results in one-to-one correspondence between magnetic anomalies and magnetic bodies, it is an analytical method that makes correlation of topography and underground structures with magnetic anomalies easier. Upward continuation is carried out for the purpose of eliminating short wavelength anomalies due to magnetic anomaly substances very near the surface of the earth, and in this case 50 m of upward continuation was carried out. Furthermore, profile curve matching analysis was carried out by model calculation on profile charts for the purpose of estimating the forms of underground magnetic anomaly rock bodies.

2-4-3 Results of Analyses

(1) Total Magnetic Intensity Distribution

The total magnetic intensity maps of the Pishkash area and the Kotodesh area are give in PL. 2-4-1 and Fig. 2-4-4 and PL. 2-4-2 and Fig. 2-4-5, respectively.

(1)-1 Pishkash Area

As can be seen on PL. 2-4-1 and Fig. 2-4-4, the total magnetic intensity in this area has a north-south zonal distribution. West of the center there is distribution of high anomalies, and east of it there distribution of low anomalies. Looking more closely, one sees that high anomalies extend in the NW-SE direction in the northwest and southern part of the area, the main ones lying between measuring lines P68 and P58 in the northwest part of the area and between measuring lines P28 and P10 in the southern part of the area. Besides that, there is distribution of short-wave anomalies from measuring lines P60 to P42 in the northwestern part of the area, which points to a surface chromite showing in that proximity. There are also several dipole anomalies, i.e. pairs of high and low anomalies, the main ones being an anomaly on measuring line P52 in the northwest part of the area, an anomaly near Guri i Pishkashit and an anomaly on measuring line P24 in the south central part of the area. The anomaly on measuring line P24 has a form extending in the north-south direction from measuring line P26 to P20.

Since the low anomalies and high anomalies distributed in zonal fashion on measuring lines P52 and P54 have distributions that do not match the geological structure extending in the direction of the measuring lines, it is considered that it is more probable that they are effects of the measuring itself than effects of magnetic rock bodies.

(1)-2 Kotodesh Area

Looking at the area as a whole, high anomalies are distributed east of a line drawn north-south through the eastern tip of measuring line K19, and low anomalies are distributed west of it. There are three high anomalies: one centering on measuring line K25, another centering on measuring line K35 and the third centering on measuring line K40 in the southern part of the area. Those three anomalies are arranged roughly in the direction NW-SE, and the Gjorduke deposit lies near the anomaly centering on measuring line K25.

In the way of low anomalies, there are short-wave anomalies of comparatively large amplitude distributed north of measuring line K15, some of them of the dipole type, i.e. accompanied by high anomalies. The cluster of short-wave anomalies noted on measuring lines K4 to K11 are arranged roughly in the east-west direction, several chromite showings being located within their range of distribution. Furthermore, clear anomalies of the dipole type, i.e. pairs of high and low anomalies were noted on both measuring line K9 and measuring line K10, extended to the west to the Katjel deposit outside the survey area.

(2) Curve Matching

Curve matching is a method whereby first an underground structure model with theoretical magnetic anomaly curves is prepared for comparison with actually measured curves and the magnetic susceptibility, upper surface depth, horizontal extent and dip of the actual structure are obtained from the parameters of the structure model in which the theoretical and actually measured curves are best matched.

(2)-1 The Pishkash Area

In the Pishkash area magnetic profiles were prepared concerning the five anomalies PM-1 to PM-5 indicated in PL. 2-4-5 and Fig. 2-4-6(1) to Fig.2-4-6(6), and the horizontal extent, upper surface depth, dip, magnetic susceptibility, etc. of the magnetic structure were obtained by the curve matching method. The shape of the curve models used for the matching was tabular in all cases.

- The PM-1 anomaly extends roughly in the E-W direction, and the model with a thickness of 20 meters, an upper surface depth of 60 m, a lower surface depth of 200 m, a 70° dip to the south and a magnetic susceptibility of 183 x 10^{-3} SI best matches it.
- The PM-2 anomaly extends roughly in the NW-SE direction, and the model with a thickness of 20 m, an upper surface depth of 60 m, a lower surface thickness of 200 m, a 70° dip to the southwest and a magnetic susceptibility of 322 x 10^{-3} SI best matches it.
- The PM-3 anomaly extends roughly in the E-W direction, and the model with a thickness of 30 m, an upper surface depth of 60 m, a lower surface depth of 200 m, a 70° dip to the south and a magnetic susceptibility of 127 x 10^{-3} SI best matches it.
- The PM-4 anomaly extends roughly in the NW-SE direction, and the model with a thickness of 20 m, an upper surface depth of 60 m, a lower surface depth of 200 m, a 70° dip to the south and a magnetic susceptibility of 141 x 10^{-3} SI best matches it.
- The PM-5 anomaly extends roughly in the N-S direction, and the model with a thickness of 20 m, an upper surface depth of 60 m, a lower surface depth of 200 m, a 70° dip to the west and a magnetic susceptibility of 169 x 10^{-3} SI best matches it.

(2)-2 The Kotodesh Area

For the Kotodesh area magnetic profiles were prepared concerning the four anomalies KM-1 to KM-4 indicated in PL. 2-4-6 and Fig. 2-4-6(6) to Fig.2-4-6(9) and model calculations were carried out in the same manner as for the Pishkash area.

- The KM-1 anomaly extends roughly in the WNW-ESE direction, and the model with a thickness of 20 m, an upper surface depth of 60 m, a lower surface depth of 200 m, a 70° dip to the SSW and a magnetic susceptibility of 157 x 10^{-3} SI best matches it.
- The KM-2 anomaly extends roughly in the NE-SW direction, and the model with a thickness of 30 m, an upper surface depth of 70 m, a lower surface depth of 200 m, a 60° dip to the SE and a magnetic susceptibility of 168 x 10^{-3} SI best matches it.

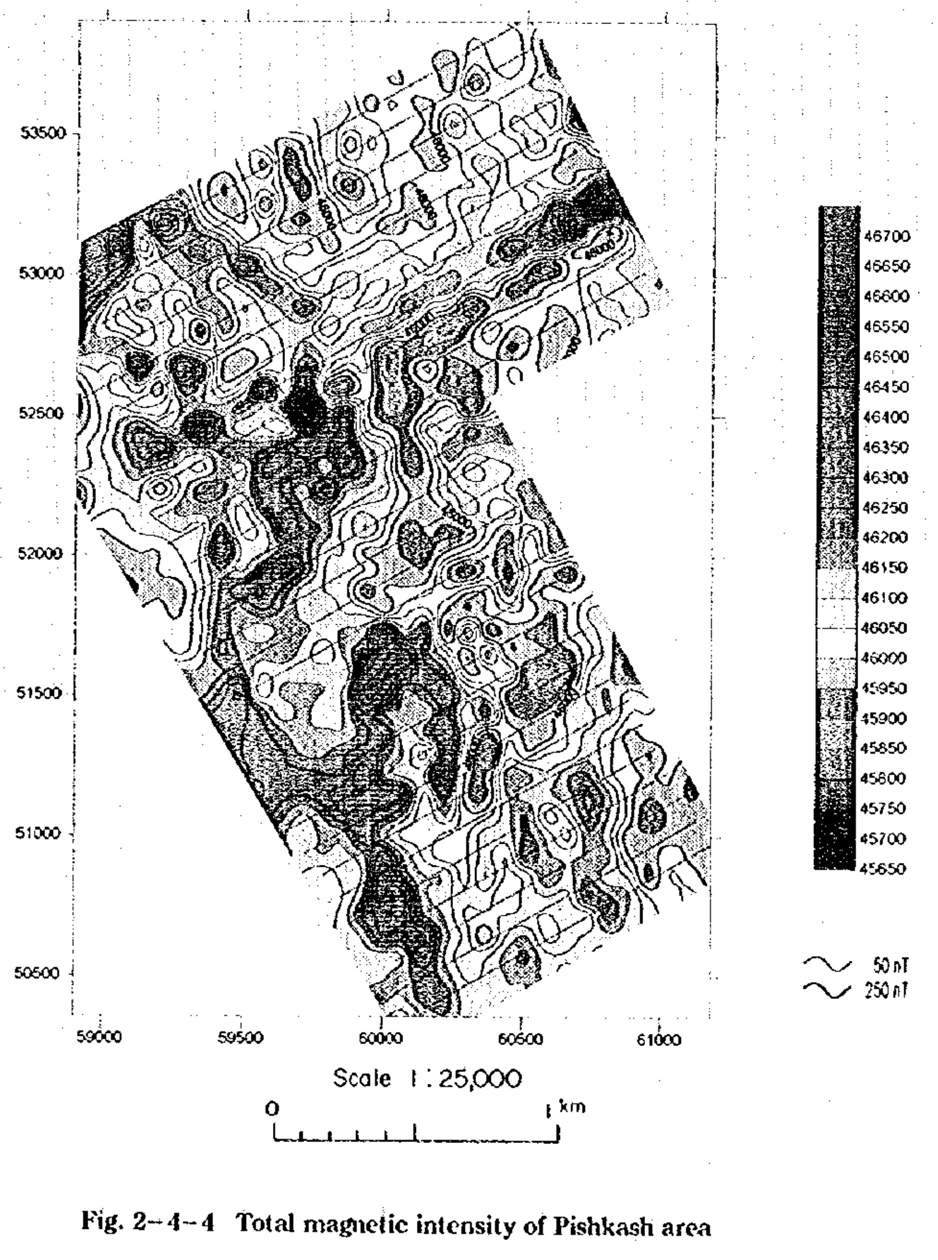

Fig. 2-4-4 Total magnetic intensity of Pishkash area

Fig. 2-4-5 Total Magnetic Intensity of Kotodesh Area

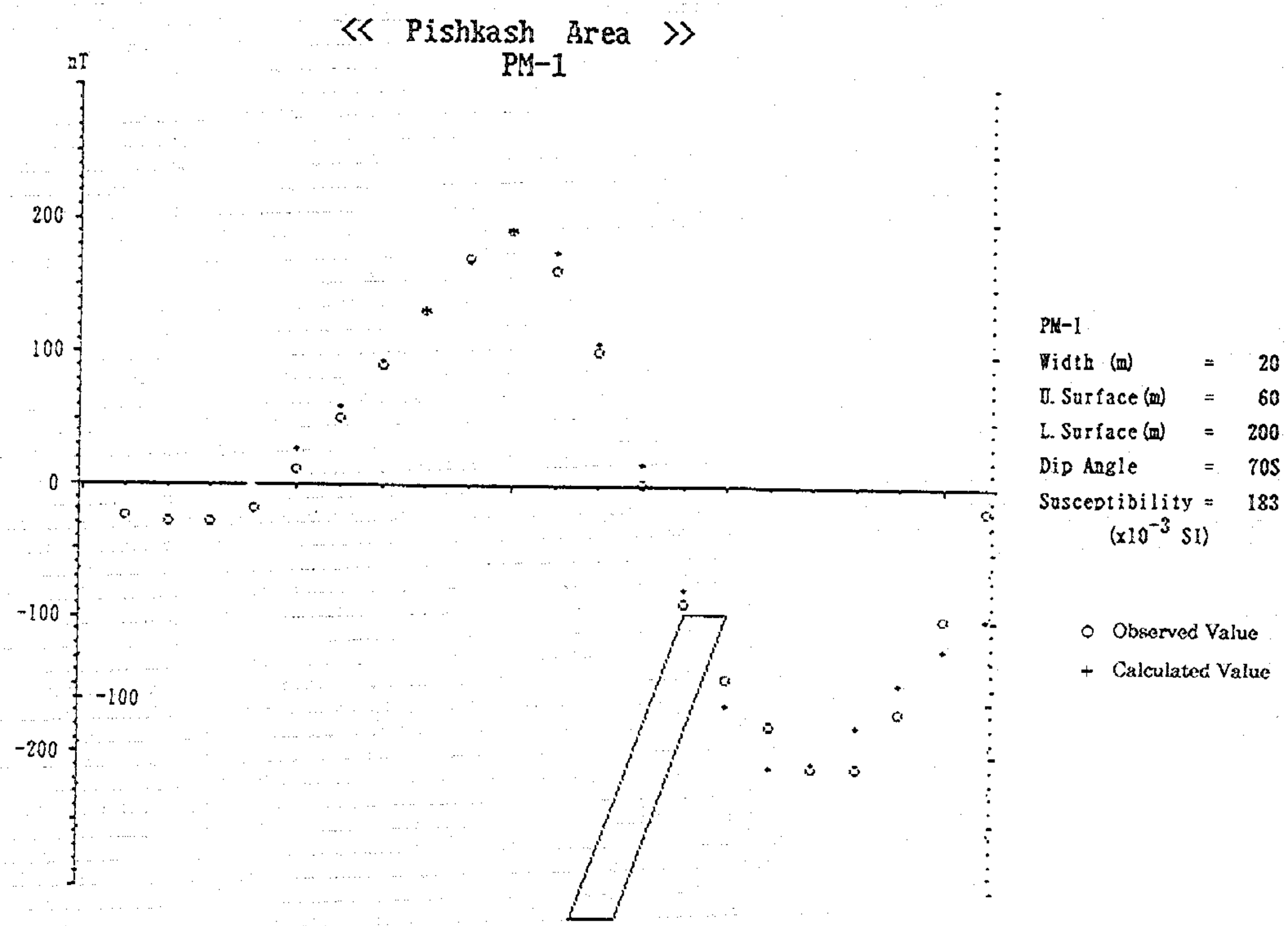

Fig. 2-4-6(1) Interpretation Profile PM-1 of Pishkash area

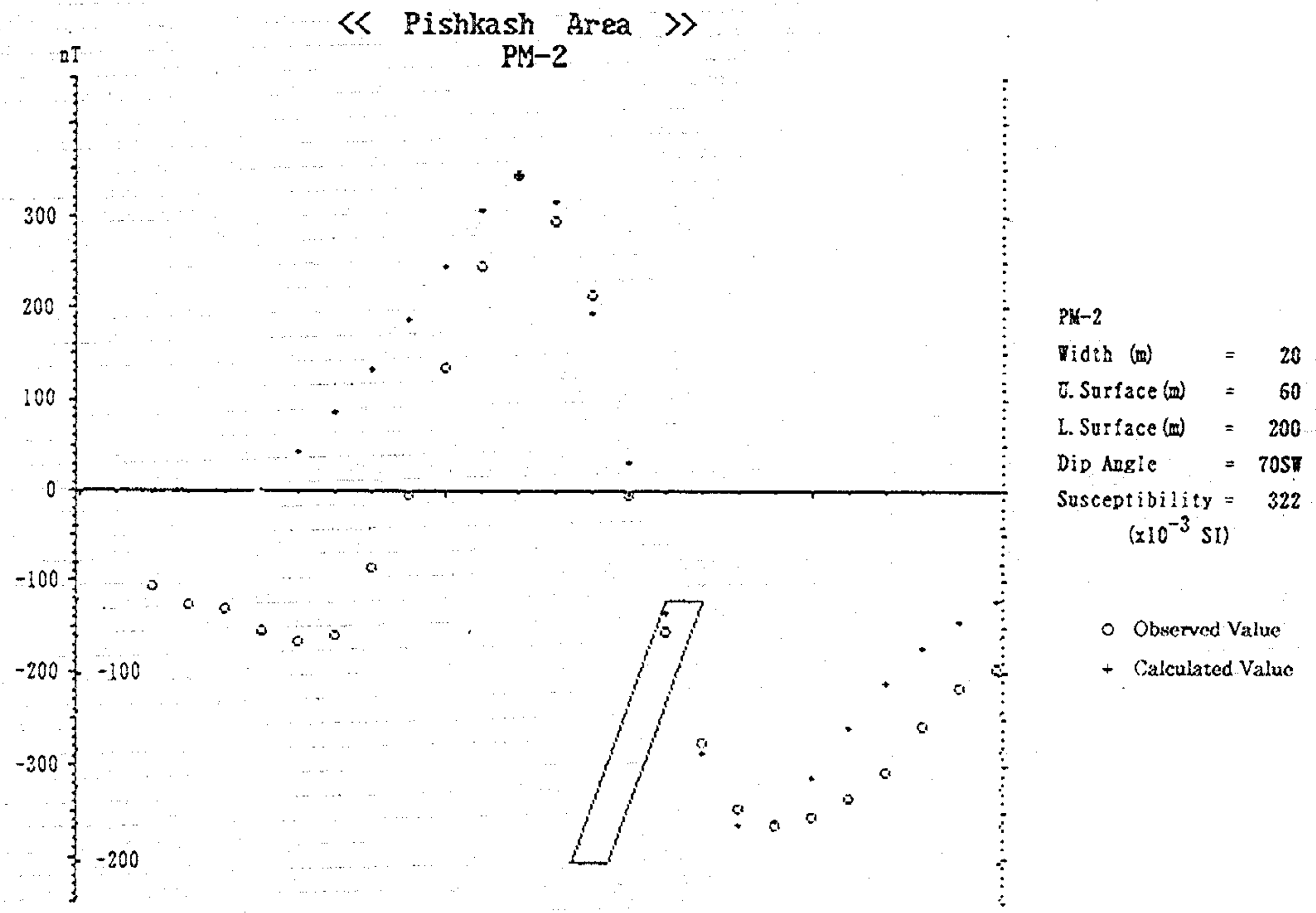

Fig. 2-4-6(2) Interpretation profile PM-2 of Pishkash area

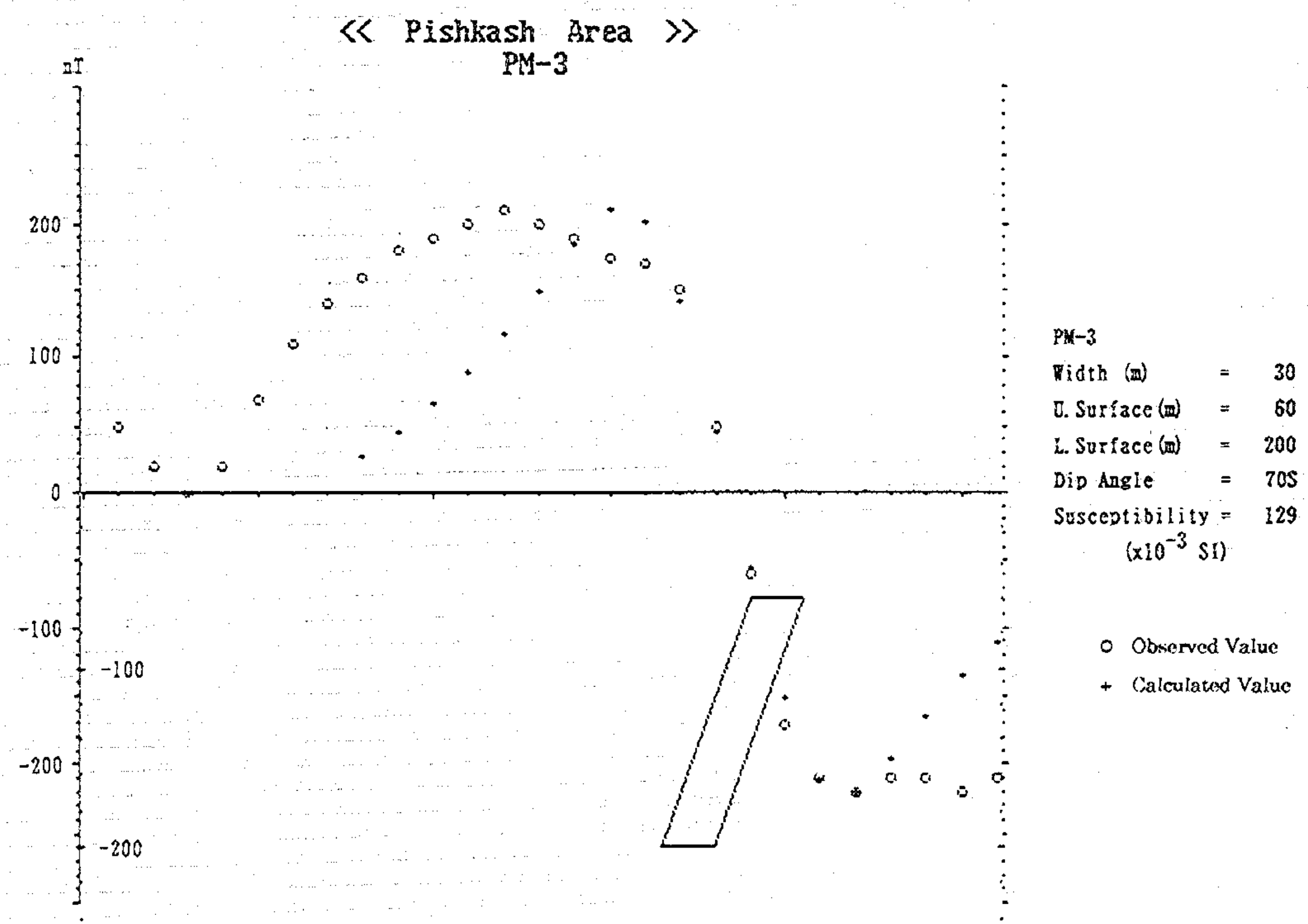

Fig. 2-4-6(3) Interpretation profile PM-3 of Pishkash area

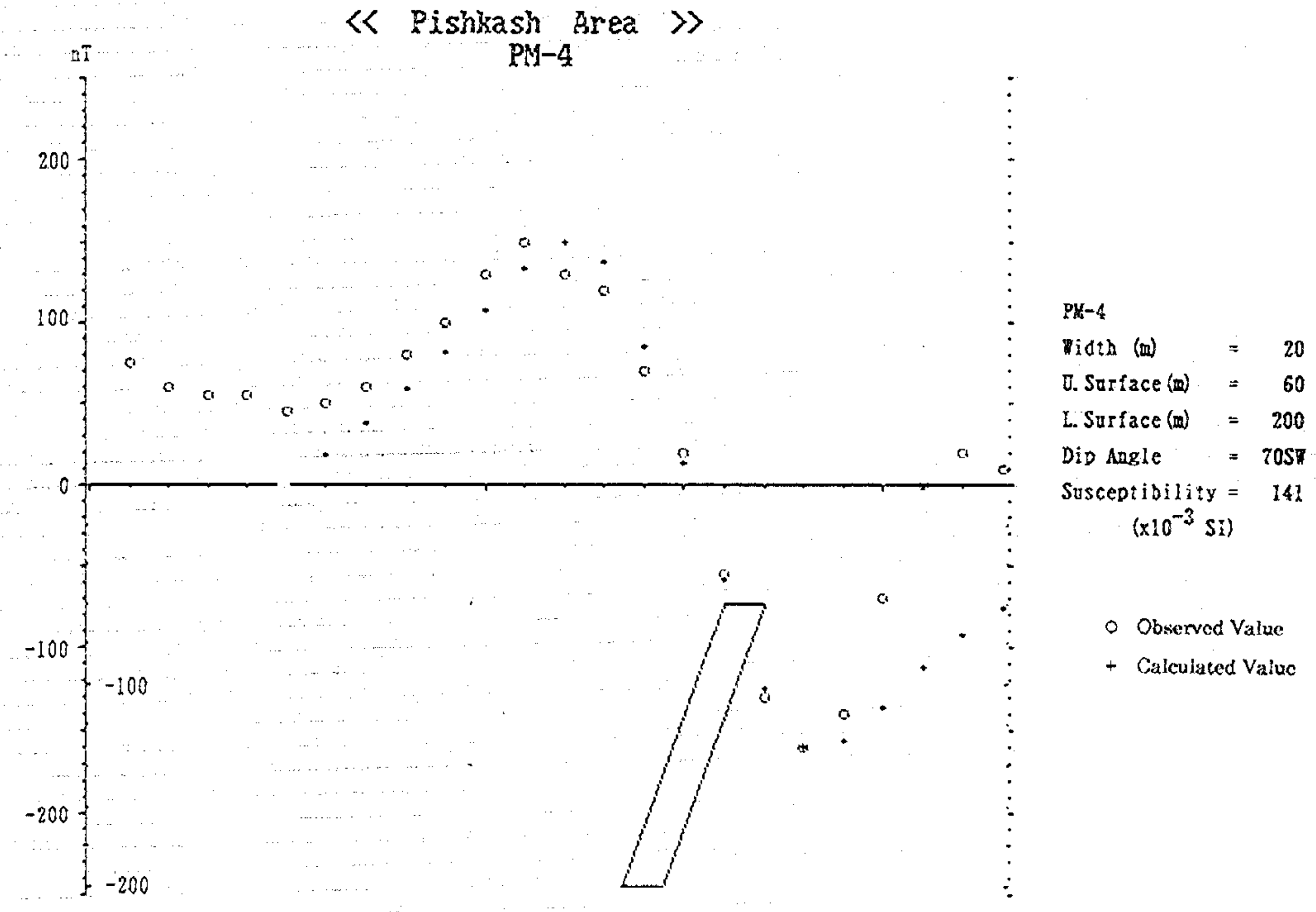

Fig. 2-4-6(4) Interpretation profile PM-4 of Pishkash area

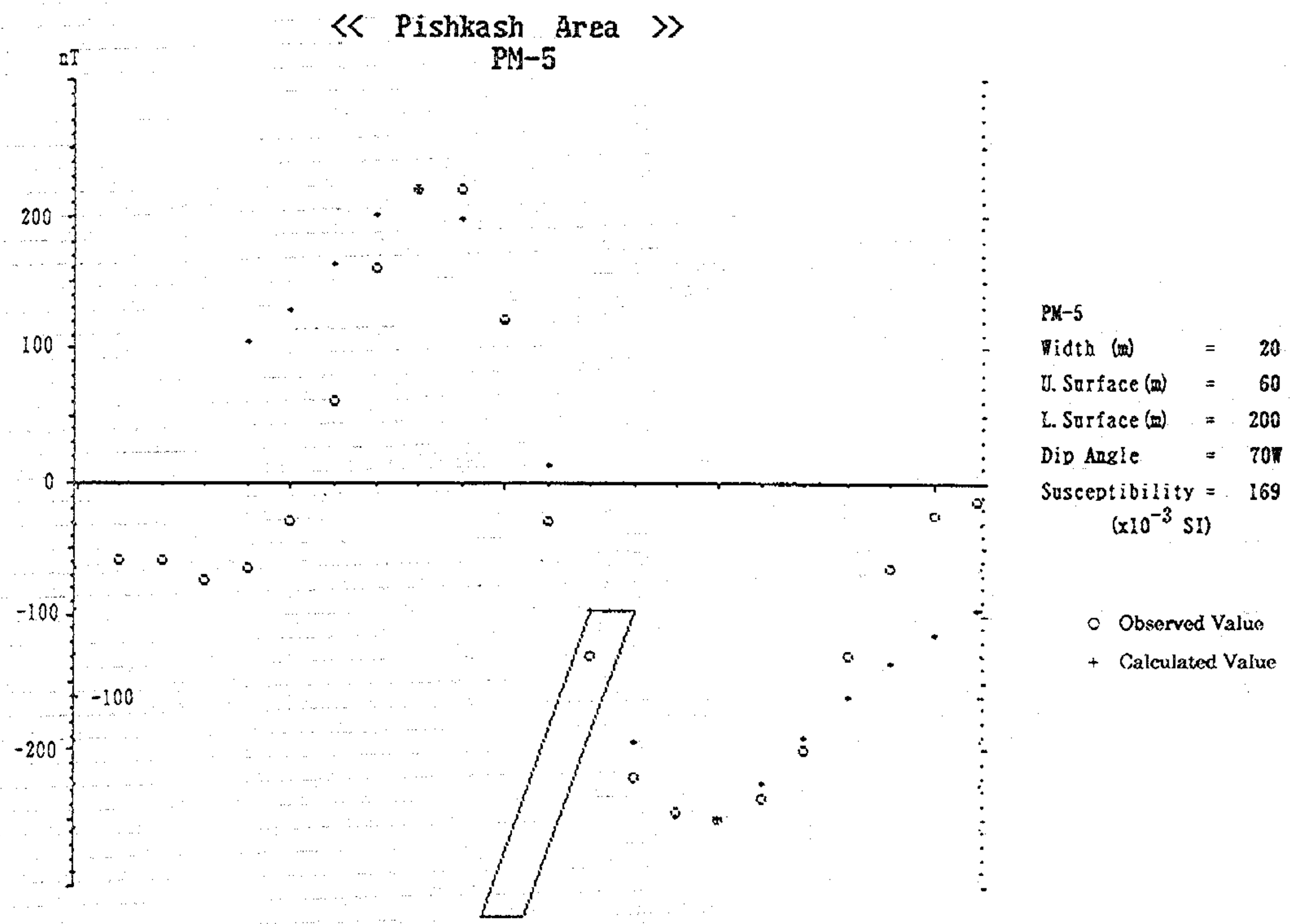

Fig. 2-4-6(5) Interpretation profile PM-5 of Pishkash area

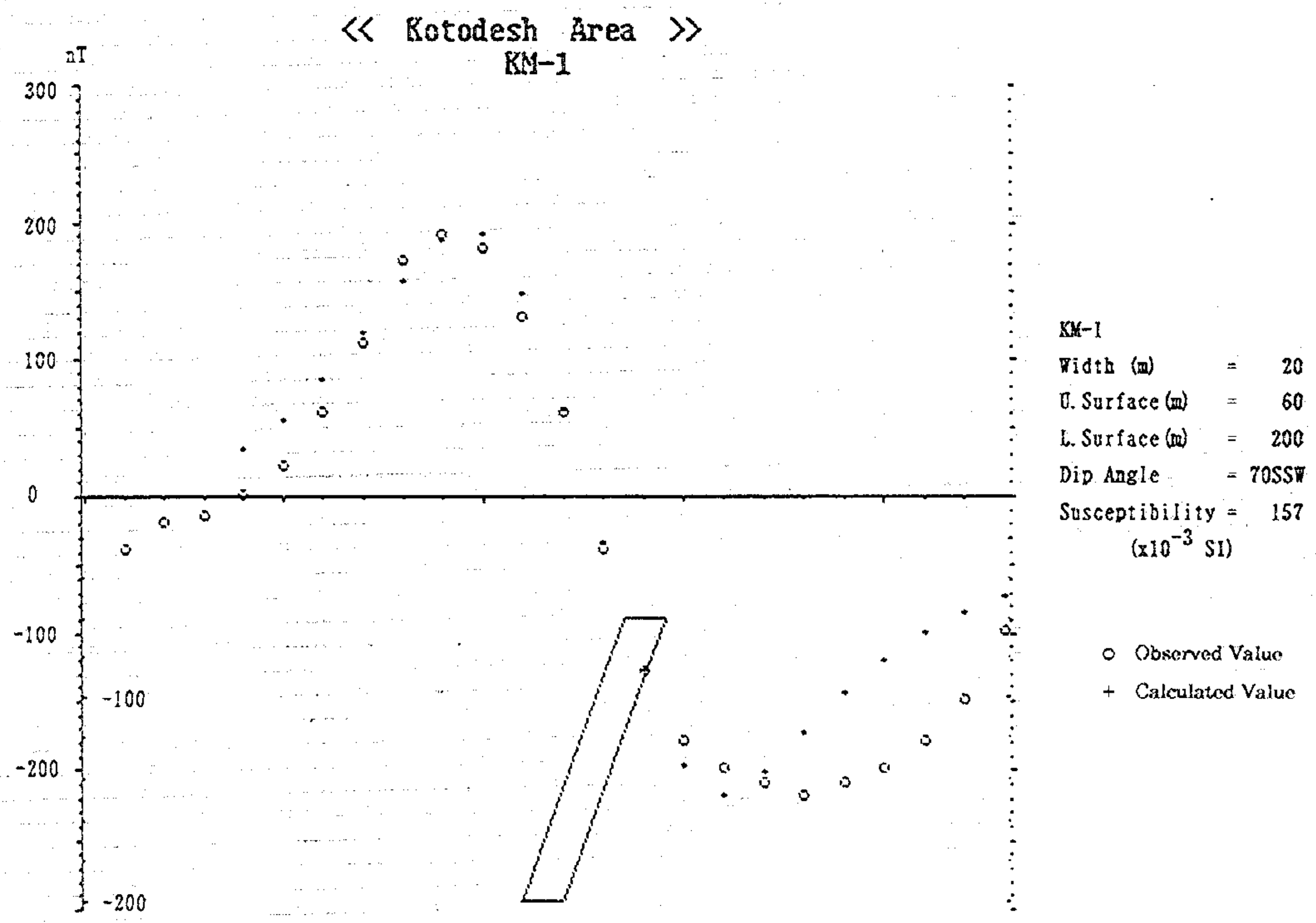

Fig. 2-4-6(6) Interpretation profile KM-1 of Kotodesh area

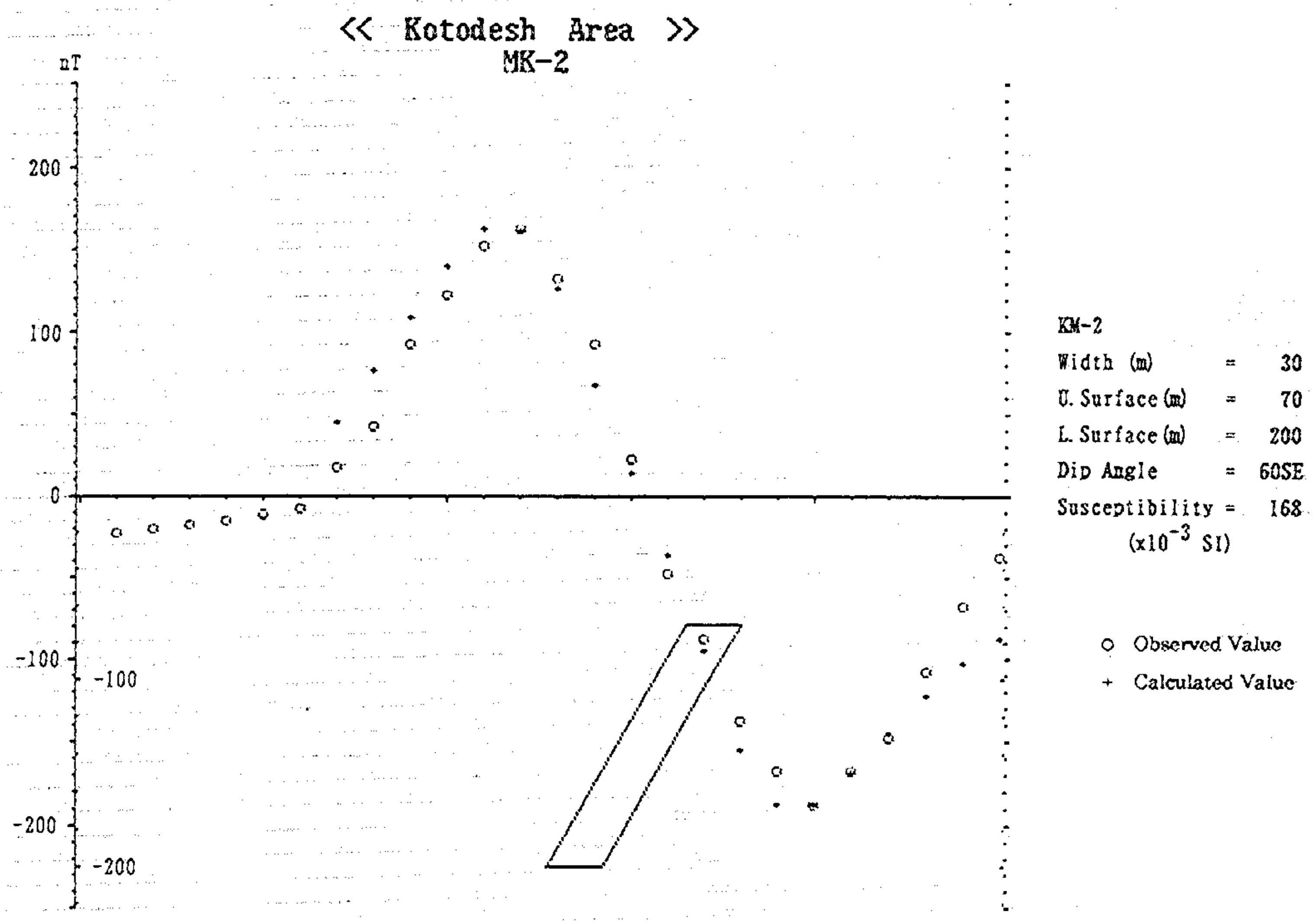

Fig. 2-4-6(7) Interpretation profile KM-2 of Kotodesh area

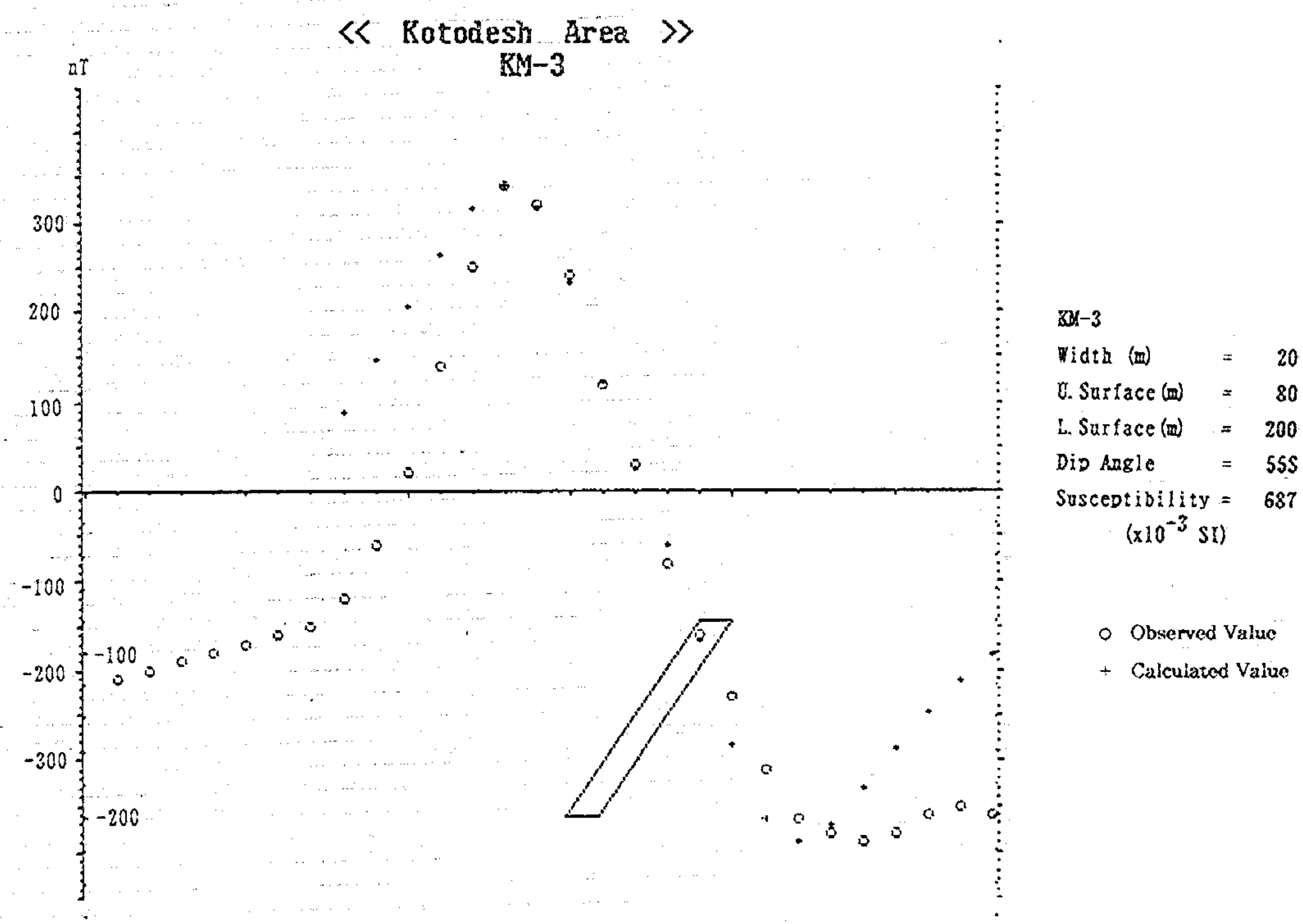

Fig. 2–4–6(8) Interpretation profile KM–3 of Kotodesh area

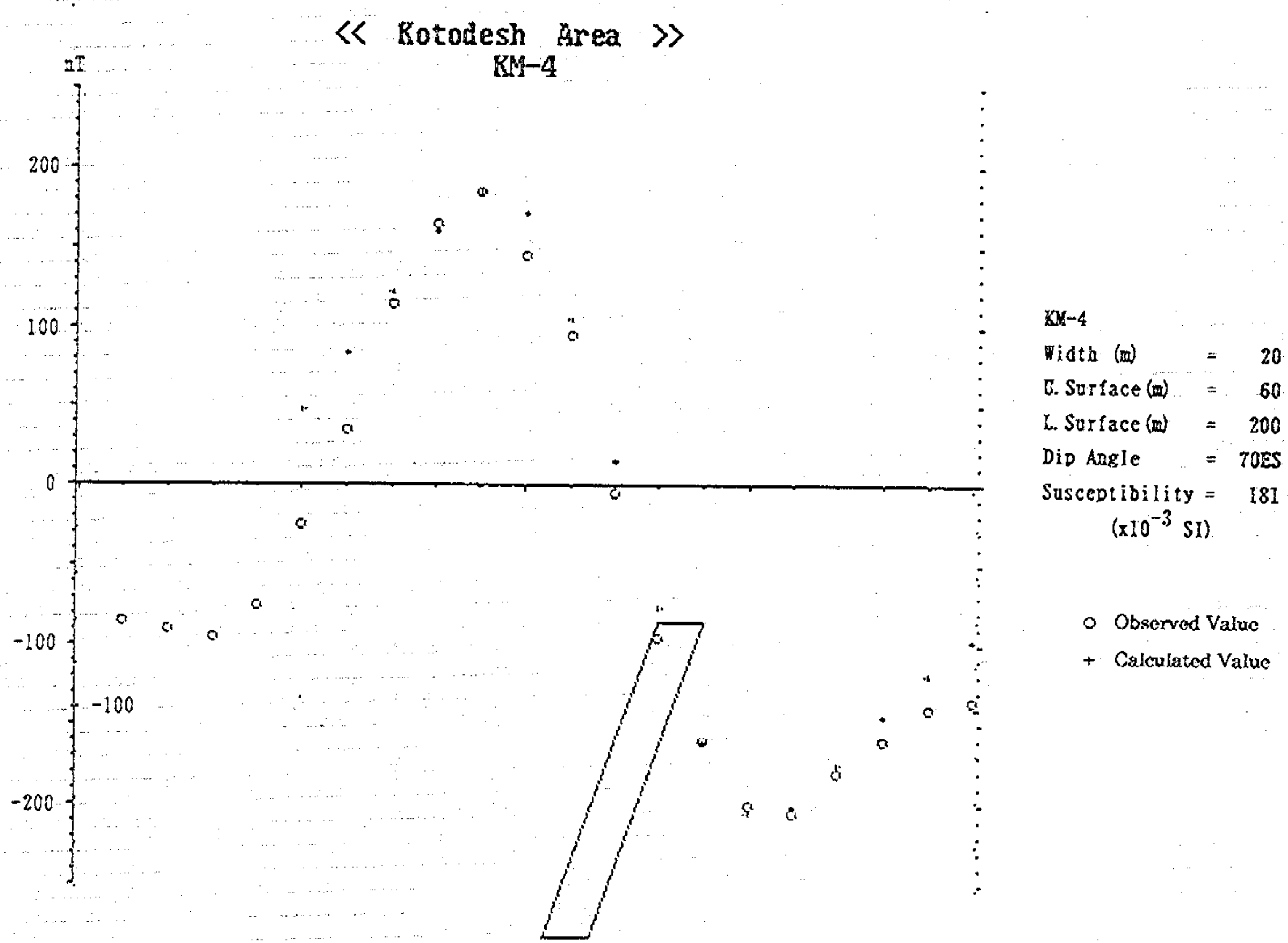

Fig. 2-4-6(9) Interpretation profile KM-4 of Kotodesh area

Table 2-4-2 Parameters of interpretation of magnetic profiles

	PM-1	PM-2	PM-3	PM-4	PM-5	KM-1	KM-2	KM-3	KM-4
Width (m)	20	20	30	20	20	20	30	20	20
U. Surface (m)	60	60	60	60	60	60	70	80	60
L. Surface (m)	200	200	200	200	200	200	200	200	200
Dip Angle ( )	70S	70SW	70S	70SW	70W	70SSW	60SE	55S	70ES
Susceptibility	183	322	129	141	169	157	168	697	181

unit of susceptibility: $x10^{-3}$ SI

Table 2-4-3 Magnetic characteristics of oriented rock samples

No	LnNo	PtNo	X	Y	Decli.	Incli.	Suscep	Rock	Remarks
P-1	38	173	60112	51971	20.1	57.6	0.2150	Hrz	N410606/E203122.1
P-2	49	296	60902	53062	-51.1	46.4	0.2760	"	N410639/E203207.5
P-3	56	82	58874	52296	55.3	16.8	0.0846	"	
P-4	66	254	60113	53589	37.7	-7.9	0.1580	"	
P-6	50	190	59959	52576	58.2	31.7	0.0657	"	
P-11	22	160	60399	51213	-92.8	-6.8	0.7320	"	N410541.3/E203137.6
P-12	22	136	60191	51093	25.3	27.2	0.7690	"	N410537.4/E203126.1
P-14	28	174	60370	51543	-97.3	-4.7	3.4600	Dun	N410552.6/E203132.9
P-16	28	216	60734	51753	46.2	-14.1	0.0523	Hrz	N410602.7/E203157.4
P-18	30	184	60407	51680	28.2	60.8	0.6050	"	N410601.3/E203124.3
K-1	22	86	65794	44195	18.6	-40.4	0.2000	"	
K-2	20	89	65668	44353	63.0	-20.3	0.1340	Dun	
K-3	17	84	65561	44638	28.5	34.2	3.2600	Hrz	
K-4	15	82	65479	44821	53.2	-32.7	0.2140	"	
K-5	11	92	65192	45117	5.8	13.0	0.1990	Dun	
K-6	7	105	64880	45399	63.2	17.0	0.1310	Hrz	
K-7	27	56	66301	43912	-2.8	40.7	0.1880	"	
K-9	32	48	66623	43519	110.9	-11.8	0.2520	Dun	N410130.8/E203613.1
K-10	36	70	66633	43062	47.6	39.7	0.3440	"	
K-11	42	74	66898	42523	21.3	29.4	0.0846	Hrz	

P-1: Sample No. of Pishkash Area
K-1: Sample No. of Kotodesh Area
LnNo: Line No.
PtNo: Point No.
Decli: Declination
Incli: Inclination
Suscep: Susceptibility (SI, $x10^{-3}$)
Hrz: harzbergite
Dun: dunite

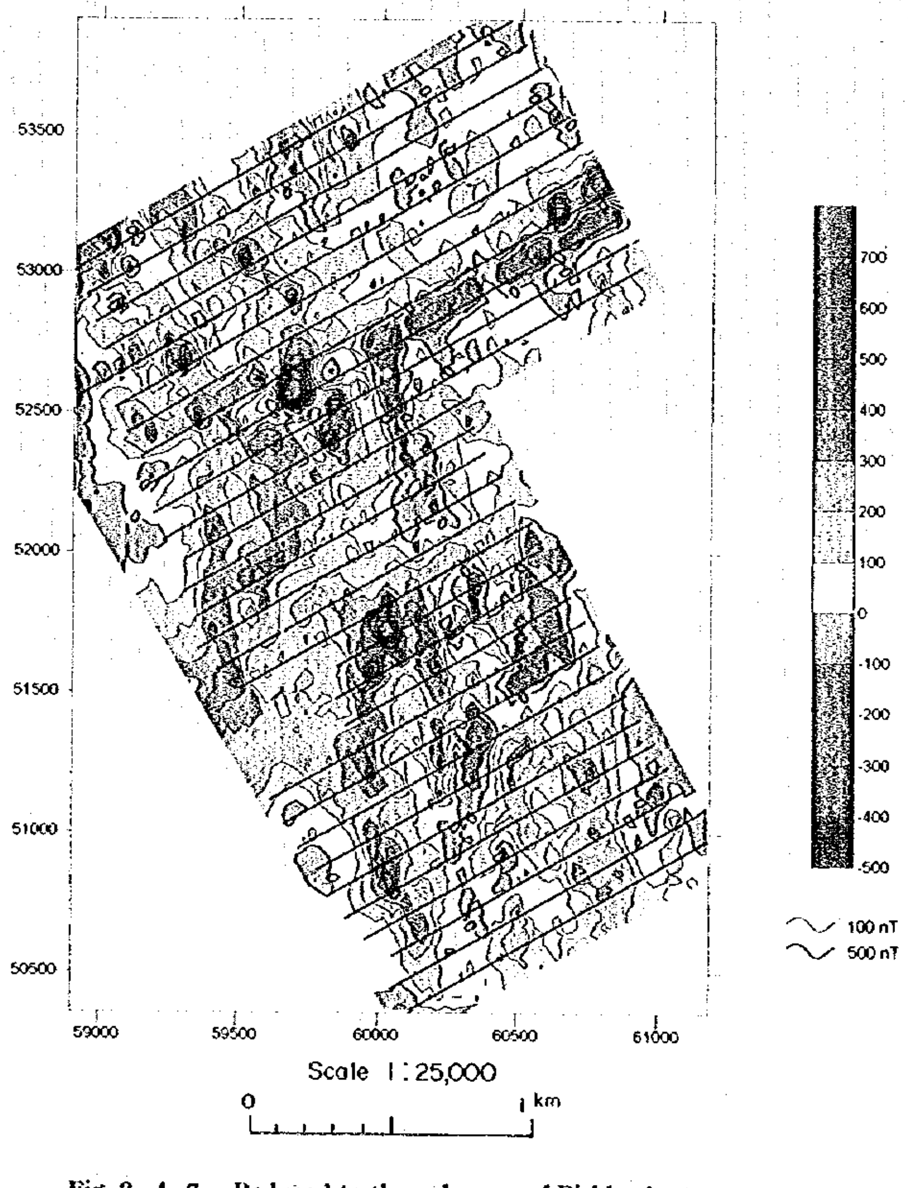

Fig. 2-4-7 Reduced to the pole map of Pishkash area

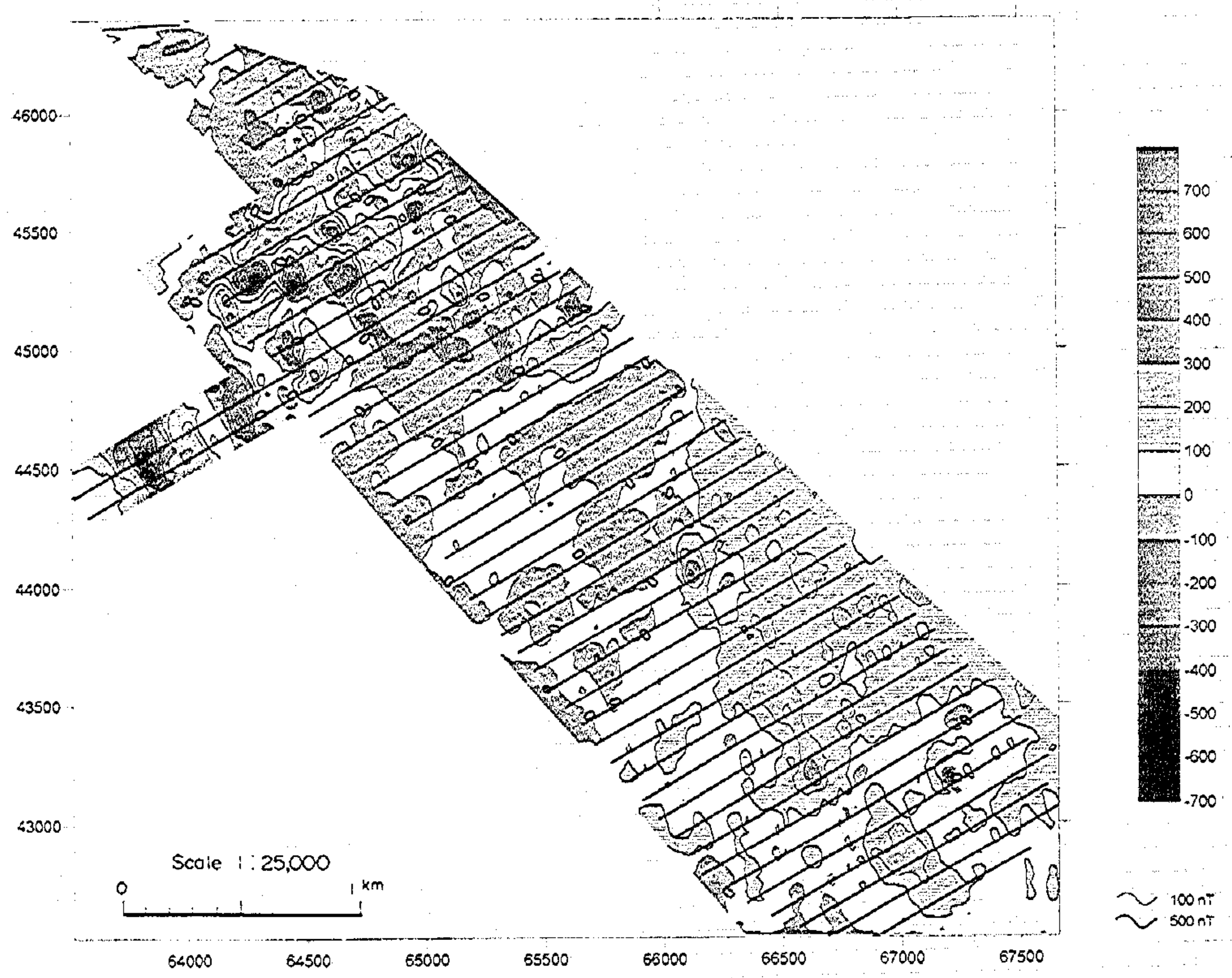

Fig. 2–4–8 Reduced to the pole map of Kotodesh area

- The KM-3 anomaly extends roughly in the WNW-ESE direction, and the model with a thickness of 20 m, an upper surface depth of 80 m, a lower surface depth of 200 m, a 55° dip to the south-southeast and a magnetic susceptibility of 697 x 10^{-3} SI best matches it.
- The KM-4 anomaly extends in the NE-SW direction, and the model with a thickness of 20 m, an upper surface depth of 60 m and a lower surface depth of 200 m, a 70° dip to the southeast and a magnetic susceptibility of 181 x 10^{-3} SI best matches it.

The results of the model calculations based on the above-mentioned curve matching are given in Table 2-4-2. For both the Pishkash area and the Kotodesh area there is considerable variation in such model calculation results: 20-30 m for thickness, 60-80 m for upper surface depth and 129-697 x 10^{-3} SI for magnetic susceptibility, although the lower surface depth is about 200 m for all of the models.

(3) Filter Analysis

(3)-1 Reduction of Total Magnetic Intensity to the Pole

The maps of reduction to the pole for the Pishkash area and the Kotodesh area are given in PL. 2-4-3 and Fig. 2-4-7 and in PL. 2-4-4 and Fig. 2-4-8, respectively.

(3)-1-1 The Pishkash Area

As a result of reduction to the pole, the scopes of the high anomalies and low anomalies with zonal distribution in the north-south direction on the total magnetic intensity maps are more limited and more clearly defined.

The high anomalies distributed in the western part of this area indicate underground distribution of magnetic bodies with relatively high magnetism, and it is considered that short-wave high anomalies, in particular, indicate the existence of bodies with high magnetism near the surface of the ground. The main short-wave high anomalies lie west of measuring line P52, near the western end of measuring line P58, at Guri i Pishkashit, etc.

On the other hand, it is considered that the low anomaly zones distributed on the east side of the area indicate the existence underground of objects with low magnetism in comparison with the area as a whole. Such low anomaly zones extend mainly from the central part of measuring line P52 southward to measuring line P40 and from the east end of measuring line P38 to south of measuring line P26.

The anomalies distributed near the middle of the southern part of the area from measuring line P28 to measuring line P20 are high anomalies paired with low anomalies, which indicates extremely high contrast in magnetism.

(3)-1-2 The Kotodesh Area

After reduction to the pole the high and low anomaly contract between the eastern half and western half of this area is sharper.

The entire eastern half demarcated by the north-south line that runs through the east end of measuring line K19 represents a high anomaly, and it is considered that that indicates that rocks with higher magnetism than west of that line are widely distributed in it. In the western part of that wide area of high anomaly represented by the eastern half of the area there are three high anomalies with particularly high values that run in the NW-SE direction, and it is considered that they indicate the existence of rock bodies with higher magnetism at comparative shallow depths. The Fushe e Madhe-Gjorduke deposit and the Shesh Bush No. 1 ore body are distributed at and nearby those high anomalies arranged in the NW-SE direction.

The entire western half of the area represents a low anomaly zone. However, short-wave, sharp-contrast high and low anomalies are arranged in the east-west direction in the northern part near the village of Kotodesh, and two sharp-contrast high anomalies close to one another are clearly expressed on measuring lines K9 and K10, which extend over the Katjel deposit. There are many known chromite showings at and near those high anomalies near the village of Kotodesh, and the Katjel deposit occurs roughly midway between those two sharp contrast high anomalies close to one another.

(3)-2 Upward Continuation

Fifty meters of upward continuation was carried out for both the Pishkash and the Kotodesh areas in order to eliminate the influence of small magnetic structures near the surface so as to be able to identify larger magnetic structures. The results of such upward continuation are indicated for the two areas in Fig. 2-4-9 and Fig. 2-4-10, respectively.

(3)-2-1 The Pishkash Area

Upward continuation eliminated extremely short-wave structures near the surface of the ground, making the overall distribution in the north-south direction on the total magnetic intensity map clearer and resulting in a total magnetic intensity distribution reflecting deeper structures.

However, although extremely short-wave magnetic anomalies due to the influence of small structures near the surface were eliminated on the total magnetic intensity map, in the northwest part of the area, characterized by distribution of short-wave magnetic anomalies, there is still a short-wave magnetic anomaly that is thought to reflect a group of small structures, and it is considered that that is an indication that in that vicinity there is continuation of small magnetic structures to a comparatively deep level.

The anomaly in the north-south direction in the area that includes Guri i Pishkashit is thought to reflect a comparatively large magnetic body extending in the north-south direction, but it is also possible that it is due to a certain extent to topographical influence since it is parallel to the direction of the ridge.

(3)-2-2 The Kotodesh Area

As a result of upward continuation the distributions of the high anomaly zone represented by the eastern half of the area and the low anomaly zone represented by the western half of the area on the total magnetic intensity map are clearer, and the running of the cluster of short-wave anomalies in the east-west direction in the north part of the western half of the area is also clearer. The high anomaly directly above the Katjel deposit, too, is clearer than before.

(4) Remnant Magnetization

The results of measurement of the remnant magnetization of the Pishkash and Kotodesh areas are given in Table 2-4-2.

(4)-1 The Pishkash Area

Of the 10 samples collected in this area for measurement of remnant magnetization bearing, 7 have a magnetization bearing of 20-58° (average value: 38.7°).

The other 3 samples are magnetized in roughly the opposite direction to those 7 samples, their average value being -80.4° . Of those 3 samples, sample P-11 (harzburgite) and sample P-14 (dunite),

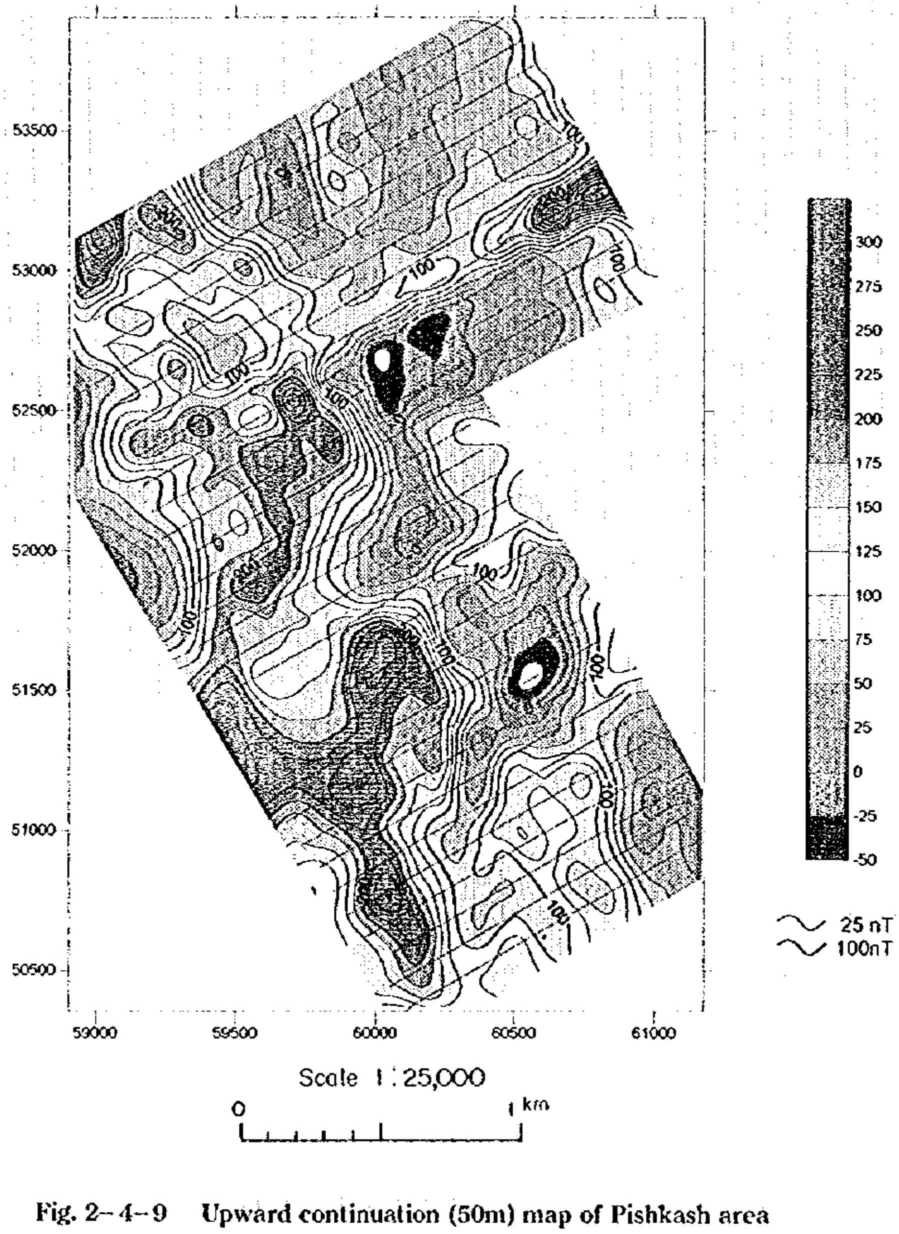

Fig. 2-4-9 Upward continuation (50m) map of Pishkash area

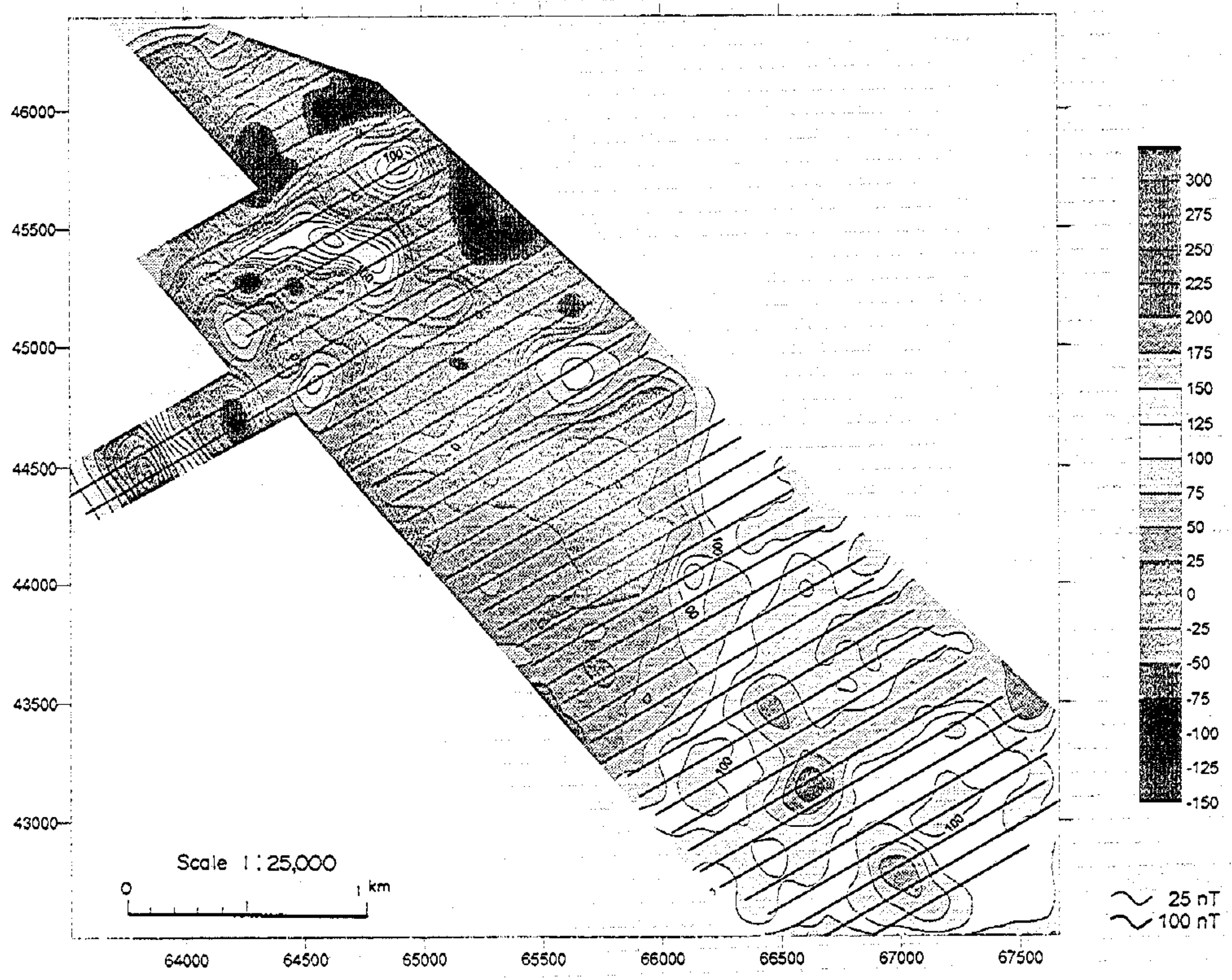

Fig. 2–4–10 Upward continuation (50m) map of Kotodesh area

which were collected at points about 300 m apart, have roughly the same direction, i.e. -92.8° and -97.3°, and their magnetic dips, -6.8° and -4.7°, are also about the same, which indicates that they belong to the same block in terms of geological structure.

But the magnetic dip variation among the 10 samples, -14° to 61°, is considerable, and that fact is considered to indicate that most of them underwent block formation as a result of folding and faults and that they were collected from blocks that ended up having different magnetic inclinations.

No difference or bias according to rock type was noted among the samples (harzburgite and dunite) taken for measurement of remnant magnetization; as in the case of the two samples mentioned above, there being samples for which harzburgite and dunite have similar remnant magnetization. That fact indicates that the harzburgite and dunite already coexisted before they were cooled off to below the Curie point.

(4)-2 The Kotodesh Area

The average declination of the 10 samples collected in this area is 41.2°. Seven of them are magnetized in the direction range 19° to 63°, with an average declination of 42.6°. Two samples taken 1.5 km apart (K-11 and K-27) are magnetized in the present magnetic north direction (5.8° and -2.8°), and another sample (K-9) has an entirely different direction of magnetization of 110.9°. There is very great dispersion among all of the samples as regards magnetic inclination: -40° to 41° (average: 6.9°). As in the case of the Pishkash area, that is considered to indicate a very high degree of block formation of with respect to geological structure.

Again as in the case of the Pishkash area, no difference or bias in remnant magnetization was noted according to the rock type of the samples that were used for measurement thereof.

(5) Magnetic Susceptibility

The results of measurement of magnetic susceptibility in the Pishkash area and the Kotodesh area are given in Tables 2-4-4 and 2-4-5, respectively.

(5)-1 The Pishkash Area

The 66 outcrops for which magnetic susceptibility was measured show values ranging from 2.73 x 10^{-3} SI to 0.75 x 10^{-3} SI (average: 5.6 x 10^{-3} SI).

As for the trend of the top-view distribution of magnetic susceptibility in the area, short-wave variation is noted in the northwestern and southern parts of the area. In the northwestern part the short-wave variation of magnetic susceptibility is 1 x 10^{-3} SI to 10 x 10^{-3} SI, the distribution being roughly the same as the distribution of the short-wave anomaly cluster on the total magnetic intensity map. In the southern part the variation is very great, 2 x 10^{-3} SI to 28 x 10^{-3} SI, the distribution being roughly the same as the distribution of the anomaly cluster that includes Guri i Pishkashit on the total magnetic intensity map.

(5)-2 The Kotodesh Area

The 26 outcrops for which magnetic susceptibility was measured show values ranging from 16.5 x 10^{-3} SI to 0.86 x 10^{-3} SI (average: 4.26 x 10^{-3} SI).

As for the trend of the top-view distribution of magnetic susceptibility in the area, there is not much variation (only 1 x 10^{-3} SI to 3 x 10^{-3} SI) in the magnetic susceptibility values of the eastern half of the area, which in its entirety represents a high anomaly on the total magnetic intensity map. But in the western half of the area, which in its entirety represents a low anomaly on the total magnetic susceptibility map, there is considerable variation (1 x 10^{-3} SI to 16 x 10^{-3} SI), particularly in the

Table 2-4-4 Magnetic susceptibility of Pishkash area

No	Line	Poin	X	Y	$x10^{-3}$ SI	No	Line	Poin	X	Y	$x10^{-3}$ SI
1	10	94	60128	50364	3.53	36	30	184	60407	51680	5.09
2	10	100	60180	50394	1.26	37	31	146	60053	51533	14.00
3	10	152	60630	50654	1.62	38	32	160	60149	51646	2.77
4	10	165	60742	50719	7.99	39	32	196	60461	51826	5.68
5	10	192	60976	50854	1.30	40	32	204	60530	51866	2.03
6	10	198	61028	50884	3.95	41	32	214	60617	51916	0.99
7	10	199	61037	50889	3.04	42	33	174	60245	51760	9.04
8	10	208	61115	50934	4.60	43	34	184	60307	51853	5.55
9	14	215	61075	51142	5.84	44	38	176	60138	51986	2.33
10	16	208	60965	51194	6.36	45	40	106	59481	51723	15.70
11	17	142	60368	50907	7.83	46	46	146	59678	52183	7.19
12	18	114	60101	50810	1.00	47	49	296	60902	53062	4.42
13	18	216	60984	51320	3.29	48	50	167	59760	52461	2.91
14	19	120	60128	50883	27.30	49	50	188	59942	52566	4.04
15	19	150	60388	51033	9.71	50	50	190	59959	52576	6.94
16	21	130	60164	51020	6.77	51	50	288	60808	53066	1.70
17	21	156	60389	51150	5.22	52	52	130	59389	52362	10.60
18	22	130	60139	51063	4.07	53	52	145	59519	52437	3.65
19	22	136	60191	51093	3.35	54	52	174	59770	52582	7.51
20	22	160	60399	51213	3.96	55	54	110	59166	52349	2.33
21	23	154	60322	51227	5.87	56	54	154	59547	52569	6.03
22	23	166	60426	51287	1.97	57	54	170	59686	52649	2.60
23	25	208	60740	51583	4.96	58	56	166	59601	52716	1.32
24	26	132	60057	51247	2.39	59	56	214	60017	52956	3.37
25	26	146	60178	51317	13.10	60	56	282	60606	53296	0.90
26	26	187	60533	51522	14.60	61	60	268	60384	53399	1.04
27	26	206	60697	51617	5.94	62	66	189	59550	53264	7.14
28	27	164	60309	51450	6.69	63	66	214	59767	53389	0.75
29	28	174	60370	51543	25.00	64	66	244	60027	53539	3.43
30	28	184	60457	51593	4.90	65	66	252	60096	53579	4.66
31	28	194	60544	51643	1.77	66	66	254	60113	53589	1.34
32	28	216	60734	51753	1.01						
33	29	206	60622	51746	5.60						
34	30	152	60130	51520	10.20						
35	30	166	60251	51590	6.87						

Table 2-4-5 Magnetic susceptibility of Kotodesh area

No	Line	Point	X	Y	$x10^{-3}SI$
1	4	66	65067	45853	16.50
2	4	145	64383	45458	3.05
3	4	180	64080	45283	9.15
4	5	130	64563	45447	3.05
5	5	132	64546	45437	2.96
6	5	138	64494	45407	9.38
7	7	107	64862	45389	2.32
8	9	100	65023	45250	6.55
9	11	92	65192	45117	1.84
10	13	90	65309	44954	6.37
11	13	108	65154	44864	1.01
12	14	65	65576	44992	3.95
13	15	81	65487	44826	1.11
14	15	82	65479	44821	10.67
15	15	96	65357	44751	1.45
16	15	157	64829	44446	1.58
17	16	46	65840	44914	8.46
18	17	84	65561	44638	1.42
19	18	90	65559	44521	6.00
20	20	89	65668	44353	0.86
21	22	86	65794	44195	2.23
22	27	56	66304	43912	2.18
23	30	35	66636	43757	2.06
24	32	48	66623	43519	3.22
25	36	70	66633	43062	1.78
26	42	74	66898	42523	1.20

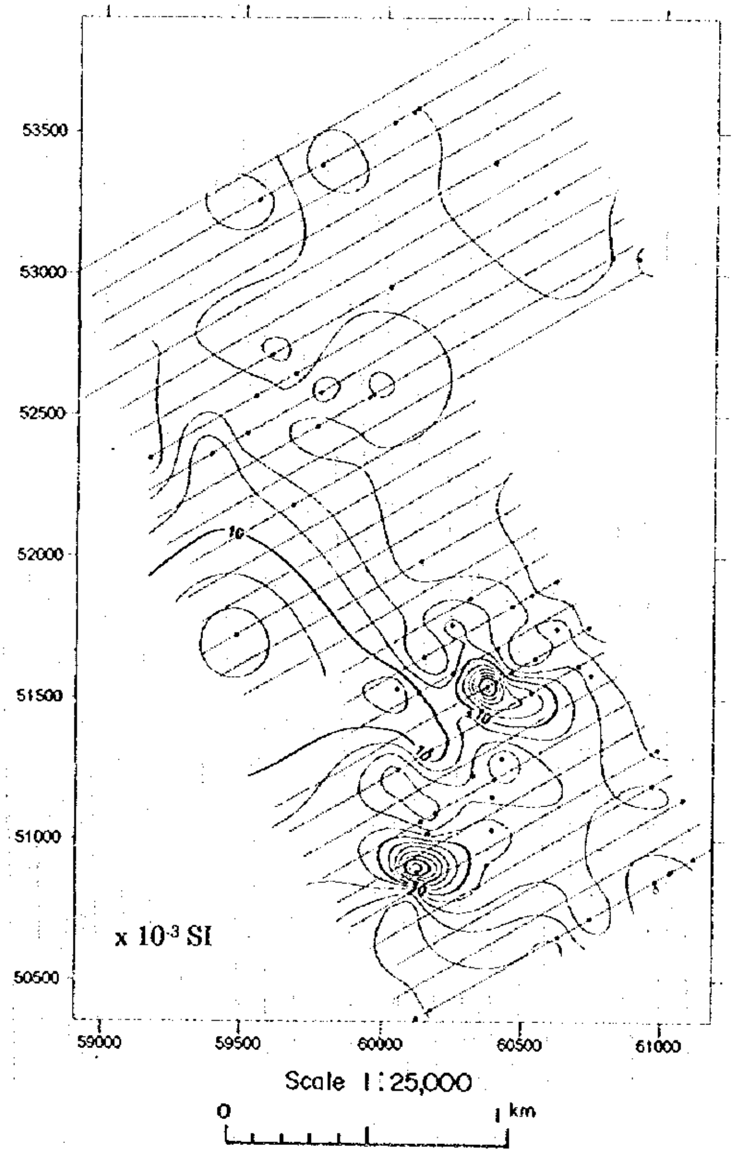

Fig. 2-4-11 Magnetic susceptibility of Pishkash area

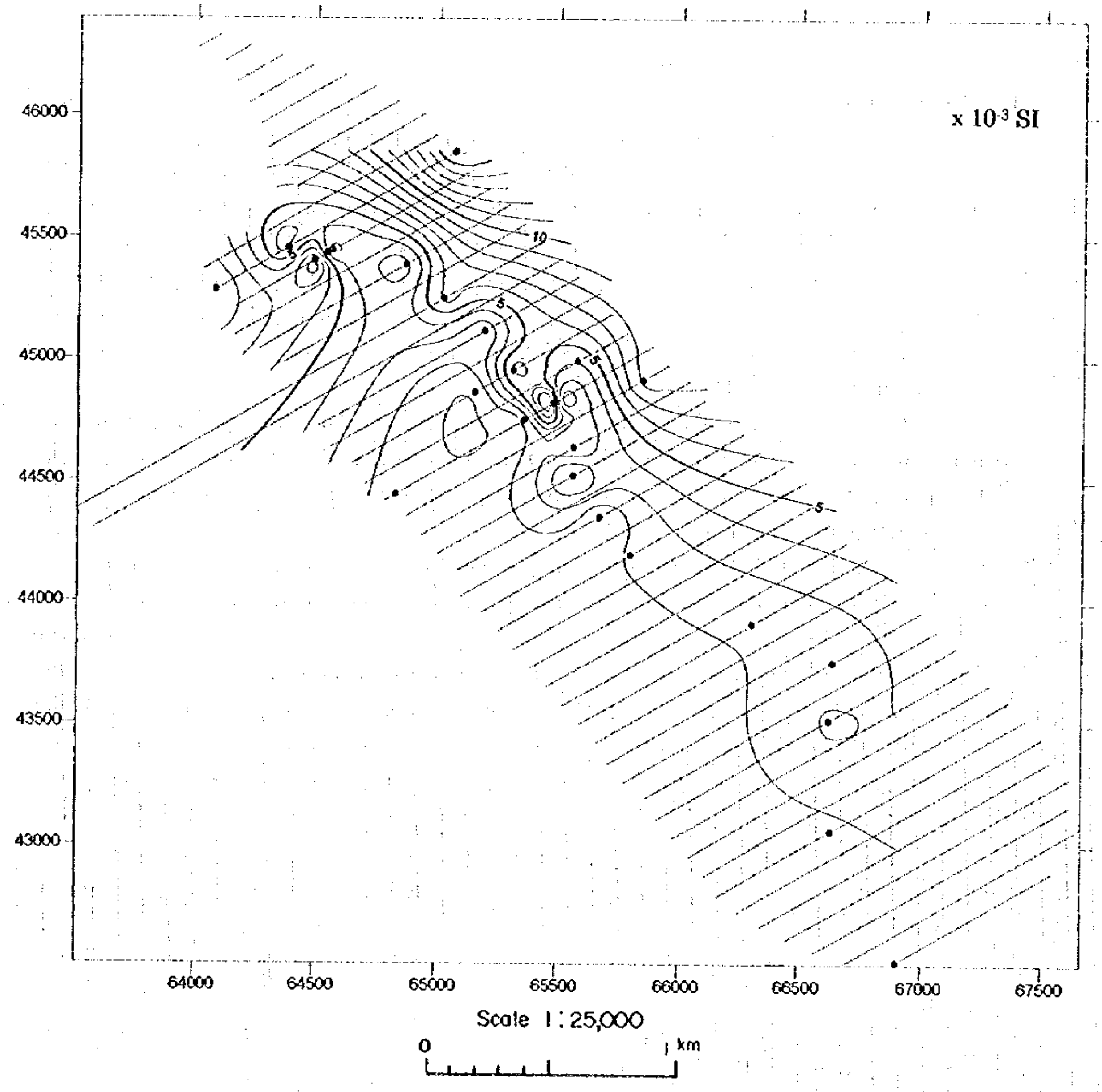

Fig. 2-4-12 Magnetic susceptibility of Kotodesh area